

**ER-associated degradation (ERAD):
Novel components and cellular regulation**

**Dissertation der
Fakultät für Biologie der
Ludwig-Maximilian-Universität
München**

vorgelegt von
Diplom-Biologe Sigurd Braun
aus Freiburg i. Br.

Juli 2005

Ehrenwörtliche Erklärung

Hiermit erkläre ich, dass ich die vorliegende Arbeit selbständig verfasst und keine anderen als die von mir angegebenen Quellen und Hilfsmittel benutzt habe. Ferner erkläre ich, dass ich weder versucht habe, eine Dissertation anderweitig einzureichen bzw. einer Prüfungskommission vorzulegen noch eine Doktorprüfung durchzuführen. Die vorliegende Dissertation ist nicht ganz oder in wesentlichen Teilen einer anderen Prüfungskommission vorgelegt worden.

München, den 25.Juli 2005

Die vorliegende Arbeit wurde zwischen Juli 2000 und April 2005 unter der Anleitung von Prof. Dr. Stefan Jentsch am Max-Planck-Institut für Biochemie, Martinsried durchgeführt.

Teile der Dissertation sind in folgenden Publikationen veröffentlicht:

Braun, S., K. Matuschewski, M. Rape, S. Thoms and S. Jentsch (2002). Role of the ubiquitin-selective CDC48(UFD1/NPL4) chaperone (segregase) in ERAD of OLE1 and other substrates. *Embo J* **21**(4): 615-21.

Richly, H., M. Rape, **S. Braun**, S. Rumpf, C. Hoegge and S. Jentsch (2005). A series of ubiquitin binding factors connects CDC48/p97 to substrate multiubiquitylation and proteasomal targeting. *Cell* **120**(1): 73-84.

Promotionsgesuch eingereicht am	27. Juli 2005
Tag des wissenschaftlichen Kolloquiums	13. September 2005
Erster Gutachter	Prof. Dr. Stefan Jentsch
Zweiter Gutachter	Prof. Dr. Peter B. Becker

Danksagung

Ganz herzlich möchte ich mich bei Stefan Jentsch bedanken. Sein stetes Interesse, die vielen Anregungen und konstruktive Kritik, schließlich aber auch die mir überlassenen wissenschaftlichen Freiräume waren Motivation und nicht zuletzt Voraussetzung für das Gelingen dieser Arbeit. Insbesondere möchte ich ihm dafür danken, dass er neben der Wissenschaft nie das Persönliche zu kurz kommen ließ und jede mögliche Unterstützung für meinen zukünftigen Weg aufgebracht hat.

Zudem möchte ich mich bei den Mitgliedern der Prüfungskommission der Ludwig-Maximilians-Universität bedanken. Insbesondere gilt mein Dank Herrn Prof. Dr. Peter Becker für die Begutachtung dieser Arbeit.

Manuela Kost danke ich, dass sie mich während meiner „Ufe“-Zeit tatkräftig unterstützt und meinen oft hektischen Anliegen Stand gehalten hat.

Ebenso möchte ich mich bei meinen Kollegen Holger Richly und Michael Rape für die außerordentlich gute Zusammenarbeit während des „escort“-Projektes bedanken.

Großer Dank gilt der gesamten Arbeitsgruppe von Stefan Jentsch, deren angenehmes, kooperatives Arbeitsklima und soziale Verbundenheit die Zeit sehr schön und meist unbeschwert hat werden lassen. Insbesondere seien hier erwähnt Carsten Höge und Michael Rape, die mich in ihrer ganz besonderen Art in meinen Anfangsbemühungen unterstützten; Georg Dönges für die vielen aufmunternden Plauschs wissenschaftlicher und nicht-wissenschaftlicher Natur; Marian Kalocay, Till Bartke und Holger Richly, mit denen oftmals das geistige Verarbeiten des Tageswerks in geselliger Runde bewältigt wurde; Sandrine Creton und Boris Pfander sowie bereits Genannte für die intensive Auseinandersetzung von geschriebenen und ungeschriebenen Erkenntnissen; alle Anwärter auf die Plätze des blauen Dunstkreises; Alexander Buchberger, der immer ein Ohr für Probleme nicht nur in Bezug auf Computer hatte. Ulla Cramer für ihren unermüdlichen Einsatz in Sachen Stammsammlung. Dirk Kempe für das Organisieren und Pflegen zahlreicher sozialer Anlässe. Neben Mitgliedern der Jentsch-Gruppe seien auch Andrea Pichler und Sowmya Swaminathan erwähnt als Anlaufstelle für vielerlei Belange.

Schließlich möchte ich ganz besonders meinen Eltern danken: dafür, dass sie mich stets auf meinem Weg unterstützt und meine Entscheidungen mitgetragen haben. Ebenso gilt mein ganz persönlicher Dank Ulrike, die mir immer liebevoll zur Seite stand, den zeitlichen Tribut an die Doktorarbeit mitrug und selbst nach „Feierabend“ den wissenschaftlichen Restergüssen geduldig zuhörte– nicht zuletzt aber auch dafür, dass trotz aller Faszination sie mich hin und wieder drängte, den schönen Dingen außerhalb der wissenschaftlichen Enklave Beachtung zu schenken.

TABLE OF CONTENT

SUMMARY	1
1. INTRODUCTION	2
1.1. The ubiquitin-conjugating system	2
1.1.1. A hierarchical enzymatic cascade controls the ubiquitylation of substrates	2
1.1.2. The ubiquitylation machinery recognizes specific degradation signals	4
1.1.3. E3 ligases determine the substrate specificity	5
1.1.4. The mode of ubiquitylation dictates the fate of the conjugated protein	7
1.2. The 26S proteasome	10
1.2.1. Multiubiquitylated substrates are degraded in a coordinated manner	10
1.2.2. Several ubiquitin receptors are implicated in substrate targeting	11
1.2.3. Non-conventional functions: the proteasome is implicated in processing	12
1.3. Specialized pathway: ER-associated degradation (ERAD)	13
1.3.1. Substrate recognition differs between luminal and membrane proteins	13
1.3.2. The identity of the protein channel involved in ER protein dislocation	14
1.3.3. ERAD occurs by a specific subset of E2/E3 enzymes	15
1.4 Other proteolytic factors within the ubiquitin-proteasome system	17
1.4.1. The Cdc48 ^{Ufd1/Npl4} complex untethers ubiquitylated proteins from non-modified partners	17
1.4.2. Cdc48/p97 cooperates with SNAREs in homotypic membrane fusion	18
1.5. Aim of this work	21
2. RESULTS	22
2.1. The fatty acid desaturase Ole1 is a substrate of ERAD	22
2.1.1. Ole1 is a naturally short-lived protein	22
2.1.2. The half-life of Ole1 is modulated by unsaturated fatty acids	23
2.1.3. Turnover of Ole1 proceeds via ERAD	26
2.2. Ubiquitin-binding factors implicated in ERAD	27
2.2.1. Requirement of the Cdc48 ^{Ufd1/Npl4} chaperone in degradation of Ole1	27
2.2.2. Accumulation of stabilized Ole1 at the membrane	29
2.2.3. General role of the Cdc48 ^{Ufd1/Npl4} complex in ERAD	30
2.2.4. Involvement of other ubiquitin-binding factors in ERAD	31
2.3. Proteolytic regulation of the ER SNARE Ufe1	34
2.3.1. Ufe1 is ubiquitylated in WT cells	34
2.3.2. The SM protein Sly1 controls the stability of Ufe1	36
2.3.3. Ufe1 stability is directly linked to interaction with Sly1	37
2.3.4. Sly1-unengaged Ufe1 is degraded by the ubiquitin/proteasome system	41

2.3.2. Function of the Sly1-dependent regulation of Ufe1 stability	43
2.3.2.1. Lack of Ufe1 regulation impairs viability	43
2.3.2.2. Ufe1 competes with Sed5 for Sly1 interaction	45
2.3.2.3. Sly1 interacts genetically and physically with Cdc48 and Shp1	46
3. DISCUSSION	49
3.1. Novel components of the ERAD pathway	49
3.1.1. The Cdc48 ^{Ufd1/Npl4} complex promotes the relocation of ERAD substrates	49
3.1.2. Ubiquitin-binding proteins escort ERAD substrates to proteasomes	50
3.1.2.1. The role of the multiubiquitylation enzyme (E4) Ufd2 in ERAD	50
3.1.2.2. Alternate soluble ubiquitin receptors mediate proteasome targeting	52
3.2. Novel substrates of ERAD	54
3.2.1. Regulation of the fatty acid desaturase Ole1	54
3.2.1.1. Ole1 is a naturally short-lived protein and ERAD substrate	54
3.2.1.2. Ole1 turnover is regulated by unsaturated fatty acids	56
3.2.1.3. Implications of Ole1 on the fatty acid homeostasis	57
3.2.2. Regulation of the syntaxin SNARE Ufe1	57
3.2.2.1. Sly1 protects Ufe1 from degradation	58
3.2.2.2. Sly1 availability balances the cellular pool of Ufe1	60
3.2.2.3. A putative function of Sly1 in homotypic membrane fusion	61
3.2.2.4. Does Ufe1 ubiquitylation provides a link to SNARE disassembly?	62
3.3. General implication of ERAD in regulatory pathways	63
4. MATERIALS AND METHODS	64
5. REFERENCES	83
ABBREVIATIONS	95

SUMMARY

The majority of eukaryotic proteins are degraded by the ubiquitin-proteasome system. In this pathway, cytosolic substrates are first earmarked for degradation by modification with ubiquitin ('ubiquitylation') and subsequently degraded by the 26S proteasome, a large protease residing in both the cytosol and the nucleus. ER-resident proteins are similarly degraded but take the route of a specialized pathway coined ER-associated degradation (ERAD). In order to reach the cytosolic ubiquitin/proteasome system, these substrates must first relocate from the ER to the cytosol, possibly with the help of protein conducting membrane channels. Previous work has shown that specific ubiquitin-conjugating enzymes (e.g. Ubc6, Ubc7) and ubiquitin ligases (e.g. Hrd1) contribute to ERAD, but how the substrates reach the proteasome remained to be clarified. Besides its function as a quality control system in recognizing and eliminating aberrant proteins, ERAD appears also to play a part in regulatory pathways.

This study focuses on the identification of novel components contributing to ERAD. It could be demonstrated that the yeast protein Cdc48 (p97 in mammals), together with its co-factors Ufd1 and Npl4, plays a key role in this process. Cdc48 belongs to the large family of AAA-type ATPases and is believed to function as a chaperone-like enzyme. Previous work has shown that the Cdc48 complex specifically acts on ubiquitylated substrates. This study indicates that the Cdc48 complex takes part in mobilization of ERAD substrates from the ER membrane for proteasomal targeting. Furthermore, degradation of some ERAD substrates involves the multiubiquitylation factor E4/Ufd2 and proteasome targeting factors of the Rad23 protein family.

Another aspect of this work addresses the regulatory functions of ERAD. The fatty acid desaturase Ole1, an integral membrane protein of the ER, was identified as a novel ERAD substrate. Intriguingly, ERAD of Ole1 is specifically regulated since the protein is particularly short lived in the presence of high levels of unsaturated fatty acids, the products of Ole1. Thus, this feedback loop provides an additional mechanism, by which the cell regulates the amount of unsaturated fatty acids. The t-SNARE (syntaxin) protein Ufe1 was characterized as another substrate of ERAD. This protein is required for homotypic membrane fusion of ER vesicles. Notably, Ufe1 degradation is negatively controlled by its binding partner Sly1, a member of the SM (Sec1/Munc18) protein family. Reciprocal mutations in the Ufe1-Sly1 interaction face result in rapid degradation of Ufe1 by ERAD. Conversely, strong overproduction of Ufe1 was found to be detrimental for cellular growth. These findings suggest that one important function of Sly1 is to control Ufe1 SNARE levels in order to ensure cellular homeostasis. In conclusion, analysis of the degradation of Ole1 and Ufe1 revealed an important contribution of ERAD to essential regulatory pathways.

1. INTRODUCTION

To ensure a dynamic state, cells have to provide regulatory mechanisms to adapt their functional state to intracellular requirements and environmental changes. This can be accomplished on one hand by altering gene expression, thereby turning on the synthesis of a different subset of proteins that execute distinct functions. On the other hand, every regulated process needs to become inactivated after it has fulfilled its function. At the protein level, this can be achieved by modulating the activity of proteins or, ultimately, by degrading them. Thus, in order to act efficiently in this regulatory process intracellular protein degradation must be highly selective.

Cellular proteases often recognize their target proteins directly by a specific amino acid sequence located close to the cleavage site ('primary signal'). However, this type of proteolysis is less suited to mediate the down regulation of a broad spectrum of substrates. In fact, this task is executed by a specialized system evolved in all eukaryotes that segregates substrate recognition from degradation and proceeds in a two-step reaction: Substrates are recognized on the basis of a primary signal by the ubiquitin-conjugating system that subsequently tags the target protein by the addition of the small protein ubiquitin ('secondary signal'). Once modified by several ubiquitin moieties, the earmarked protein is targeted to the 26S proteasome independently of their primary sequence. This large multi-subunit protease complex harbors a number of different proteolytic active sites in a high local concentration within a gated chamber. Thus, this specific molecular architecture provides high efficiency through processive peptide hydrolysis while it prevents unwarranted degradation by sequestering the active sites within the cavity (Pickart and Cohen, 2004). How substrate recognition and degradation particularly are accomplished will be discussed in the following chapters.

1.1. The ubiquitin-conjugating system

1.1.1. A hierarchical enzymatic cascade controls the ubiquitylation of substrates

Ubiquitin is a small, heat-stable protein with a globular, robust fold and is highly conserved within all eukaryotes. In *Saccharomyces cerevisiae* ubiquitin is encoded by a gene family. All members of this family encode for fusions of two or more proteins that become post-translationally processed. The genes *UBI1*, *UBI2* and *UBI3* provide most of the ubiquitin for vegetative growth, and their gene products all include small carboxyl extension proteins, which are found in their matured form as ribosomal subunit proteins (Finley *et al.*, 1989). Cellular stress induces the expression of the multiubiquitin gene

UBI4 that encodes five tandemly repeated copies of the ubiquitin coding sequence (Finley *et al.*, 1987). Therefore, ubiquitylation generally requires the proteolytic processing of the carboxy terminus from the ubiquitin precursors, yielding the mature form of a peptide of 76 amino acids that ends with a double glycine residue motif (Pickart, 2001).

Processed ubiquitin is conjugated to proteins via a reversible isopeptide linkage between its C-terminal glycine residue and a lysine chain of the target protein. This modification requires the subsequent action of three classes of enzymes. The first step requires the ubiquitin-activating enzyme (E1), which catalyzes the formation of a ubiquitin-adenylate intermediate through ATP hydrolysis. The ubiquitin-AMP intermediate is subsequently transferred to a conserved cysteine residue within the E1 enzyme yielding a stable E1-ubiquitin thioester (McGrath *et al.*, 1991). In all eukaryotes the E1 enzyme is encoded by one essential gene (in *S. cerevisiae* *UBA1*, ubiquitin activating enzyme 1) (Pickart, 2001). In a second step, activated ubiquitin is passed by transesterification to a cysteine residue of a ubiquitin conjugating enzyme (UBC or E2), which binds specifically to the ubiquitin-loaded E1 molecule. In *S. cerevisiae* there exist 13 different UBC proteins sharing a conserved core domain of about 150 amino acids. They all conjugate either ubiquitin, or the ubiquitin-like proteins SUMO (Ubc9), or RUB1 (Ubc12), respectively (Jentsch, 1992; Johnson, E. S. and Blobel, 1997; Liakopoulos *et al.*, 1998; Schwarz *et al.*, 1998). *In vitro* the transfer of ubiquitin to substrates can sometimes be carried out directly by the E2 enzyme, but *in vivo* this reaction is in most cases

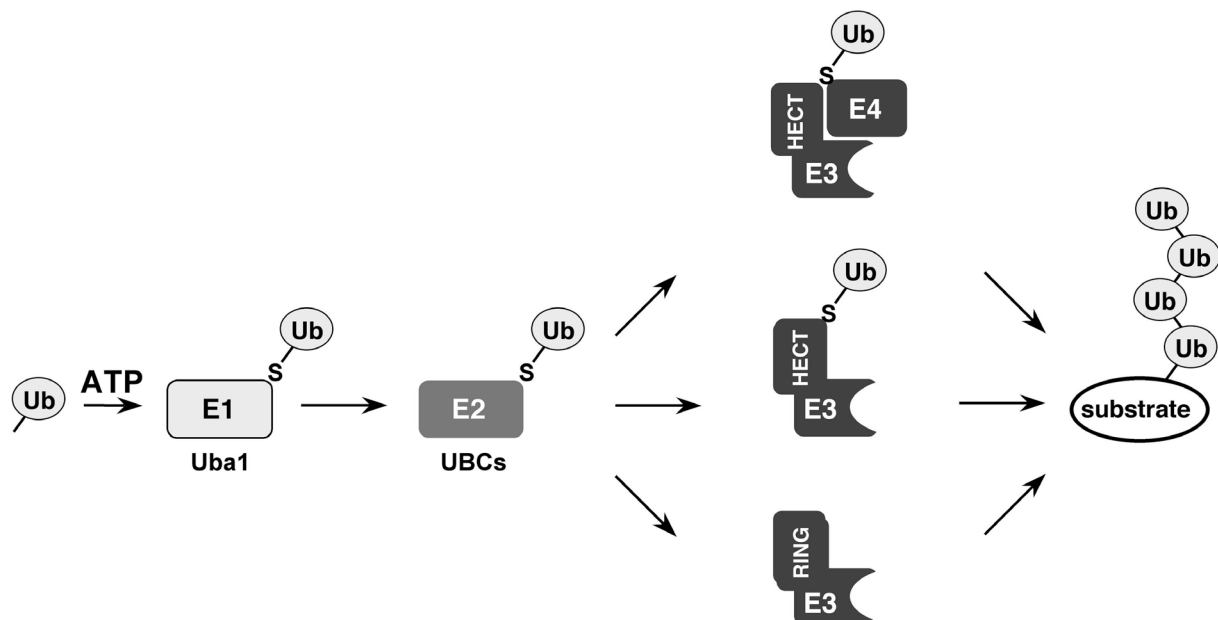


Figure 1-1: The enzymatic thioester cascade of the ubiquitin conjugation system. Ubiquitin is activated by Uba1 (E1) and then passed to several UBCs (E2s). Ubiquitylation of substrates occurs usually in conjunction with ubiquitin ligases (E3s), which are most responsible for substrate specificity. Some multiubiquitylation reactions may require an additional factor (E4). See text for details.

accomplished in conjunction with another class of enzymes, called ubiquitin ligases (E3). This group of enzymes recognizes both the target protein and the E2-ubiquitin-thioester, thereby mediating the transfer of ubiquitin to a lysine ϵ -amino group of the substrate. The transfer occurs either directly from the E2 to the substrate in the case of so-called RING finger E3s, or includes the formation of an E3-ubiquitin thioester intermediate analogous to the UBCs, when catalyzed by members of HECT E3 ligase family, (see 1.1.3.) (Pickart, 2001). Once conjugated by this enzymatic cascade ubiquitin itself is often targeted for further ubiquitylation reactions by using one of its internal lysine residues for modification, often by employing the same E2 and E3 constituents of the preceding reaction. However, in some cases, an additional factor (E4) is required, which functions as a multiubiquitylation factor in conjunction with the common ubiquitylation machinery (Koegl *et al.*, 1999; Imai *et al.*, 2002; Hoppe *et al.*, 2004). Successive conjugating reactions result in the formation of a multiubiquitin chain on the substrate and are a prerequisite for the successful targeting to the 26S proteasome.

Besides ubiquitin, there exist several ubiquitin-like (UBL) proteins. Although they show only a weak sequence homology to ubiquitin, they share a similar three-dimensional protein fold. Likewise, SUMO (small ubiquitin modifier) and RUB1 (related to ubiquitin) are also attached to substrates by an analogous conjugation machinery. However, modification by these UBLs does not result in targeting to the 26S proteasome but fulfills rather a function in regulating the interaction of the substrates with other proteins (for a review see Jentsch and Pyrowolakis, 2000).

1.1.2. The ubiquitylation machinery recognizes specific degradation signals

The selectivity of the ubiquitylation reaction is ensured by the specific recognition of a degradation signal within the target protein. All degradation signals consist at least of two distinct parts: a recognition motif for the E2/E3 enzymes (ubiquitylation or primary signal) and one or more appropriate lysine residue(s), at which ubiquitin moieties can be conjugated (ubiquitylation site).

The recognition motif or degron can be located within the polypeptide in a sequence- or structure-confined manner mediating the constitutive turnover of the target protein (Laney and Hochstrasser, 1999). Degradation of such substrates depends therefore primarily on the presence and activity of the E3. An example for this type of recognition is the C-terminal domain (CTD) of the large subunit of yeast RNA polymerase II. The CTD contains the heptapeptide repeat sequence SPTSPSY, which is necessary and sufficient for ubiquitylation (Huibregtse *et al.*, 1997). Conversely, substrates may be only degraded after they have been targeted through post-translational

modification mediated by a specific signal transduction cascade. This regulatory mechanism allows coordinating protein degradation with specific cellular events (e.g. cell cycle progression) and is found for instance in polypeptides containing the PEST (proline-, aspartate-, serine- and threonine-rich) sequence that directs phosphorylation and subsequent degradation of various proteins (Rogers *et al.*, 1986). Alternatively, the recognition motif of a substrate may be masked by its binding to a partner protein. Upon the dissociation of the partner, the degron becomes solvent-exposed and is recognized by its cognate E3. This situation is found for the yeast transcription factor $\alpha 2$ that is only stable when another transcription factor, **a1**, is bound to the hydrophobic Deg1 sequence of $\alpha 2$ (Chen, P. *et al.*, 1993). Similarly, a hydrophobic stretch being naturally buried within the protein core might be recognized as degradation signal after it has become exposed, e.g. under denaturing conditions or after misfolding of the protein. Recognition of these non-native structures might be generally implemented in protein quality control and may explain how aberrant proteins are specifically recognized and degraded (Laney and Hochstrasser, 1999).

1.1.3. E3 ligases determine the substrate specificity

Among the different cellular UBCs involved in ubiquitylation, only Ubc3 (Cdc34) is essential for viability in *S. cerevisiae*. However, the other UBCs do not simply represent isoenzymes with redundant functions. In contrast, the disparate phenotypes of the corresponding UBC mutants demonstrate, that they are involved in different cellular processes. However, substrate specificity is still predominantly mediated by the large class of E3 enzymes being directly involved in recognition of and binding to the degradation motif of the individual substrate.

E3 enzymes have a modular composition that can be divided into a variable substrate recognition domain and into a conserved catalytic domain that consists of either a HECT or a RING finger motif. Although unrelated in sequence or structure, both catalytic modules recognize similarly their cognate E2-ubiquitin partners, while they differ considerably in the mechanism of the conjugation reaction (Pickart, 2001).

All members of the HECT (homologous to E6-AP carboxy terminus) E3 family include a C-terminal ~350 amino acid catalytic domain with a conserved cysteine, which undergoes a thioester intermediate with ubiquitin during the conjugation mechanism. The founding member of this class, the human E6-AP (E6 associated protein), promotes in conjunction with the viral protein E6 the degradation of the tumor suppressor p53 (Huibregtse *et al.*, 1995; Scheffner *et al.*, 1995). In all HECT family members, the N-terminal region is responsible for the specific interaction with substrates and includes specific protein-protein interaction motifs. One well-characterized HECT E3 is the yeast

Rsp5 enzyme, which is essential for viability and involved in several pathways. Rsp5 contains three WW domains that are known to bind to phosphoserines and phosphothreonines. According to this finding, some substrates of Rsp5 (e.g. plasma membrane receptors) have been shown to be degraded in a phosphorylation-dependent manner (Pickart, 2001). Other motifs recognized by WW domains are proline-rich sequences. This type of recognition signal is found for example in the transcription factors Spt23 and Mga2, which both display a (P)PXY motif and are ubiquitylated by Rsp5 (Hoppe *et al.*, 2000; Shcherbik *et al.*, 2004).

The other class of ubiquitin ligases is characterized by a RING (really interesting new gene) finger motif that encompasses a series of histidine and cysteine residues being involved in the coordination of two zinc ions. In contrast to the HECT domain the RING finger does not form a thioester with ubiquitin. Instead it serves as a molecular scaffold for the specific and catalytically productive binding of the E2 enzyme (Pickart, 2001).

Several RING finger proteins are part of multi-subunit E3s (Feldman *et al.*, 1997; Skowrya *et al.*, 1997), in which the demands for the recognition of a broad substrate spectrum are addressed by the use of different exchangeable modular adaptors. The

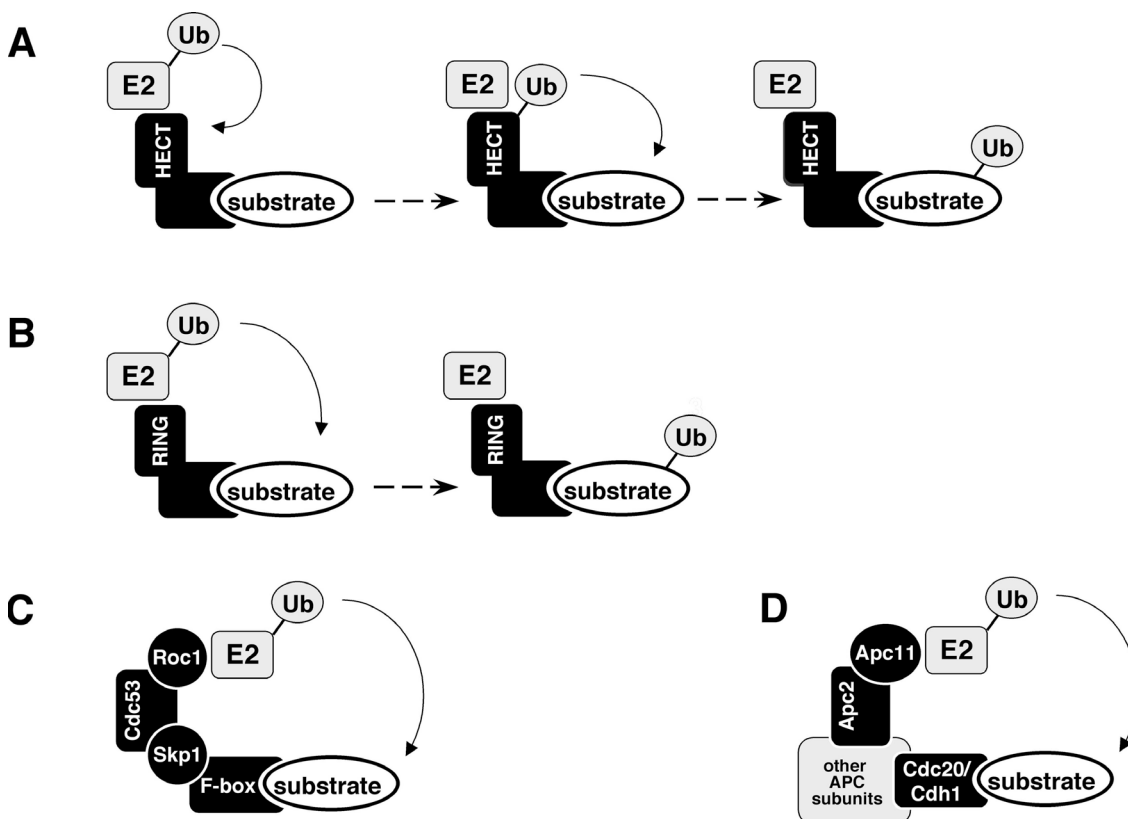


Figure 1-2: Ubiquitin transfer by HECT and RING finger ubiquitin ligases.

A. HECT ligase. **B.** Monomeric RING finger ligase. **C** and **D** multimeric RING finger ligases: SCF complex (C), APC/C complex (D). See text for details.

most prominent members are the SCF (Skp1-Cul1-E-box) and the APC/C (anaphase promoting complex/cyclosome) complex. Both comprise a central scaffold subunit belonging to the cullin family. In the SCF complex, the cullin Cul1 (Cdc53 in yeast) binds with its C-terminus to the RING finger protein Roc1 (Rbx1 or Hrt1) and with its N-terminus to Skp1, which serves as an adaptor for different substrate recruitment factors called F-box proteins. Similarly, the APC/C includes the cullin-related protein Apc2, the RING finger protein (Apc11) and one of the exchangeable substrate recruitment factors Cdc20 and Hct1. Besides these basal components, further subunits are enclosed in the APC/C, whose functions mostly remain to be clarified (Petroski and Deshaies, 2005). A common feature of nearly all multi-subunit RING E3s is that they recognize and ubiquitylate their substrates in a regulated fashion. Post-translational modifications of substrates, like phosphorylation, operate as molecular switches and direct the substrates to their cognate recruitment factors like the various F-box proteins in case of the SCF complex (Petroski and Deshaies, 2005).

1.1.4. The mode of ubiquitylation dictates the fate of the conjugated protein

So far the best understood function of ubiquitin is its role in substrate targeting for proteasome-dependent degradation by the attachment of a multiubiquitin chain. However, meanwhile it became evident that ubiquitylation provides besides its proteolytic property further 'non-conventional' functions, indicating a general role in cellular protein targeting. Remarkably, its different functions can be mechanistically discriminated by the mode of how ubiquitin is attached to the target protein: whether the substrate is modified by a single (mono-ubiquitylation) or by several moieties (multiubiquitylation), and aside which internal lysine residue is used for chain formation. The outcome of the modification differs considerably in terms of signaling. A multiubiquitin chain is structurally not recognized as a multiplied signal of a single ubiquitin molecule but represents an entirely different signal and chains linked differently by the use of distinct lysine residues even alter remarkably in their structure (Pickart, 2001).

Multiubiquitylation can proceed by different lysine linkages. Among ubiquitin's 7 lysine residues, only K48 is essential for viability (Finley *et al.*, 1994), and a single K48-linked multiubiquitin chain is sufficient to target a substrate to proteasomes (Chau *et al.*, 1989). This indicates that the K48 chain linkage represents the 'canonical' signal for proteasome-dependent proteolysis. However, apart from K48-linked chains other multiubiquitin chains have been observed. K29-linked chains seem also to be involved in proteasome targeting even though it is not yet clear whether they are only involved in chain initiation while further chain extension is conducted by a switch to K48-linkage (Koegele *et al.*, 1999; Saeki *et al.*, 2004). Similarly, K11-linked chains can signal protea-

somal degradation *in vitro*, nevertheless a specific *in vivo* function has not been addressed so far (Baboshina and Haas, 1996). Conversely, substrates being modified by K6-linked chains are directed to proteasomes but not degraded, and this modification has been implicated in DNA repair (Morris, J. R. and Solomon, 2004; Nishikawa *et al.*, 2004). Likewise, ubiquitin chains linked by K63 (the most abundant chains after K48 linkage) provide entirely non-proteolytic functions. They are known to signal in different pathways like DNA damage tolerance, the inflammatory response, protein trafficking, and ribosomal protein synthesis (Pickart and Fushman, 2004). For instance, upon DNA damage, the polymerase processivity factor PCNA (proliferating cell nuclear antigen) that serves as a molecular scaffold for other factors, can selectively be modified either by mono- or K63-linked multiubiquitin, thereby recruiting different translesion polymerases (Hoegge *et al.*, 2002). Similarly, K63-linked chains on TRAF6 are directly implicated in the recruitment of competent signaling complexes during the NF- κ B signal transduction pathway, which in turn leads to the phosphorylation and activation of the $\text{I}\kappa\text{B}\alpha$ kinase (IKK) and thereby to the degradation of the NF- κ B inhibitory subunit $\text{I}\kappa\text{B}\alpha$ (Deng *et al.*, 2000; Wang, C. *et al.*, 2001).

Besides multiubiquitylation mono-ubiquitylation provides also distinct regulatory non-proteasomal targeting functions. This type of modification is implicated in diverse cellular pathways as DNA damage (as mentioned before for PCNA), chromatin modification, transcription or endocytosis.

Histone 2A (H2A) was the first substrate discovered to be ubiquitylated, but the function of these modification was mysterious for long time, since it does not influence the H2A stability (Goldknopf and Busch, 1977). Meanwhile, other histone proteins (H1, H2B, H3 and the histone variant H2A.Z) were found to be similarly mono-ubiquitylated. Ubiquitylation of H2B requires *in vitro* and *in vivo* the E2 Ubc2/Rad6 (Jentsch *et al.*, 1987; Robzyk *et al.*, 2000) and is a prerequisite for methylation of H3 at K4, which is required for the establishment of silent chromatin at telomeres (Sun and Allis, 2002). This observation led to the assumption that modification by ubiquitin contributes aside other post-translational modifications to the 'histone code' (Jenuwein and Allis, 2001). The outcome of histone ubiquitylation might result in an altered structure of histones either directly, or indirectly by the subsequent recruitment of other modifying enzymes, controlling thereby the transcriptionally active state of chromatin (Osley, 2004).

Besides its contribution to the general chromatin status through histone modification, mono-ubiquitylation influences as well the transcriptional activity of some transcription factors. In *S. cerevisiae* the heterologous transcription factor VP16 is only active after mono-ubiquitylation by the SCF^{MET30} E3 ligase (Salghetti *et al.*, 2001). Likewise, the yeast transcription factor Spt23 exists after its mobilization as a mono-ubiquitylated protein (see 1.3.1.) (Hoppe *et al.*, 2000). These observations raised the idea, that mono-

ubiquitylation is involved in 'licensing' of certain transcription factors, which might be necessary to recruit other co-factors to DNA at the promoter. However, the contribution of ubiquitylation to transcriptional activation might be more complex. Indeed, in some cases also a requirement for proteasomal activity or a recruitment of proteasomal sub-particles to active promoters have been reported (Gonzalez, F. *et al.*, 2002; Morris, M. C. *et al.*, 2003). Interestingly, most of the unstable transcription factors studied so far show a sequence overlap between their transcriptional activation domain (TAD) and the degradation signal (Salghetti *et al.*, 2000), and recently an E3 ligase activity has been observed to associate with RNA polymerase (Brower *et al.*, 2002). These intriguing findings give rise to the 'suicidal model', in which a transcription activation signal resembles to a degradation signal, thereby restricting the activity of a transcription factor to a short time window (Muratani and Tansey, 2003).

Finally, the function of mono-ubiquitylation has been comprehensively studied in receptor-mediated endocytosis and lysosomal targeting. In yeast several plasma-membrane-bound receptors are mono-ubiquitylated by the E3 ligase Rsp5 at their cytoplasmic tails. Mono-ubiquitylation has been shown to induce the internalization of these receptors (Hicke and Dunn, 2003). This modification is subsequently recognized by the so-called UIM (ubiquitin-interacting motif) sequence present in several members of the intracellular endocytotic apparatus (Hofmann and Falquet, 2001; Shih *et al.*, 2002). After sorting into early endosomes, the ubiquitylated receptors are incorporated into lysosomes and after invagination of the membranes into multi-vesicular bodies (MVBs), degraded by lysosomal proteases. Notably, targeting of ubiquitylated proteins into the MVBs requires also the sequential recognition of the ubiquitin moiety by three 'endosomal complexes required for transport' (ESCRT-I-III) (Katzmann *et al.*, 2001; Babst *et al.*, 2002a; Babst *et al.*, 2002b). Interestingly, this pathway is also endured for sorting from the trans-Golgi network directly to the vacuole; however, for this route rather multi-ubiquitylation seems to be the sorting signal, which is mediated by Rsp5 in conjunction with two other factors, Bul1 and Bul2 (Helliwell *et al.*, 2001).

In conclusion, ubiquitylation generally represents a targeting or recruitment signal mediating protein-protein interaction. Like phosphorylation, this modification is reversible by the action of de-ubiquitylation enzymes, thereby ensuring that only appropriately conjugated proteins meet their targets. The fate of ubiquitin-conjugates depends primarily on the mode of ubiquitylation. Whereas mono-ubiquitylation is preferentially involved in trafficking or sorting, multiubiquitylation (with the exception of K63- and K6-linked chains) usually targets conjugates to proteasomal proteolysis. However, as observed for instance for transcription factors, both types of modifications together might be combined, resulting in a complex regulatory system.

1.2. The 26S proteasome

1.2.1. Multiubiquitylated substrates are degraded in a coordinated manner

Multiubiquitylated proteins are targeted to 26S proteasomes that are present in the cytosol and the nucleus of every eukaryote. This multi-subunit, self-compartmentalized protease comprises a 20S core complex bearing different, rather non-specific proteolytic sites within its cavity, and two axial 19S regulatory caps (Pickart and Cohen, 2004).

The barrel-like core particle consists of a stack of 4 rings each composed of 7 homologous subunits: two central identical β -rings and two distal identical α rings (Groll *et al.*, 1997). Although α and β -subunits are sequence-related, only the β -ring harbors the proteolytic sites encoded by three different β -subunit genes (in total 6 proteolytic sites per core particle). The α -subunits are implicated in forming the gate with their α -specific N-terminal extensions, thereby restricting the access to the proteolytic chamber (Groll *et al.*, 2000). In absence of the 19S regulatory particle the entry to the interior chamber is closed.

The 19S regulatory complex includes at least 17 different subunits and is assembled from two main subcomplexes: the base that contains 6 ATPase (Rpt1-6) forming a hexameric ring plus 2 non-ATPase subunits (Rpn1-2), and the lid that sits on top of the base and bears 8 non-ATPase subunits (Rpn2-9) (Pickart and Cohen, 2004). The Rpn10 subunit is localized to the base-lid interface and contributes to the stable lid association with the base (Glickman *et al.*, 1998). The individual subunits provide different functions: recognition of the ubiquitin conjugates, which is accomplished most probably by several ubiquitin receptors; substrate unfolding by ATPase subunits of the base; substrate translocation into the pore by opening the channel, which is controlled by the ATPase Rpt2; recycling of the conjugated ubiquitin moieties by de-ubiquitylation

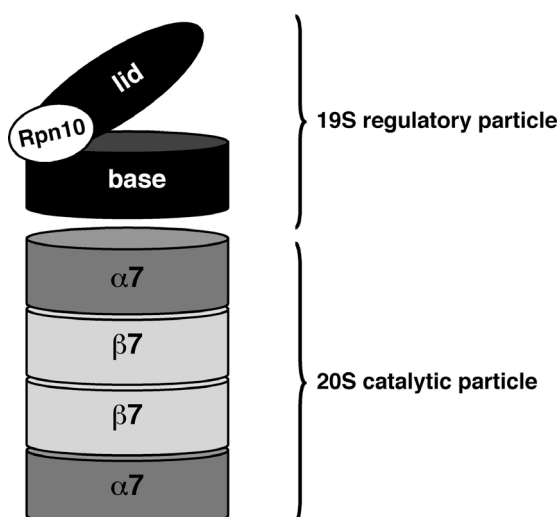


Figure 1-3: The 26S proteasome.

The 26S proteasome consists of the 20S catalytic particle and the 19S regulatory particle. The 20S particle harbors the proteolytic sites within a central cavity formed by 4 stacked rings of 7 α and β subunits each. The 19S particle can be further subdivided into base and lid. The lid is comprised of non-ATPase (Rpn) subunits and is involved in de-ubiquitylation of the multiubiquitin chain. The base mediates unfolding of substrates and pore opening through its ATPase (Rpt) subunits. In addition the base is implicated in recognition of multiubiquitylated substrates. The protein Rpn10 binds to both the lid and the base and promotes their stable association. Apart from this function, Rpn10 serves as a soluble ubiquitin receptor.

of the substrate executed by the lid subunit Rpn11 (other de-ubiquitylating enzymes that associate with the proteasome may assist to this process) (Pickart and Cohen, 2004). Polypeptides inserted into the central cavity are digested usually into peptides of a length ranging from 3 to 22 amino acids (Kisselev *et al.*, 1999).

Most notably, the different functions of the 26S proteasome are apparently coordinated (Pickart and Cohen, 2004): substrate unfolding seems to be preceded by a successful engagement with a loosely folded region of the substrate (which follows the weak and reversible tethering of the multiubiquitin chain) and is itself a prerequisite for translocation into the chamber. Likewise, de-ubiquitylation by Rpn11 that cleaves only at the one ubiquitin moiety proximal to the substrate is strictly ATP-dependent and does not occur before substrate unfolding. This observation suggests that upon engagement and unfolding, the multiubiquitylated substrate is moved into a fixed position required for successful processing of the ubiquitin chain. Even though ubiquitin itself can be principally unfolded and degraded by the 26S proteasome, this process occurs extremely slowly due to ubiquitin's extraordinary stable fold, indicating that de-ubiquitylation also provides a regulatory function during the substrate translocation into the proteolytic cavity.

1.2.2. Several ubiquitin receptors are implicated in substrate targeting

Substrates modified by 4 ubiquitin moieties are efficiently targeted to the 26S proteasome (Thrower *et al.*, 2000). However, the question of which of the individual subunits recognize the multiubiquitin signal has long been under debate. Rpn10 (S5a in metazoans) has been proposed as a proteasomal ubiquitin receptor since it contains a UIM (ubiquitin interacting motif), and the non-assembled subunit shows high affinity to multiubiquitin chains (Deveraux *et al.*, 1994; Hofmann and Falquet, 2001). Nonetheless, the deletion of *RPN10* is not lethal in yeast and displays only mild defects on protein turnover (van Nocker *et al.*, 1996). Moreover, as part of proteasomes Rpn10 has not been found to be associated with multiubiquitin chains (Lam *et al.*, 2002). Thus, it is unlikely that Rpn10 represents the sole receptor for multiubiquitin. The yeast proteins Rad23 and Dsk2 comprise also a specific recognition motif for ubiquitin conjugates, the UBA (ubiquitin associated) domain (Hofmann and Falquet, 2001; Wilkinson, C. R. *et al.*, 2001). Additionally, they display a UBL (ubiquitin-like) motif that mediates their association with proteasomes (Schauber *et al.*, 1998; Kim *et al.*, 2004). Although Rad23 and Dsk2 are non-essential proteins and present in proteasomes markedly below stoichiometric amounts (Schauber *et al.*, 1998; Verma *et al.*, 2004), mutants of Rad23 lacking the UBL domain indeed display synthetic defects with $\Delta rpn10$, suggesting that both types of receptors function in a redundant manner in proteasome targeting

(Lambertson *et al.*, 2003). However, the recent discovery of the strong association of the ATPase subunit Rpt5 (mammalian S6') with multiubiquitin chains when bound to proteasomes implied that this candidate actually represents the primary receptor for ubiquitin conjugates (Lam *et al.*, 2002). Nonetheless, whether Rpt5 works in conjunction with the other ubiquitin receptors or rather independently has still to be determined.

1.2.3. Non-conventional functions: the proteasome is implicated in processing

Substrates are usually proteolyzed within the central cavity into small fragments that are small enough to exit the proteasome through its narrow ports. But surprisingly, some ubiquitin-conjugates have been found to be only partially degraded by the 26S proteasome. This process, referred to as regulated ubiquitin/proteasome-dependent processing (RUP), was first discovered for the heterodimeric transcription factor NF- κ B. One of its two subunits is translated as an inactive precursor protein (p105) and ubiquitin-proteasome-dependent degradation of its C-terminal domain is required to convert p105 into its mature form p50 (Fan and Maniatis, 1991; Palombella *et al.*, 1994). Remarkably, two distant relatives of NF- κ B p105, the yeast transcription factor Spt23 and Mga2, are similarly processed (Hoppe *et al.*, 2000). They are synthesized *in vivo* as membrane-bound precursors (p120) that are anchored by their C-terminus in the ER-membrane. Activation requires their processing by the 26S proteasome yielding a soluble N-terminal fragment (p90), which is subsequently translocated into the nucleus. This raised the intriguing question of how protein domains are spared from proteasomal degradation.

Notably, within the Rel homology domain residing in the N-terminus of p105, a highly stable region was discovered that prevents complete proteolysis (Lin, L. and Kobayashi, 2003). A structurally related motif, the IPT (Ig-like/plexin/transcription factor) domain was found in Spt23 and Mga2, which seems to be equally important for regulated processing (Rape *et al.*, 2001; Rape and Jentsch, 2004). Since the N-terminus of NF- κ B and Spt23/Mga2 is left intact while the C-terminus especially in the case of the membrane-bound transcription factors is not accessible, it was concluded that degradation has to initiate from an internal, loosely folded polypeptide loop that could be easily unfolded and transferred into the central proteasome cavity. Based on this assumption degradation would proceed until the proteasome would reach those regions that resist unfolding due to tightly folded domains. Segments beyond these barriers would then be not degraded but released from the proteasome (Rape and Jentsch, 2004).

1.3. Specialized pathway: ER-associated degradation (ERAD)

Since all components of the ubiquitin-proteasome system reside in the cytosol and/or the nucleus, proteins from other compartments destined for proteasomal proteolysis have to be re-translocated prior to their degradation. The endoplasmic reticulum (ER) forms a specialized compartment for protein folding and maturation and about 20% of the human genes have been predicted to encode for secretory proteins (Lander *et al.*, 2001). Due to the high protein content, misfolding of singular proteins or failures in the assembly of multiprotein complexes ultimately provokes the formation of toxic protein aggregates within the ER lumen. To avoid this situation, two quality control systems exist in the ER, which cooperate with each other: Hydrophobic patches of misfolded proteins are immediately sensed by the unfolded protein response (UPR). Activation of the UPR results in the transcriptional upregulation of specific proteins that increase the biosynthetic capacity of the ER (e.g. ER-resident chaperones). Concomitantly, aberrant proteins are specifically recognized, exported to the cytoplasm and subsequently degraded by the ubiquitin/proteasome system. The last process has been referred to as ER-associated degradation (ERAD) (Ellgaard and Helenius, 2003; Ahner and Brodsky, 2004). Interestingly, yeast cells can tolerate impairments of one of the two control systems under normal growth conditions, however, mutants defective in both are inviable (Friedlander *et al.*, 2000).

1.3.1. Substrate recognition differs between luminal and membrane proteins

Luminal and integrative membrane substrates of ERAD were initially thought not to differ significantly in the way they are degraded - with one exception: the recognition of aberrant soluble proteins takes exclusively place within the ER lumen. Thus, luminal substrate recognition has to specifically address this circumstance. Whereas E2 enzymes involved in ERAD (see 1.3.3.) are almost entirely cytosolic, some membrane spanning E3 enzymes face partially the ER lumen, supplying a potential contribution to substrate recognition (Hampton, 2002). Nonetheless, additional factors play important roles in recognition of abnormal proteins in the ER lumen. The Hsp70 chaperone BiP (Kar2 in yeast) binds to hydrophobic stretches and regulates together with its Hsp40 co-chaperones the binding and release of aggregation-prone misfolded proteins. Mutants of those chaperones are actually impaired in degradation (Ahner and Brodsky, 2004). Another mechanism of protein surveillance is provided by monitoring the retention time of secretory proteins within the ER compartment. In higher eukaryotes, prolonged retention of immature glycoproteins by calnexin and calreticulin results in trimming of mannose residues and enables another lectin, EDEM, to bind to and target the trimmed glycoprotein for degradation. A similar cycle seems to exist also for *S. cerevisiae* (Ahner

and Brodsky, 2004). Surprisingly, some soluble substrates apparently are first transported to the Golgi and subsequently retrieved to the ER prior to their degradation (Caldwell *et al.*, 2001; Vashist *et al.*, 2001).

Conversely, substrate recognition and degradation of several ER-membrane proteins do not rely on luminal chaperones. Instead, these substrates require the cytoplasmic Hsp70 Ssa1. In addition, E3 ligases seem to be primarily implicated in substrate recognition, at least for ER-membrane proteins that expose their aberrant domains to the cytosolic side (Ahner and Brodsky, 2004).

1.3.2. The identity of the protein channel involved in ER protein dislocation

To become accessible to the cytoplasmic degradation machinery, luminal proteins have to be entirely translocated into the cytosol, whereas ER-membrane proteins have at least to be extracted out of the membrane. Export of both types of ER proteins is believed to occur by an aqueous channel, by which substrates are able to overcome the hydrophobic barrier of the ER membrane. Genetic and biochemical data suggested that the Sec61 ER import channel is also involved in the dislocation process (Wiertz *et al.*, 1996; Pilon *et al.*, 1997; Plemper *et al.*, 1997; Zhou and Schekman, 1999). This translocation channel also provides the ability of lateral opening, which would facilitate not only the direct insertion of polytopic integral membrane proteins into the lipid bilayer membrane, but also their extraction out of it (Menetret *et al.*, 2000). However, considering the fact that this channel would have to operate in a bidirectional manner, a specific regulation has to be presumed. Additionally, some ERAD substrates are still glycosylated after translocation (Blom *et al.*, 2004) and therefore it was concluded that any channel involved in retrograde transport has to impart a pore size large enough to allow the passage of glycosylated proteins (Hirsch *et al.*, 2004).

Class I MHC molecules have been shown to be degraded by ERAD in human cytomegalus virus (CMV)-infected cells. Recently, a polytopic ER protein, Derlin-1, was found to interact with class I MHC molecules during their dislocation process. Interestingly, Derlin-1 is also found in association with the CMV encoded protein US11 that specifically targets class I MHC for ERAD (Lilley and Ploegh, 2004; Ye *et al.*, 2004). Based on this observation, it was hypothesized that Derlin-1 constitutes a pore for protein export. However, MHC-class I turnover induced by another CMV encoded protein, US2, does not rely on Derlin-1 (Lilley and Ploegh, 2004). Moreover, the yeast homolog of Derlin-1, Der1, has been shown to be involved only in the turnover of some luminal ER proteins (Knop *et al.*, 1996; Vashist *et al.*, 2001; Taxis *et al.*, 2003) and some membrane spanning substrates that specifically dispose their aberrant domain towards the ER lumen (Vashist and Ng, 2004). These findings make it rather unlikely that Derlin-1

and Der1 are exclusively required for substrate dislocation. Likewise, any direct data demonstrating that these proteins form a pore still are lacking, which leaves the question about the identity of the protein conducting channel open.

Finally, the question of how retrograde transport through the pore occurs mechanically remains just as elusive. Import into the ER requires energy that is provided either during co-translational translocation by the ribosomal translation machinery or during post-translational translocation by ATP consumption of the ER-resident HSP70 chaperones Kar2 and Lhs1 through several rounds of substrate binding on the luminal side (Wilkinson, B. M. *et al.*, 1997). Thus the post-translational import mechanism might operate according to the 'Brownian ratchet' model, by which a randomly for- and backward slipping is converted into a vectorial motion (Neupert and Brunner, 2002). In analogy, the attachment of ubiquitin moieties to a partially translocated substrate was shown to be a prerequisite for retrotranslocation, possibly by preventing the polypeptide from slipping back into the ER (Biederer *et al.*, 1997). Alternatively, retrotranslocation might involve also an active pulling force. Some of the energy is most likely supplied by the ATP-depending processes of peptide unfolding and hydrolysis taken place at and within the proteasome. Most notably, a direct involvement of the 26S proteasome in membrane extraction of an integral membrane protein could be demonstrated (Mayer *et al.*, 1998). However, the question whether the proteasome activity is sufficient for the removal of ERAD substrates has been remained unanswered.

1.3.3. ERAD occurs by a specific subset of E2/E3 enzymes

Aberrant proteins emerging at the cytosolic site of the ER membrane are ubiquitylated by E2 and E3 enzymes specifically adapted for this task. UBC6 and UBC7 represent the prototypes of UBCs involved in ERAD (Sommer and Jentsch, 1993; Biederer *et al.*, 1996). Both are tethered to the ER membrane either by a single transmembrane domain (Ubc6) or by binding to the anchor protein Cue1 (Ubc7) (Biederer *et al.*, 1997), suggesting that a direct localization of these enzymes is a prerequisite for ERAD. However, for some ERAD substrates, also a participation of the cytosolic E2 Ubc1 has been demonstrated (Friedlander *et al.*, 2000; Bays *et al.*, 2001). How it is recruited to the ER membrane remained obscure.

Two specific ERAD E3 ligases have been identified in *S. cerevisiae*. Both are RING finger type E3s and integrated into the membrane by several transmembrane segments. Degradation of several integral membrane proteins like Hmg2 (3-hydroxy-3-methylglutaryl coenzyme A reductase) is controlled by an ubiquitin-ligase complex that consists of the polytopic RING protein Hrd1 and the single membrane span protein

Hrd3. The luminal domain of Hrd3 is assumed to function in substrate sensing as well as in regulation of the cytosolic Hrd1 E3 ligase activity by a transmembrane signaling, which is mechanistically so far not understood (Bays *et al.*, 2001; Gardner *et al.*, 2001a). The substrate spectrum of the HRD complex is obviously not restricted to membrane proteins, since a luminal substrate has been shown to be degraded in a Hrd1-dependent manner as well (Friedlander *et al.*, 2000). However, some known ERAD substrates are not recognized by Hrd1/Hrd3, and recently another ER-resident multi-spanning ubiquitin ligase, Doa10, was identified (Swanson *et al.*, 2001). Interestingly, mutants that are deficient for both, Hrd1 and Doa10, are more sensitive towards ER stress and display a more elevated UPR than the respective single mutants, suggesting overlapping functions (Friedlander *et al.*, 2000).

How substrate recognition is mediated by these ubiquitin ligases could be already partially addressed. The HRD complex seems to be able to discriminate between distinct folding states of its substrates. In particular, Hmg2 that acts in the mevalonate pathway is regulatory degraded by a negative feedback mechanism. High levels of the mevalonate pathway intermediate farnesyl pyrophosphate (FPP) directly stimulate Hmg2 ubiquitylation and degradation. Remarkably, degradation requires the membrane spans of Hmg2, suggesting that the signal for degradation derives directly from the membrane. Therefore the so-called 'structural transition model' has been proposed, by which presence of FPP somehow alters the structure of Hmg2 thereby inducing a deg-

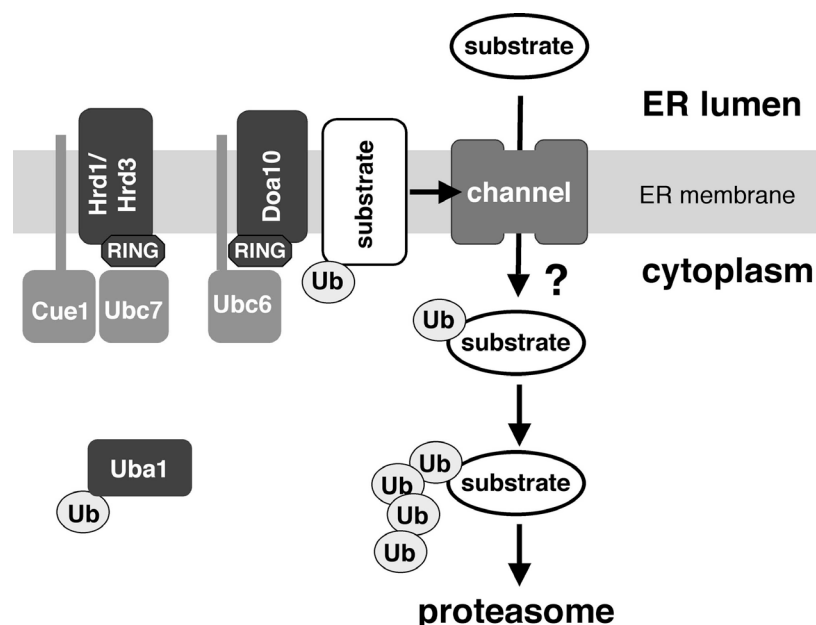


Figure 1-4. The ubiquitin conjugation system during ERAD.

Whereas luminal substrates are supposed to be ubiquitylated as they emerge at the cytosolic site, membrane proteins might be modified even before they have completed their dislocation. Ubiquitylation is largely mediated by the membrane-associated UBCs Ubc6 and Ubc7, which work in conjunction with different E3s as the RING finger ubiquitin ligases Hrd1 or Doa10. Other factors like Hrd3 may also contribute by influencing the substrate specificity or by regulating the ligase activity.

radiation signal recognized by the HRD complex (structural transition model) (Hampton, 2002). Such a quality control sensing mechanism could be principally envisaged also for other substrates of the HRD complex, although the specific recognition motif within Hrd1 or Hrd3 has not been isolated so far.

Conversely, Doa10 appears to contain distinct protein-protein interaction motifs, by which substrate recognition could occur. For instance it displays a putative WW motif. In consistence with this finding, Ubc6 that is itself an ERAD substrate and contains a PPxY motif is degraded in dependence on Doa10 (Swanson *et al.*, 2001). However, Doa10 seems to provide also further determinants, as other substrates are discerned by a different recognition motif. For instance, Doa10 recognizes the Deg1 signal derived from the yeast $\alpha 2$ transcription factor and degrades variants bearing this degron. Remarkably, Deg1 comprises an amphiphatic helix that possibly participates in coiled-coil structures and Doa10 displays at its very N-terminus a short stretch predicted to undergo coiled-coil interactions (Swanson *et al.*, 2001).

1.4 Other proteolytic factors within the ubiquitin-proteasome system

Various genetic screens identified additional factors that are involved in ubiquitin-dependent proteolysis or sorting, but surprisingly they neither belong to the E1/E2/E3 ubiquitin-conjugating system nor they are components of the proteasome. A great number of these factors displays the property to recognize ubiquitylated substrates, suggesting that they might function downstream of ubiquitin conjugation prior to proteasomal degradation or signaling. Among them are several so-called UFD proteins (ubiquitin-fusion-degradation) that were originally isolated in a screen searching for mutants stabilizing a short-lived artificial ubiquitin-protein fusion (Johnson, E. S. *et al.*, 1995; Ghislain *et al.*, 1996): The E4 Ufd2 exhibits a role in multiubiquitylation of oligo-ubiquitylated substrates (Koegl *et al.*, 1999), whereas Ufd1 was later found to function in conjunction with Npl4 as a substrate recruitment factor for ubiquitylated proteins in the oligomeric Cdc48^{Ufd1/Npl4} complex (Meyer *et al.*, 2000; Hitchcock *et al.*, 2001; Rape *et al.*, 2001).

1.4.1. The Cdc48^{Ufd1/Npl4} complex untethers ubiquitylated proteins from non-modified partners

Cdc48 (p97 in mammals) was originally identified by a screen for mutants with cell cycle defects (cell division cycle). It belongs to the family of AAA-type ATPases (ATPase associated with different cellular activities) and forms a homohexameric ring that possesses chaperone-like activity (Zhang *et al.*, 2000; DeLaBarre and Brunger, 2003). Like other members of the large AAA family Cdc48 contains an N-terminal protein-

protein interaction domain and two copies of the AAA-ATPase domain (Walker *et al.*, 1982). Upon concerted ATP hydrolysis, Cdc48 undergoes a rotational conformation change, thereby converting chemical bond energy into physical force (Rouiller *et al.*, 2002). Its N-terminal domain serves to recruit discrete adaptor proteins that are assumed to specify its function. Combined with the adaptor p47, mammalian p97 is involved in membrane fusion (Kondo *et al.*, 1997; Dreveny *et al.*, 2004). In contrast, recruitment of the heterodimeric adapter Ufd1-Npl4 was assumed to direct p97 to ubiquitin-dependent proteolysis although its role in this pathway was initially not clear (Meyer *et al.*, 2000).

Insight into the molecular function of the Cdc48^{Ufd1/Npl4} complex was obtained by the study on the regulation of the yeast transcription factors Spt23 and Mga2. Both transcription factors function within a regulon called the OLE pathway that controls the synthesis of unsaturated fatty acids by regulating the expression of the fatty acid desaturase Ole1 (Hoppe *et al.*, 2000). Spt23 and Mga2 are tethered to the ER membrane by a single membrane span and form homo- or heterodimers. To become functionally active, they have to be processed into the active p90 form by the 26S proteasome (see 1.2.3). Processed p90 is still tethered to its non-cleaved p120 partner protein and needs to become mobilized for its complete activation. Biochemical and genetic studies converged to demonstrate that this step is accomplished by the chaperone-like complex Cdc48^{Ufd1/Npl4}. The chaperone recognizes Spt23 preferentially in its ubiquitylated form and untethers processed p90 from the ER membrane in dependence of ATP (Rape *et al.*, 2001). Interestingly, consistently with the observed function, the Ufd1/Npl4 dimer as well as Cdc48 itself show a general preference for binding to ubiquitin, and thus the Cdc48^{Ufd1/Npl4} complex might act on other ubiquitylated proteins so segregate them from non-modified proteins (Rape *et al.*, 2001; Meyer *et al.*, 2002).

1.4.2. Cdc48/p97 cooperates with SNAREs in homotypic membrane fusion

Whereas Cdc48/p97 in conjunction with Ufd1/Npl4 has been linked to ubiquitin-dependent proteolysis, p97 in complex with p47 was presumed to function ubiquitin-independent in membrane fusion processes (Latterich *et al.*, 1995; Kondo *et al.*, 1997; Hetzer *et al.*, 2001).

Membrane fusion has been suggested to operate by a mechanism following the SNARE hypothesis (Sollner *et al.*, 1993; Rothman, 1994): SNARE (α SNAP receptor) proteins are anchored on the opposing membranes of vesicles, which are about to fuse, and form energetically favorable tetrahelical coiled-coil bundles through intermolecular interactions of their SNARE domains. The SNARE assembly works like a molecular zipper (*trans*-SNARE complex formation) that brings the membranes into close proximity

and promotes thereby fusion. After fusion, the SNARE proteins are found in a highly stable *cis*-SNARE complex present on the newly formed membrane. Their recycling requires the ATP-consuming segregation by the AAA-ATPase NSF (N-ethylmaleimide-sensitive factor), which is recruited to the *cis*-SNARE complex via its co-factor α SNAP (soluble NSNF-attachment protein). In yeast, the disassembly of SNARE complexes is mediated by Sec18 and Sec17, respectively.

Whereas most membrane fusion processes rely exclusively on NSF, homotypic membrane fusion of ER and Golgi vesicles requires (in addition) p97, which is actually highly homologous to NSF, and has therefore been proposed to function by a similar mechanism. Together with p47, p97 mediates the reassembly of mitotic Golgi fragments (Kondo *et al.*, 1997). p47 contributes apparently by recruiting p97 to the SNARE syntaxin 5, and by modulating the ATPase activity of p97 (Meyer *et al.*, 1998; Rabouille *et al.*, 1998). Likewise, Cdc48 has been reported to mediate homotypic membrane fusion of ER vesicles by binding to the syntaxin homolog Ufe1, most probably also in combination with an adaptor protein (Latterich *et al.*, 1995; Patel, S. K. *et al.*, 1998). In yeast, a protein with considerable homology to p47, Shp1, has been identified and proposed to function similarly to p47 (Kondo *et al.*, 1997).

While p47 was initially supposed to function analogous to α SNAP (Rabouille *et al.*, 1998), it was recently shown that p47 and its putative yeast homolog Shp1 bind specifically to ubiquitin and ubiquitin-conjugates (Meyer *et al.*, 2002; Hartmann-Petersen *et al.*, 2004; Schuberth *et al.*, 2004). Moreover, cycles of ubiquitylation and de-ubiquitylation are required for mitotic Golgi reassembly, although the target has not been identified (Wang, Y. *et al.*, 2004). Thus, it might be possible that either a regulatory factor or SNARE proteins themselves are targeted by ubiquitylation, thereby regulating either the assembly or disassembly of SNAREs. Remarkably, the syntaxin Ufe1 was recently reported to be linked to ubiquitylation-dependent regulation (Lin, A. *et al.*, 2001). Thus, ubiquitin recognition and binding seems to be conserved throughout the cellular functions of the different p97/Cdc48 complexes.

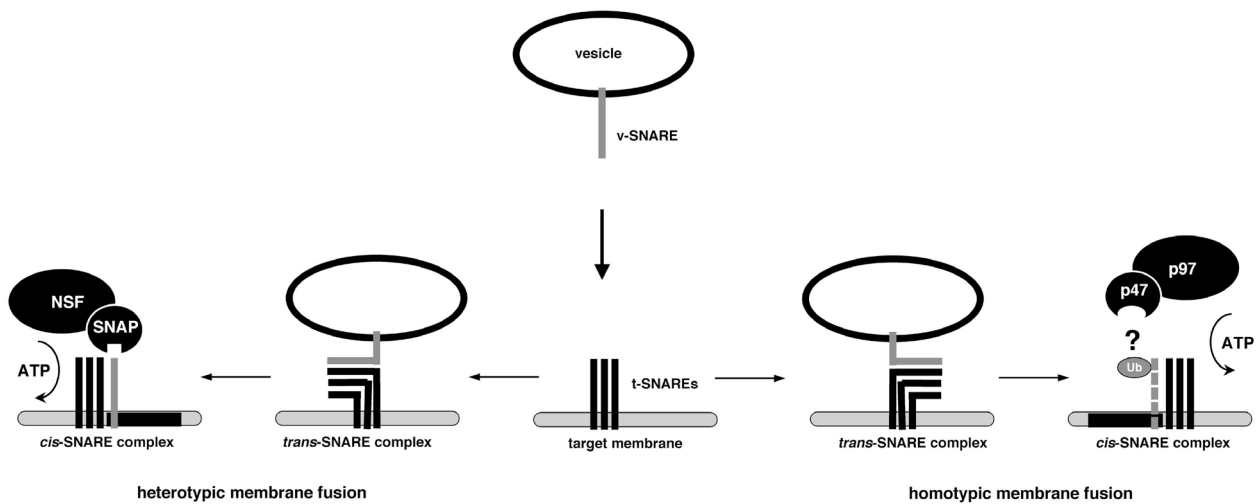


Figure 1-5: SNARE-mediated membrane fusion.

Membrane-anchored SNARE proteins of opposing vesicles (v, vesicle; t, target membrane) form ternary helical bundles by their SNARE domains resulting in a stable *trans*-SNARE complex. This brings the membranes in close proximity and enables them to fuse. To allow new rounds of SNARE assemblies, the *cis*-SNARE complex on the newly formed membrane has to be disassembled by a AAA ATPase under ATP consumption. In case of heterotypic membrane fusion disassembly is promoted in mammals by NSF, which is recruited to SNAREs via α SNAP. In case of homotypic membrane fusion of Golgi or ER vesicles, this process is mediated by p97 in conjunction with p47. SNARE molecules might be directly recognized by p47. However, due to the ability of p47 to bind to ubiquitin-conjugates, SNARE recruitment might probably be also regulated through SNARE ubiquitylation acting as a recruitment signal and/or degradation signal.

1.5. Aim of this work

This study focuses on the identification of novel components in the ERAD pathway and the investigation of its regulatory role in the turnover of newly identified ERAD substrates.

Whereas previous work has addressed the means of substrate recognition and ubiquitylation, the mechanisms how substrates are relocated from the ER and targeted to the 26S proteasome are still elusive. The scope of this study is the investigation of proteolytic factors having been recently isolated as ubiquitin-binding proteins with respect to a possible contribution to ERAD. Particularly the potential function of the recently identified ubiquitin-selective chaperone Cdc48^{Ufd1/Npl4} will be addressed (Rape *et al.*, 2001).

To date ERAD has been thought to be involved primarily in quality control; however, recent findings anticipate an additional role in regulatory functions. Thus, another aspect of this work is the identification of novel native (i.e. not abnormally folded) substrates of ERAD and to study the regulated degradation of these ER proteins with respect to the mechanisms and physiological functions. Among putative substrates, the Δ -9 fatty acid desaturase Ole1 is a likely candidate to be a short-lived protein due to the tight transcriptional control of the *OLE1* gene by the OLE pathway (Hoppe *et al.*, 2000). Moreover, the negative feedback regulation by unsaturated fatty acids at the expression level of *OLE1* assumes that Ole1 may be also regulated at the protein level (McDonough *et al.*, 1992; Gonzalez, C. I. and Martin, 1996; Hoppe *et al.*, 2000; Rape *et al.*, 2001). Another candidate to be analyzed is the syntaxin homolog Ufe1 that resides in the ER membrane. This SNARE protein is involved in homotypic membrane fusion, which is mediated by the assistance of the AAA-type ATPase Cdc48 that physically and genetically interacts with Ufe1 (Latterich *et al.*, 1995; Patel, S. K. *et al.*, 1998). The recent finding that Ufe1 becomes unstable in a conditional mutant of the kinase Pkc1 (Lin, A. *et al.*, 2001) suggests that the half-life of Ufe1 may also be regulated by ERAD.

2. RESULTS

2.1. The fatty acid desaturase Ole1 is a substrate of ERAD

The Δ -9 fatty acid desaturase Ole1 is a polytopic integral membrane protein of the ER with its catalytic center facing the cytosol. It catalyzes the conversion of saturated into unsaturated fatty acids (UFAs) at the ER membrane and thereby determines UFA levels within the yeast cell. The abundance of the essential Ole1 enzyme is controlled by a regulon, coined the OLE pathway. This pathway is uniquely controlled by the ubiquitin-proteasome system and requires a two-step mechanism for its activation: a cleavage of the ER-membrane-bound transcription factors Spt23 and Mga2 achieved by the 26S proteasome, and the mobilization of the processed transcription factors by the chaperone-like complex Cdc48^{Ufd1/Npl4} (Hoppe *et al.*, 2000; Rape *et al.*, 2001). Activation by this mechanism enables the active transcription factor to localize to the nucleus and drive the expression of the *OLE1* gene. Over- and underexpression of *OLE1* is toxic for yeast cells. Intriguingly, the OLE pathway is regulated by a negative feedback mechanism by UFAs at different levels, i.e. the processing of the precursor transcription factors, the *OLE1* transcription and the *OLE1* mRNA half-life (McDonough *et al.*, 1992; Choi *et al.*, 1996; Gonzalez, C. I. and Martin, 1996; Hoppe *et al.*, 2000). Thus, in order to respond appropriately to these multiple regulatory loops Ole1 would have to be a short-lived protein.

2.1.1. Ole1 is a naturally short-lived protein

To test this hypothesis epitope-tagged ^{3myc}*OLE1* was expressed in WT yeast cells from an extra copy, stably integrated into the genome under the control of the *GAL1-10* promoter. This ensures that *OLE1* expression is uncoupled from the OLE pathway and independent of the fatty acid-regulated *OLE1* mRNA decay that requires the 5'UTR of *OLE1*. Furthermore, expression from such a heterologous system allows promoter shut-off experiments since the *GAL1-10* promoter is only active in the presence of galactose but repressed upon addition of glucose to the medium. In combination with the translational inhibitor cycloheximide any *de novo* protein synthesis is efficiently blocked. This permits to study exclusively the turnover of the protein. By following protein levels ^{3myc}Ole1 was indeed found to be short-lived *in vivo* under normal growth conditions (Figure 2-1A, left panel). To rule out the possibility that the short half-life is caused by altered UFA levels upon the heterologous expression of *OLE1*, a similar experiment was conducted with an enzymatically inactive mutant of Ole1. To generate this mutant, two conserved essential histidine residues in the desaturase domain (Shanklin *et al.*, 1994) were exchanged to alanine residues by site-directed mutagenesis (Figure 2-1B).

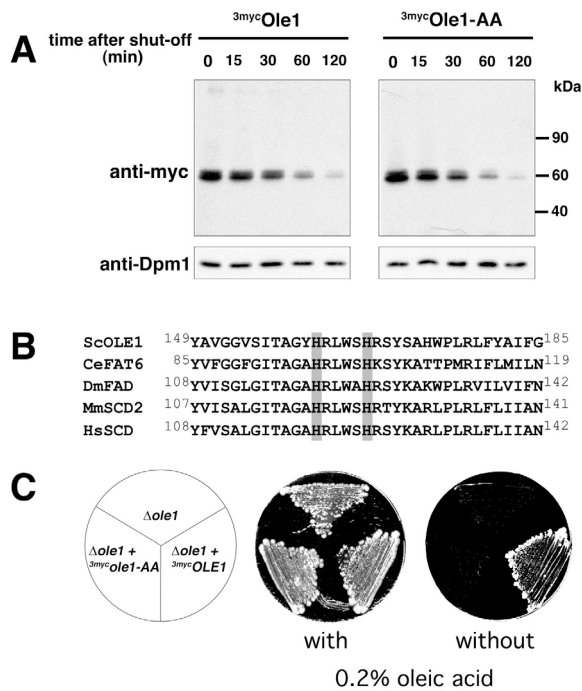


Figure 2-1. OLE1 is a short-lived *in vivo*.

(A) Expression shut-off experiments with WT cells co-expressing $3mycOLE1$ and the mutant variant $3mycole1-AA$ under the control of the *GAL1-10* promoter. Cells were grown in YPGal to an OD_{600} of 0.5 at 23°C and shifted for another 2 hours to 37°C. The experiment was started by adding glucose and cycloheximide to the medium. At each time point indicated, the cellular level of both epitope-tagged Ole1 variants was analyzed by anti-myc immunoblots (upper panel). As a control, the blots were reprobed with an antibody against the stable ER-membrane protein dolichol phosphate mannose synthase, Dpm1 (lower panel). (B) Sequence comparison of $\Delta 9$ -fatty acid-desaturases from different organisms (Sc, *Saccharomyces cerevisiae*; Ce, *Caenorhabditis elegans*; Dm, *Drosophila melanogaster*; Mm, *Mus musculus*; Hs, *Homo sapiens*). The two conserved His residues, which were replaced by Ala residues in the mutant *ole1-AA* variant, are shaded in gray. (C) Growth of the $\Delta ole1$ deletion strain expressing either none, $3mycOLE1$, or

mutant $3mycole1-AA$ in presence and absence of oleic acid, respectively. The lethal phenotype of $\Delta ole1$ in absence of unsaturated fatty acids in the growth medium can only be suppressed by expressing the functional desaturase.

The inability of the $3mycOle1-AA$ variant to produce UFAs in yeast cells was assessed by expressing this mutant in a $\Delta ole1$ strain, which is only viable in the presence of oleic acid in the medium. Whereas expression of WT epitope-tagged $3mycOle1$ suppresses the lethal phenotype of the $\Delta ole1$ deletion, the mutant protein $3mycOle1-AA$ did not show complementation in the absence of oleic acid (Figure 2-1C). Albeit the mutation renders this protein enzymatically inactive the half-life of $3mycOle1-AA$ was not altered when compared with WT $3mycOle1$ in a promoter shut-off experiment (Figure 2-1A, right panel). Thus, the short half-life is an intrinsic property of the Ole1 protein and seems to be essential to provide a tight regulation of UFA availability upon the needs of the cell.

2.1.2. The half-life of Ole1 is modulated by unsaturated fatty acids

The strict regulation of the cellular amount of fatty acid pools requires several levels of regulation (e.g. transcription factor processing, *OLE1* transcription, mRNA decay). Therefore it was tempting to assume that Ole1 turnover might also be subject to a negative feedback mechanism. To investigate whether UFAs influence the half-life of Ole1, promoter shut-off experiments were performed with the physiological inactive $3mycOle1-AA$ variant in the absence and presence of palmitoleic acid (16:1) or oleic acid (18:1), respectively, both being natural endproducts of the desaturase reaction (Figure 2-2A). Whereas the half-life of $3mycOle1-AA$ is about 30 min under normal growth

conditions, it is reduced by a factor of about 0.5 in the presence of palmitoleic acid ($t_{1/2} \sim 15$ min; Figure 2-2B). Surprisingly, the presence of oleic acid did not cause a similar effect; in contrast the turnover of $^{3\text{myc}}\text{Ole1-AA}$ was even diminished under this condition ($t_{1/2} \sim 40$ min; Figure 2-2B). However, considering the different physical properties of palmitoleic and oleic acid (see below), this result might be caused by a titration effect of endogenous fatty acids. Fatty acids are usually taken up from the medium and incorporated into cellular lipid bilayer membranes. Especially high amounts of exogenous UFAs cause directly a reduction of the endogenous fatty acids in membrane phospholipids (Bossie and Martin, 1989). The lipid bilayer membrane is influenced in its physical properties directly by its fatty acid constituents. Particularly, the number of unsaturated chemical bonds and the length of the fatty acids affect both the fluidity and the thickness of the membrane. Under normal growth conditions palmitoleic acid and oleic acid together contribute equally to the cellular pool and make up already 70% of fatty

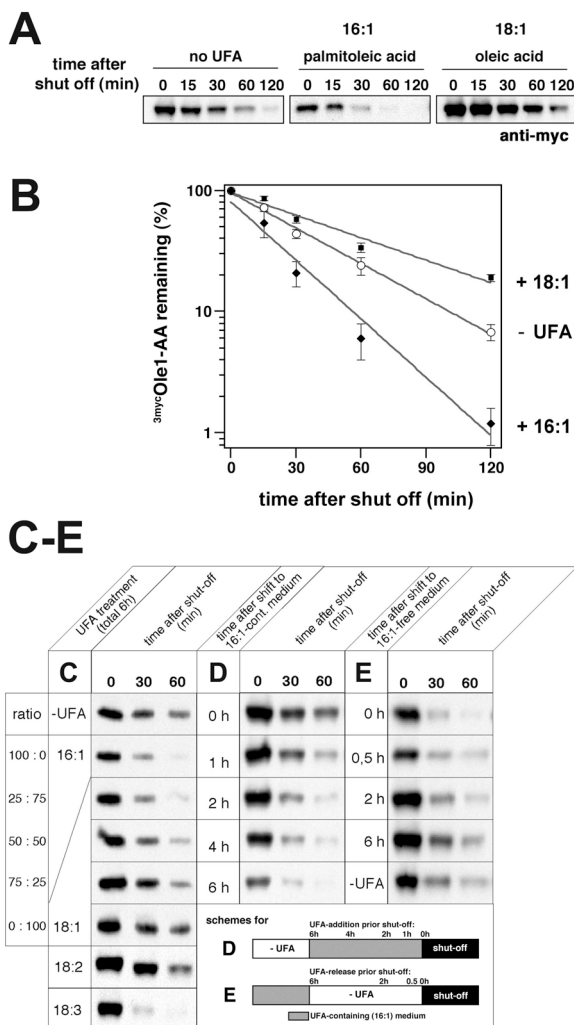


Figure 2-2. Unsat. fatty acids (UFAs) modulate the half-life of Ole1. (A) Promoter shut-off with WT cells expressing $^{3\text{myc}}\text{ole1-AA}$ in absence, or presence of 0.2% palmitoleic (16:1) or oleic acid (18:1), respectively, in the medium. (B) Quantification of the $^{3\text{myc}}\text{Ole1-AA}$ decay after promoter shut-off experiments in absence or presence of oleic acid (18:1) and palmitoleic acid (16:1). Symbols and bars represent the mean and the standard error (S.E.) of 4-5 independent experiments. (C) Promoter shut-off experiments similar to (A) but in presence of different ratios of palmitoleic acid (16:1) and oleic acid (18:1), linoleic acid (18:2) and linolenic acid (18:3). The total amount of single or combined unsaturated fatty acids in the medium (YPD) was 0.2% (D) Similar to (C) but cells were incubated for different time intervals in medium supplemented with 0.2% palmitoleic acid (16:1) before the promoter shut-off was performed. (E) Similar to (C) but cells were first incubated for several hours in medium supplemented with 0.2% palmitoleic acid (16:1) and, then transferred to UFA-free medium for different time intervals before the promoter shut-off was performed. The schemes below indicate the order and time intervals of the different UFA treatments prior to the start of the shut-off experiment in (E) and (D).

acids within the lipid bilayer membrane. Both fatty acids contain a single unsaturated bond at the same position (C-9), but differ in their carbon chain length skeleton (16 and 18 C-atoms, respectively). Interestingly, it was previously shown that the OLE pathway is stronger affected by palmitoleic acid than oleic acid (Gonzalez, C. I. and Martin, 1996; Hoppe *et al.*, 2000). Thus, the ratio between both UFAs within the membrane could be critical for the regulation of the OLE pathway.

To test the idea whether an altered ratio of UFAs influences the half-life of Ole1, promoter shut-off experiments were performed in the presence of varying concentrations of oleic and palmitoleic supplied to the growth medium. Indeed, the turnover of $^{3\text{myc}}$ Ole1-AA directly correlated with the relative amount of palmitoleic acid. The degradation of $^{3\text{myc}}$ Ole1-AA was also increased when the total amount of both fatty acids was raised (Figure 2-2C; the ratio of 50:50 of 18:1 and 16:1 resulted in a reduction of the half-life). Similarly, the number of double bonds within the fatty acid backbone correlated with an increased turnover of $^{3\text{myc}}$ Ole1-AA, as shown for linoleic acid (18:2) and linolenic acid (18:3) (Figure 2-2C, bottom lanes). In accordance with these dose-dependent effects, the half-life of $^{3\text{myc}}$ Ole1-AA was also gradually reduced when cells had been incubated in the presence of palmitoleic acid for longer time intervals before the promoter shut-off experiment was started (Figure 2-2D). Intriguingly, this effect could be steadily reversed when cells were kept in UFA-free medium for different time intervals after an initial incubation in the presence of palmitoleic acid-supplemented medium (Figure 2-2E).

Conversely, the half-life of $^{3\text{myc}}$ Ole1-AA was substantially prolonged when cells were incubated in the presence of completely saturated palmitic acid (16:0) (data not shown). Likewise, turnover of $^{3\text{myc}}$ Ole1-AA was affected in mutants deficient in the production of endogenous UFAs by a defect in the OLE pathway: Deletion mutants of *OLE1* or *SPT23* and *MGA2*, respectively, were depleted for UFAs by shifting the cells to UFA-free medium for 17 h before the $^{3\text{myc}}$ Ole1-AA turnover was examined (yeast cells tolerate depletion of endogenous UFAs without affecting viability up to 20 cell divisions).

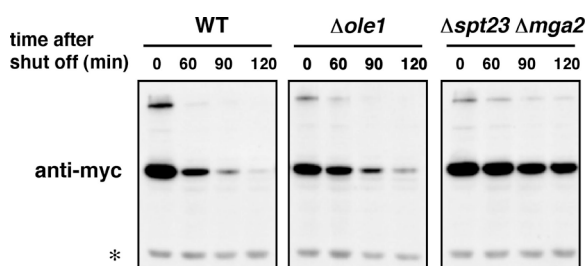


Figure 2-3. Half-life of $^{3\text{myc}}$ Ole1-AA is prolonged in cells deficient of WT OLE1. Promoter shut-off in WT, $\Delta ole1$ and $\Delta spt23 \Delta mga2$ cells expressing $^{3\text{myc}}$ ole1-AA. In order to deplete mutants defective in endogenous UFA production cells were grown for 17 h in absence of oleic acid in the medium before the promoter shut-off experiment was performed. The asterisk denotes a cross-reactive band of the anti-myc antibody.

In both deletion mutants, ^{3myc}Ole1-AA degradation was significantly slowed down (Figure 2-3). Interestingly, ^{3myc}Ole1-AA degradation was even more affected in the $\Delta spt23 \Delta mga2$ double mutant than in the $\Delta ole1$ mutant. Most notably, addition of UFAs to the medium was unable to restore the WT degradation rate of ^{3myc}Ole1-AA in the $\Delta spt23 \Delta mga2$ mutant (data not shown). These data suggest that Ole1 turnover is deregulated in cells deficient of Spt23 and Mga2 and that both transcription factors may have additional, redundant functions besides the transcriptional activation of *OLE1*, as the single mutants behaves like WT cells in respect to ^{3myc}Ole1-AA turnover (data not shown).

Taken together, UFAs display a negative feedback mechanism also on the Ole1 protein half-life. The extent of this regulation correlates on one hand reciprocally with the length of the fatty acid skeleton and the saturation of the carbon atom bonds and on the other hand directly with the relative amount of the respective fatty acid present within the lipid bilayer membrane.

2.1.3. Turnover of Ole1 proceeds via ERAD

Luminal and integral membrane proteins of the ER destined for degradation are predominantly disposed by the ER-associated degradation (ERAD) pathway. Turnover occurs by the cytosolic ubiquitin-proteasome pathway and requires the retrograde translocation of the substrate prior to its degradation. To explore whether Ole1 turnover is mediated by ERAD, several mutants deficient in ERAD were investigated. As shown in Figure 2-4, ^{3myc}Ole1-AA was substantially stabilized in a mutant strain deficient in both major ubiquitin conjugating enzymes involved in ERAD, Ubc6 and Ubc7 (Jungmann *et al.*, 1993; Sommer and Jentsch, 1993). A similar effect was observed for a deletion mutant of *CUE1* that encodes an ER-membrane anchor for Ubc7 (Biederer *et al.*, 1997). Several different E3 ligases have been reported to assist in ERAD including Hrd1, Doa10 and Rsp5 (Gardner *et al.*, 2001b; Swanson *et al.*, 2001; Haynes *et al.*, 2002), however deletion mutants of those E3 enzymes displayed only a minor or no effect on Ole1 degradation (Figure 2-4; data not shown). This implies that Ole1 down regulation may involve additional ligases. ^{3myc}Ole1-AA was significantly stabilized in a temperature-sensitive mutant of *CIM5* that encodes an essential subunit of the 19S cap of the proteasome (Ghislain *et al.*, 1993). Likewise, strong stabilization of ^{3myc}Ole1-AA was observed in *sec61-R2*, a strain carrying an allele of Sec61 that is known to exhibit strong defects in retrograde translocation of ERAD substrates (Zhou and Schekman, 1999).

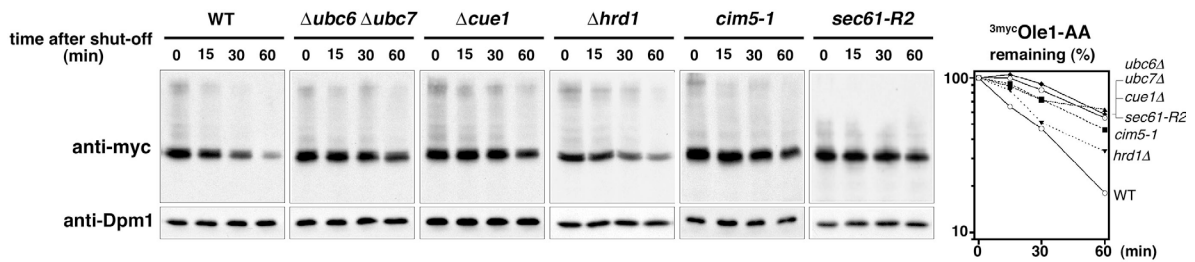


Figure 2-4. Ole1 turnover is mediated by ERAD. Expression shut-off experiments at 37°C with different ERAD mutants expressing the mutant ^{3myc}ole1-AA variant. Experimental procedures were identical to those described in Figure 2-1A. Shown are the protein levels for ^{3myc}Ole1-AA (upper panels) and as a control for Dpm1 (lower panels). The left panel shows the quantification of the ^{3myc}Ole1-AA decay.

In conclusion, these data demonstrate that Ole1 is a naturally short-lived protein, which is degraded by ERAD involving the ubiquitin-proteasome system and the Sec61 translocon. The degradation of the Ole1 protein is regulated by fatty acid pools - most probably in the immediate vicinity of Ole1 at the membrane – and executed by ERAD, emphasizing an important regulatory role for the ERAD pathway besides its function in quality control.

2.2. Ubiquitin-binding factors implicated in ERAD

2.2.1. Requirement of the Cdc48^{Ufd1/Npl4} chaperone in degradation of Ole1

ERAD substrates have to be expelled from the ER prior to their degradation. Substrates are assumed to take the route of a proteinous channel like the Sec61 translocon. However, the precise mechanism of the dislocation process has not been resolved. In particular, the means how energy for the retrograde transport is provided has remained elusive. Recently, a chaperone-like complex, designated Cdc48^{Ufd1/Npl4}, has been described to bind preferentially ubiquitin-protein conjugates (Rape *et al.*, 2001). This complex comprises the catalytic subunit Cdc48, an AAA-type ATPase, and two cofactors, Ufd1 and Npl4. It has been shown that the Cdc48^{Ufd1/Npl4} complex is essential for the OLE pathway by mediating the ATP-dependent liberation of the ubiquitylated SPT23 transcription factor from the ER membrane (Rape *et al.*, 2001). This specific property – recruitment and ATP-dependent mobilization of ubiquitin-conjugates – suspected the Cdc48^{Ufd1/Npl4} complex to be a possible candidate in promoting the retrograde transport of ERAD substrates through the ER channel.

To test the idea whether the Cdc48^{Ufd1/Npl4} complex acts as a ubiquitin-dependent chaperone at the cytosolic side for ERAD substrates, ^{3myc}OLE1-AA was expressed in the temperature-sensitive mutants *cdc48-6*, *ufd1-2* and *npl4-1* (Latterich *et al.*, 1995;

DeHoratius and Silver, 1996; Hoppe *et al.*, 2000). The degradation of $^{3\text{myc}}$ Ole1-AA was followed after the cells had been shifted to the non-permissive temperature for 3 hours. As shown in Figure 2-5A, $^{3\text{myc}}$ Ole1-AA was significantly stabilized in all three mutants. Since the Cdc48^{Ufd1/Npl4} complex is crucial for the activation of the OLE pathway, which controls the production of UFAs (Rape *et al.*, 2001), the observed stabilization of Ole1 may be caused unspecifically by a depletion of endogenous UFAs. However, a control experiment performed in the presence of oleic acid led to the same result (Figure 2-5B). These data demonstrate that the Cdc48^{Ufd1/Npl4} complex is directly involved in the degradation of the ERAD substrate Ole1.

The mammalian homolog of Cdc48, p97, is known to form at least two distinct complexes. Together with p47 it is implicated in homotypic membrane fusion (Kondo *et al.*, 1997), whereas in combination with Ufd1 and Npl4 it is involved in ubiquitin-dependent proteolysis (Meyer *et al.*, 2000). To investigate whether ERAD of Ole1 requires specifically the Cdc48^{Ufd1/Npl4} complex or whether also the alternative Cdc48/p97^{p47} complex may mediate ERAD, the yeast homolog of p47 was analyzed. The protein encoded by the putative p47 homolog, Shp1, shares 30% identical (50% similar) residues with its mammalian counterpart. Shp1 has recently been shown to interact with Cdc48 physi-

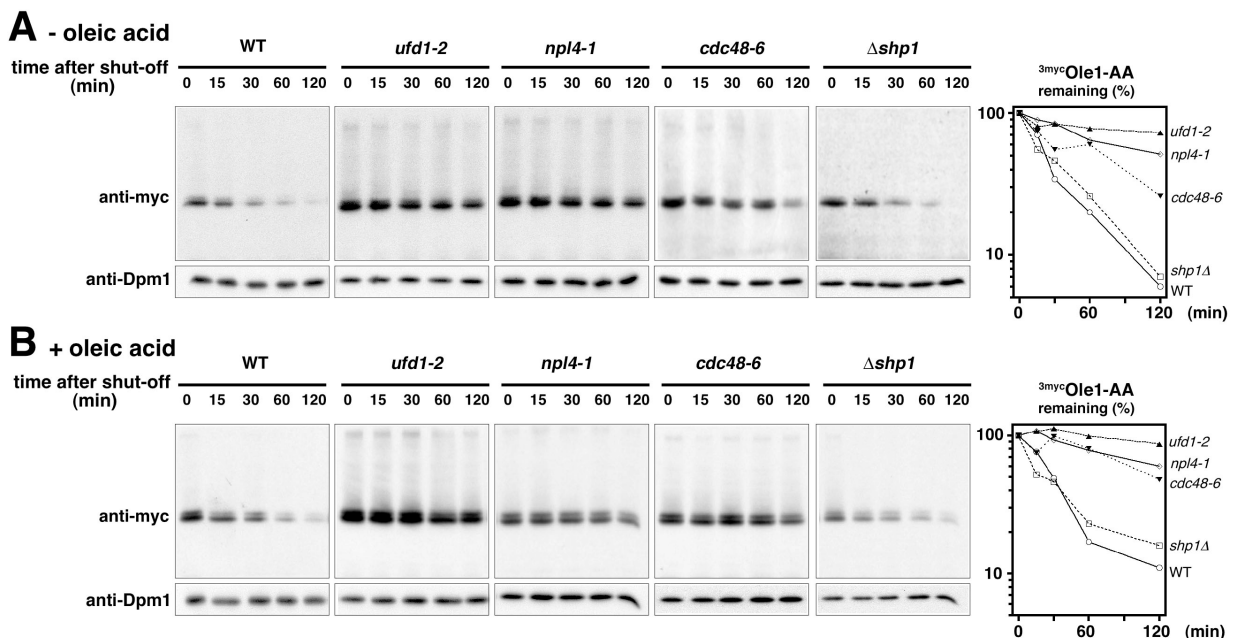


Figure 2-5. Involvement of the CDC48^{UFD1/NPL4} segregase in Ole1 degradation. (A) Expression shut-off experiments with the ts mutants *ufd1-2*, *npl4-1*, *cdc48-6* and the deletion strain Δ *shp1* expressing the mutant $^{3\text{myc}}$ *ole1-AA* variant in absence of oleic acid (at 37°C). Shown are the protein levels for $^{3\text{myc}}$ Ole1-AA (upper panels) and as a control for Dpm1 (lower panels). The left panel shows the quantification of the $^{3\text{myc}}$ Ole1-AA decay. (B) The same experiment as in (A) was performed in the presence of 0.2% oleic acid.

cally as shown by two-hybrid assays and co-immunoprecipitation experiments (Braun *et al.*, 2002), suggesting that also yeast Cdc48 is able to form two complexes, Cdc48^{Ufd1/Npl4} and Cdc48^{Shp1}. To examine whether SHP1 is involved in ERAD of Ole1, ^{3myc}Ole1-AA was expressed in a *shp1* deletion mutant and its turnover was analyzed. As shown in Figure 2-5 (A and B right panel), ^{3myc}Ole1-AA was as unstable in *shp1* mutants as in WT cells. From this data it can be concluded that ERAD of Ole1 does not involve Cdc48^{Shp1} but specifically requires the Cdc48^{Ufd1/Npl4} chaperone.

2.2.2. Accumulation of stabilized Ole1 at the membrane

Because Cdc48 as well as its adaptors Ufd1 and Npl4 bind specifically ubiquitylated proteins (Rape *et al.*, 2001; Richly *et al.*, 2005), it is conceivable that the chaperone functions downstream of the ubiquitylation event. In the case of ERAD of Ole1, the Cdc48^{Ufd1/Npl4} complex might thus be involved in the removal of Ole1 from the ER membrane. However, direct evidence for such a function of Cdc48^{Ufd1/Npl4} in the retrograde process so far was lacking. To address this particular question, cell fractionation studies were performed with extracts from *ufd1-2* cells expressing ^{3myc}Ole1-AA. As shown in Figure 2-6 (left panel) stabilized ^{3myc}Ole1-AA was detected predominantly in the microsomal pellet fraction, demonstrating that the dislocation process was not completed in this mutant. This result indicates that the activity of the Cdc48^{Ufd1/Npl4} chaperone is required at the membrane prior to proteasomal degradation of the substrate. Cdc48^{Ufd1/Npl4} might cooperate with the proteasome since it was shown in a former study that ERAD substrates accumulate at the ER membrane in mutants defective in proteasomal activity (Mayer *et al.*, 1998) Indeed ^{3myc}Ole1-AA was found to be stabilized at membranes in a mutant of *PRE1*, which encodes a subunit of the 20S proteasome core complex (Figure 2-6 right panel). This observation suggests that retrograde transport and proteasomal degradation occur in a physically and mechanistically coupled manner.

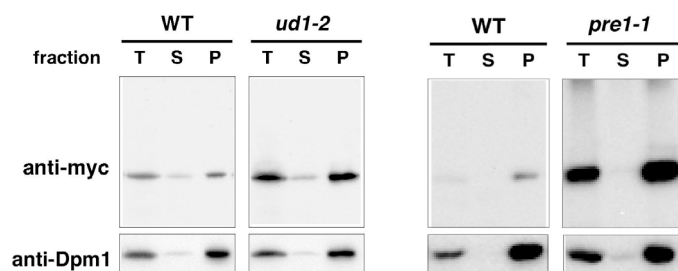


Figure 2-6. Accumulation of stabilized OLE1 at the membrane. Shut-off expression experiments were performed at 37°C with WT, *ufd1-2* and *pre1-1* cells expressing the ^{3myc}ole1-AA variant. 30 minutes after adding cycloheximide and glucose, cells were harvested and lysates subjected to cell fractionation. Equal amounts of total extract (T), soluble (S) and pellet (P) fraction were analyzed by immunoblotting with anti-myc (upper panel) and anti-Dpm1 (lower panel) antibodies.

2.2.3. General role of the Cdc48^{Ufd1/Npl4} complex in ERAD

Since Spt23 mobilization and Ole1 extraction from the membrane are both mediated by Cdc48^{Ufd1/Npl4} and in fact very similar, one may assume that they represent a unique mechanism specifically adapted for the OLE pathway. Alternatively, the Cdc48^{Ufd1/Npl4}-mediated process of recognition and mobilization of ubiquitin-conjugates may be broadly used in retrograde transport of ERAD substrates. To address this question, the turnover of several well characterized yeast ERAD substrates was investigated in mutants of the Cdc48^{Ufd1/Npl4} complex: The HMG-CoA reductase-2 (Hmg2) is a polytopic integral membrane protein being involved in sterole biogenesis and has been shown to be naturally short-lived (Hampton, 1998). ^{DEG1}Sec62^{FLAG} (DSF) is an engineered short-lived variant of the ER-membrane protein Sec62 (Mayer *et al.*, 1998), bearing the Deg1 degradation signal derived from the short-lived transcription factor MAT α 2 (Chen, P. *et*

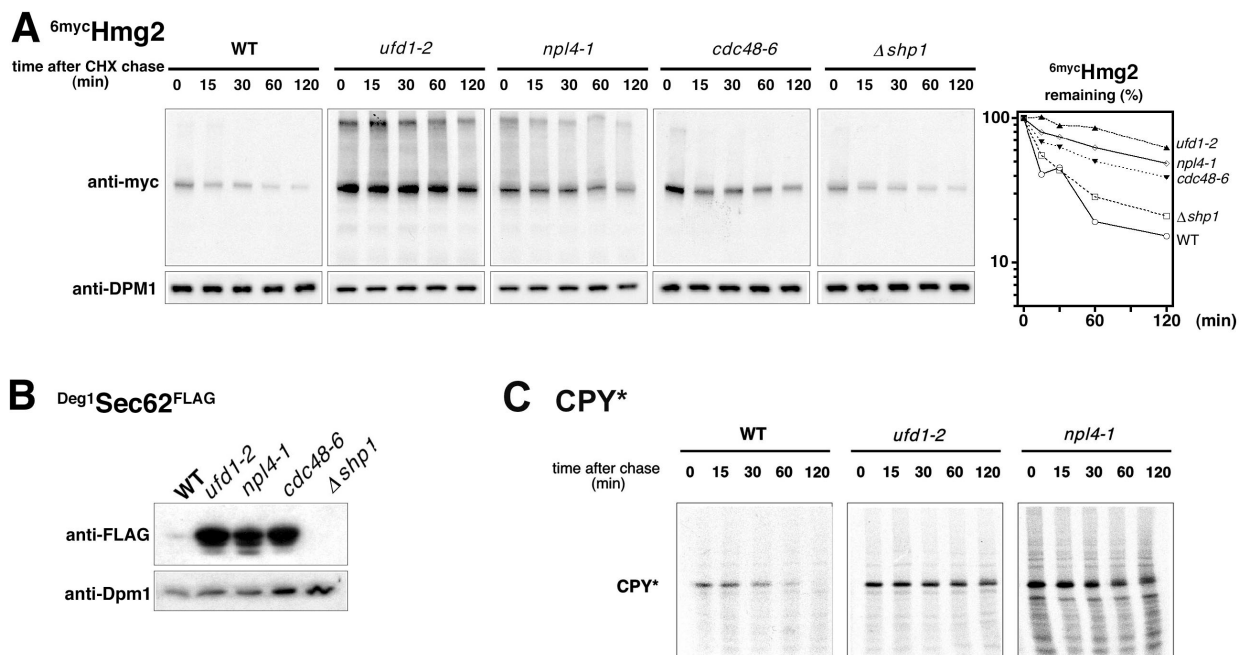


Figure 2-7. General role of the CDC48^{UFD1/NPL4} segregase in ERAD. (A) Expression shut-off (cycloheximide chase) at 37°C with WT and *ufd1-2*, *npl4-1*, *cdc48-6* Δ *shp1* cells expressing ^{6myc}HMG2. After adding cycloheximide to the medium samples were taken at time points indicated and protein extracts were prepared. The protein level of epitope-tagged ^{6myc}Hmg2 is shown by anti-myc immunoblots (upper panel). As a control blots were reprobbed with an antibody against Dpm1 (lower panel). The right panel shows the quantification of the ^{6myc}HMG2 decay. **(B)** Steady state level of the unstable ^{DEG1}Sec62^{FLAG} variant expressed in WT, *ufd1-2*, *npl4-1*, *cdc48-6* and Δ *shp1* cells. The steady state level of the epitope-tagged Sec62 variant was analyzed by using an anti-FLAG antibody (upper panel). As a control blots were reprobbed with an antibody against Dpm1 (lower panel). **(C)** Pulse chase experiment with WT, *ufd1-2* and *npl4-1* cells expressing CPY* from its endogenous locus. Cells were pulsed by adding 25 μ Ci/OD ³⁵S-methionine for 15 minutes. Samples were taken at time points indicated and subjected to immunoprecipitation with a CPY-specific antibody under denaturing conditions. Shown here is the radiogramm after SDS-PAGE.

al., 1993). CPY* is a mutant form of the soluble vacuolar protease carboxypeptidase Y that is retained within the lumen of the ER and immediately degraded via ERAD (Finger *et al.*, 1993). As shown in Figure 2-7, both membrane proteins, Hmg2 and DSF were strongly stabilized in *cdc48*, *ufd1* and *npl4* mutants at their non-permissive temperature, as demonstrated by a cycloheximide chase experiment and examination of steady state levels, respectively (Figure 2-7A and B). Likewise, turnover of the soluble protein CPY* was significantly diminished in *ufd1-2* and *npl4-1* mutants as judged by a pulse-chase experiment (Figure 2-7C). Furthermore, none of the proteins tested were stabilized in the *shp1* mutant (Figure 2-7, right panels, and data not shown). In conclusion, the data obtained by this set of experiments suggest that the ubiquitin-selective Cdc48^{Ufd1/Npl4} chaperone is generally involved in ERAD and represents a constitutive component of the ERAD machinery.

2.2.4. Involvement of other ubiquitin-binding factors in ERAD

Recently, it was demonstrated that Cdc48 cooperates with other different ubiquitin-binding factors in proteasome-targeting of various proteolytic substrates (Richly *et al.*, 2005). In particular, recruitment of ubiquitin-conjugates to Cdc48^{Ufd1/Npl4} is mediated largely by the heterodimer Ufd1/Npl4 (see Figure 2-8A), which has also been shown to bind like Cdc48 to ubiquitylated proteins (Meyer *et al.*, 2000). Upon substrate recruitment, Cdc48 directs proteins modified with 1-2 ubiquitin molecules to the ubiquitylation processivity factor (E4) Ufd2 (Kögl *et al.*, 1999; Figure 8-2B), thereby controlling the formation of the multiubiquitin chain on the substrate. Finally, multiubiquitylated substrates are delivered to soluble ubiquitin receptors as Rad23 (Figure 28C), which has been known to mediate the direct transfer of substrates to the proteasome (Kim *et al.*, 2004). Cdc48 seems to play a central role in this pathway making contacts to all ubiquitin binding proteins either directly (i.e. to Ufd1 and Ufd2) or indirectly (i.e. to Rad23 via Ufd2; see Figure 2-8D and Richly *et al.*, 2005). Due to the common role of Cdc48 in the degradation of Ole1 and other ERAD substrates, it was tempting to speculate that this pathway might also be utilized for ERAD.

In collaboration with Holger Richly, the contribution of Ufd2 and Rad23 to ERAD was investigated by studying the degradation of several ERAD substrates in deletion mutants of *UFD2* and *RAD23*. Indeed, Ole1, Hmg2, and the engineered variant Deg1-FLAG^{Deg1}Sec62 (which is analogous to Deg1^{Deg1}Sec62^{FLAG} except that it carries the FLAG epitope N-terminally of Sec62) were found to be moderately, but significantly stabilized in $\Delta ufd2$ and $\Delta rad23$ mutants, respectively (Figure 2-9A and B upper panel, and data

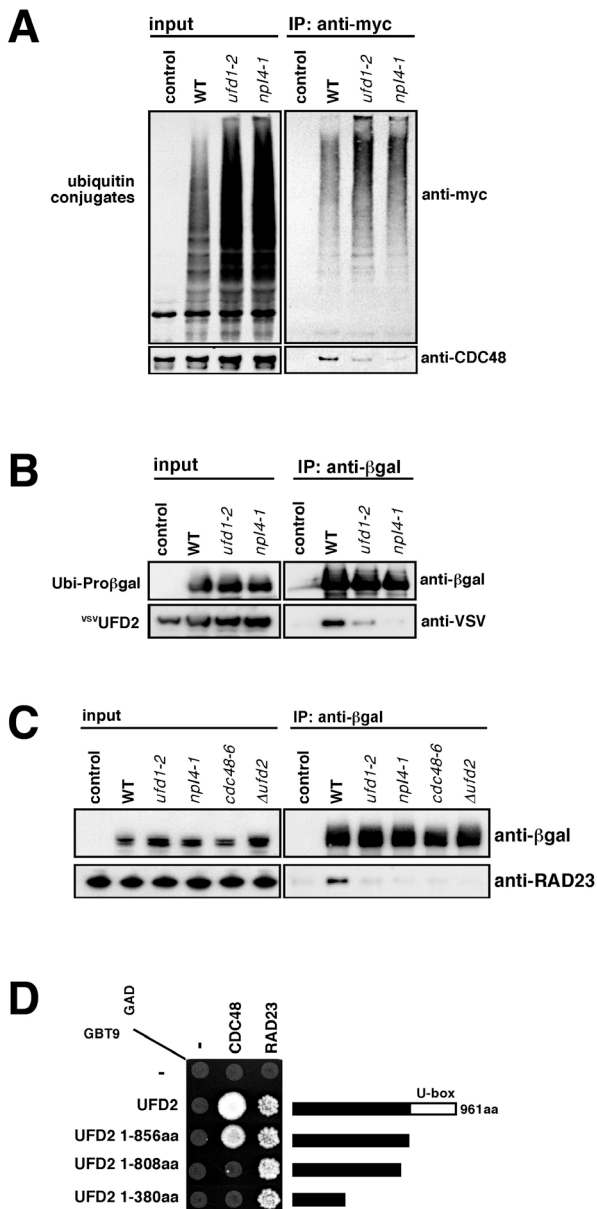


Figure 2-8. Substrate handing over by ubiquitin-binding proteins. (A) The interaction of CDC48 with ubiquitylated proteins is reduced in *ufd1-2* and *npl4-1* mutant cells grown at 37°C. Ubiquitin-conjugates were immunoprecipitated from WT, *npl4-1*, and *ufd1-2* cells overexpressing myc-tagged ubiquitin. Coprecipitated Ccd48 was detected by anti-Ccd48 immunoblots in WT, but hardly in *ufd1-2* and *npl4-1* cells. Control indicates WT cells overexpressing non-tagged ubiquitin. **(B)** Ufd2 binds Ubi-Proβgal with lower affinity in *ufd1-2* and *npl4-1* mutant cells. Ubi-Proβgal was immunoprecipitated from cleared lysates with β-galactosidase-specific antibodies. Coprecipitated Rad23 was detected by anti-Rad23 immunoblots. Control indicates WT cells not expressing Ubi-Proβgal. Temperature sensitive mutants were shifted to 37°C for 3 hours in medium supplemented with oleic acid. **(C)** Rad23 binds Ubi-Proβgal with lower affinity in *ufd1-2*, *npl4-1*, *cdc48-6* and Δ *ufd2* mutant cells. Experimental procedure as in (B). **(D)** Ufd2 can bind to Cdc48 and Rad23 simultaneously via different domains. Two-hybrid interaction of full-length or C-terminal deletion constructs of Ufd2 with Ccd48 and Rad23. Empty vectors are indicated by '-'. The Ufd2 constructs used are schematically shown on the right. The U-box located at the C-terminus of Ufd2 is structurally similar to RING finger domains and is required for the multi-ubiquitylation activity of Ufd2. The experiment shown in (B) was performed by M.Rape.

not shown). Since Rad23 was known to display partially overlapping functions with a related protein, Dsk2, ERAD was also examined in a *dsk2* deletion mutant. Again, only a minor effect could be observed for ^{Deg1-FLAG}Sec62 and the two other substrates in the Δ *dsk2* strain (Figure 2-9B, lower panel; data not shown). However, in the Δ *rad23* Δ *dsk2* double mutant, all three ERAD substrates were almost completely stabilized, indicating that Rad23 and Dsk2 function in parallel pathways and thus are able to functionally replace each other. Notably, ^{Deg1-FLAG}Sec62 was only marginally more stabilized in Δ *ufd2* Δ *rad23* and Δ *ufd2* Δ *dsk2* double mutants than in a Δ *ufd2* single mutant, substantiating the finding that Ufd2 and Rad23/Dsk2 function in the same pathway (Figure 2-9B, upper and lower panel). In addition to the Ufd2/Rad23-dependent degradation pathway,

degradation can occur via an alternative ubiquitin receptor, Rpn10, which is partially associated with proteasomes (Koegl *et al.*, 1999; Elsasser *et al.*, 2004; Richly *et al.*, 2005). ^{Deg1-FLAG}Sec62 was hardly stabilized in a single deletion mutant of *RPN10*, but the double mutant $\Delta ufd2 \Delta rpn10$ showed a strong stabilization of this substrate comparable to the effect observed in the $\Delta rad23 \Delta dsk2$ mutant (Figure 2-9B, upper panel). Thus, at least for some ERAD substrates as ^{DEG1-FLAG}Sec62 and Ole1 (data not shown), both degradation routes can be used to ensure efficient proteolysis. In conclusion, these data demonstrate that, in addition to the Cdc48^{Ufd1/Npl4} chaperone, the downstream-acting factors Ufd2, Rad23, and Dsk2 also contribute to ERAD pathways. Moreover, these findings also indicate that Ufd2/Rad23- and Rpn10-dependent pathways are partially redundant in ERAD.

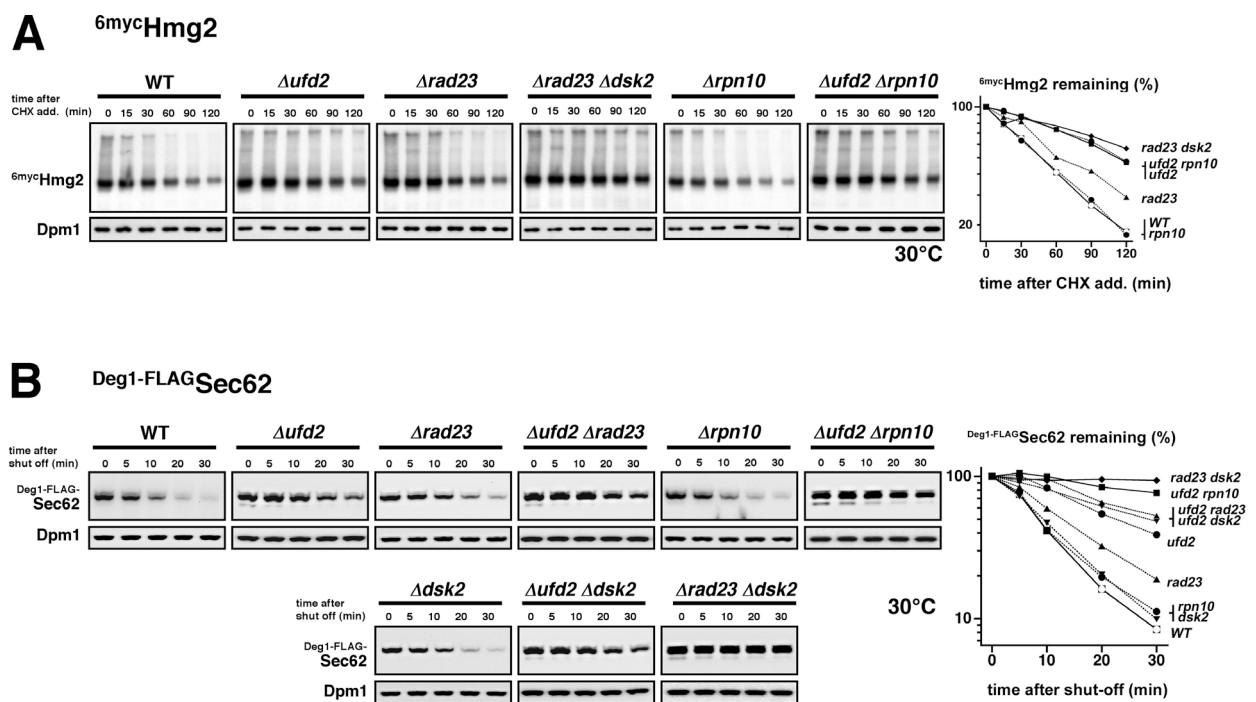


Figure 2-9. Involvement of Ufd2, Rad23, Dsk2, and Rpn10 in ERAD. (A) Expression shut-off experiments at 30°C with WT, $\Delta ufd2$, $\Delta rpn10$, $\Delta rad23$ single mutants, and $\Delta ufd2 \Delta rpn10$ and $\Delta rad23 \Delta dsk2$ double mutants expressing ^{6myc}HMG2. Samples were taken at the time points indicated and analyzed by anti-myc immunoblots. The stable ER-membrane protein DPM1 was used as control. **(B)** Expression shut-off experiments similar to (A) with cells expressing the ERAD substrates ^{Deg1-FLAG}SEC62. Samples were analyzed by anti-FLAG immunoblots. The graphs shows in (A) and (B) show the quantification of the ^{6myc}Hmg2 and ^{Deg1-FLAG}Sec62 decay, respectively (time point zero was set as 100%).

In summary, downstream of the constitutive component Cdc48^{Ufd1/Npl4}, ERAD proceeds via an interplay of several ubiquitin-binding factors that function partially in parallel degradation pathways. This mechanism may prevent the escape of substrates after they have reached the cytosol and ensures thereby efficient targeting to the 26S proteasome.

2.3. Proteolytic regulation of the ER SNARE Ufe1

The intriguing finding that Cdc48 functions at the ER membrane in several ubiquitin/proteasome-dependent processes (i.e. transcription factor processing, ERAD) prompted the study to analyze other substrates of Cdc48 with respect to regulation of ubiquitylation. An excellent candidate was the membrane tail-anchored protein Ufe1 (unknown function essential). This ER SNARE protein mediates together with Cdc48 homotypic membrane fusion of ER vesicles (Patel, S. K. *et al.*, 1998). Moreover, Ufe1 was reported to be unstable in a conditional *pkc1-2* mutant dependent on Ubc7 (Lin, A. *et al.*, 2001).

2.3.1. Ufe1 is ubiquitylated in WT cells

To assess the influence of ubiquitylation on Ufe1 regulation, it was first important to address the question whether Ufe1 is ubiquitylated under normal growth conditions in WT cells. So far it was only reported that in the conditional *pkc1-2* mutant Ufe1 becomes unstable (Lin, A. *et al.*, 2001).

In order to study ubiquitylation of Ufe1, an antibody was raised against the N-terminal half of Ufe1 recombinantly expressed in *E.coli*. Immunoblots with this antibody revealed that Ufe1 exists predominantly at steady state in a non-modified form in whole cell extracts of WT cells (Figure 2-10A, left panel, lane 1). The specificity of the antibody was demonstrated by expressing *UFE1* chromosomally tagged with a C-terminal 6HA-epitope (*UFE1*^{6HA}) that results in an up-shift of the Ufe1-specific band in the migration pattern after SDS-PAGE (Figure 2-10A, left panel, lane 2). Interestingly, by co-expressing an N-terminal-tagged form of ubiquitin (^{myc}Ub), the mobility of an additional, faint band in the immunoblot was changed to a slower migrating form (Figure 2-10A, lane 4 versus lane 3). This change in the mobility corresponds to 2-3 kDa, approximately the size of the myc-tag. The difference in the mobility between non-modified Ufe1 and this additional band corresponds to 8-12 kDa. Based on this finding Ufe1 was supposed to form (mono-) ubiquitin-conjugates in WT cells.

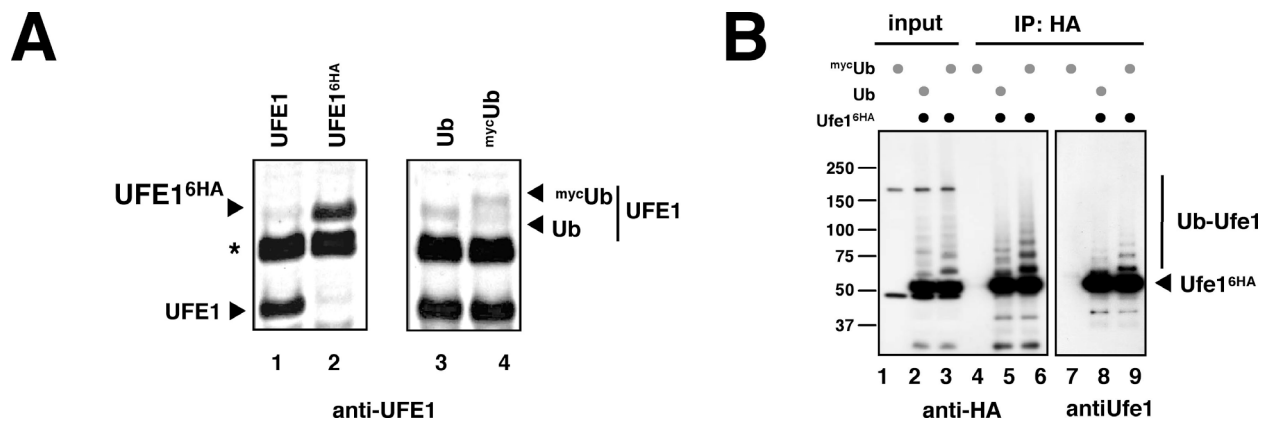


Figure 2-10. The ER SNARE Ufe1 protein is ubiquitylated in WT cells. (A) left panel: WT cells expressing non-modified or a C-terminal HA-epitope fusion of *UFE1* from its chromosomal locus (lane 1 and 2). Right panel: WT cells co-expressing ubiquitin or an N-terminal myc-epitope-fusion of ubiquitin (lane 3 and 4). Steady state levels of Ufe1 were analyzed with a Ufe1-specific antibody (B) Immunoprecipitation of Ufe1^{6HA} under denaturing conditions. Non-modified or HA-tagged *UFE1* was expressed in $\Delta ufe1$ cells from a CEN plasmid under the control of its own promoter. Cells were additionally expressing ubiquitin or myc-tagged ubiquitin, respectively, from a 2 μ plasmid under the control of the inducible copper promoter. Denaturing condition were used for preparation of whole cell extracts and immunoprecipitations. The input and the immunoprecipitated material were analyzed by immunoblots with anti-HA (left panel) and anti-UFE1 (right panel) antibodies.

To confirm these data, *UFE1*^{6HA} was expressed in $\Delta ufe1$ cells and lysates were subjected to anti-HA immunoprecipitations under denaturing conditions. When analyzing the input and the immunoprecipitated material with an anti-HA antibody, besides non-modified Ufe1^{6HA} additional bands were observed. These formed a ladder indicative of ubiquitin-conjugates (Figure 2-10B, lane 2-3 and 5-6). This ladder was also detected when the immunoprecipitated material was analyzed with an anti-Ufe1 antibody (Figure 2-10B, lane 8-9), but was absent when Ufe1 was expressed without an HA-tag (lane 1, 4 and 7). Moreover, co-expression of myc-ubiquitin led again to a significant up-shift of the ladder (compare lane 2 with 3, lane 5 with 6 and lane 8 with 9). Thus, a minor pool of Ufe1 is ubiquitylated at steady state. Although the ubiquitin conjugation appears not to be restricted to mono-ubiquitin, there seems to be a preference for shorter chains.

Depending on the substrate, the ubiquitylation reaction may be restricted to a specific lysine residue. In order to investigate this possibility for Ufe1, single arginine replacement mutants of all 30 lysine residues of the coding sequence of *UFE1* were generated. However, in none of the single mutants the ubiquitylation pattern was detectable changed (data not shown), indicating that alternate lysine residues in Ufe1 may be used for the modification.

2.3.2. The SM protein Sly1 controls the stability of Ufe1

Based on the finding that Ufe1 is ubiquitylated in WT cells, it was of particular interest to test whether Ufe1 is a short-lived protein. To this end, a cycloheximide chase experiment was performed. When WT cells were kept at room temperature, Ufe1 was hardly turned over within a period of 2 hours (Figure 2-11A, upper left panel). However, when cells were shifted to 37°C upon addition of cycloheximide, the turnover of Ufe1 was moderately, but significantly, increased (Figure 2-11A, upper right panel). Interestingly, when the cycloheximide chase experiment was performed over a longer time period, Ufe1 levels did not further decline, which may indicate that only a specific pool of Ufe1 is subject to degradation (data not shown). The slightly increased degradation of

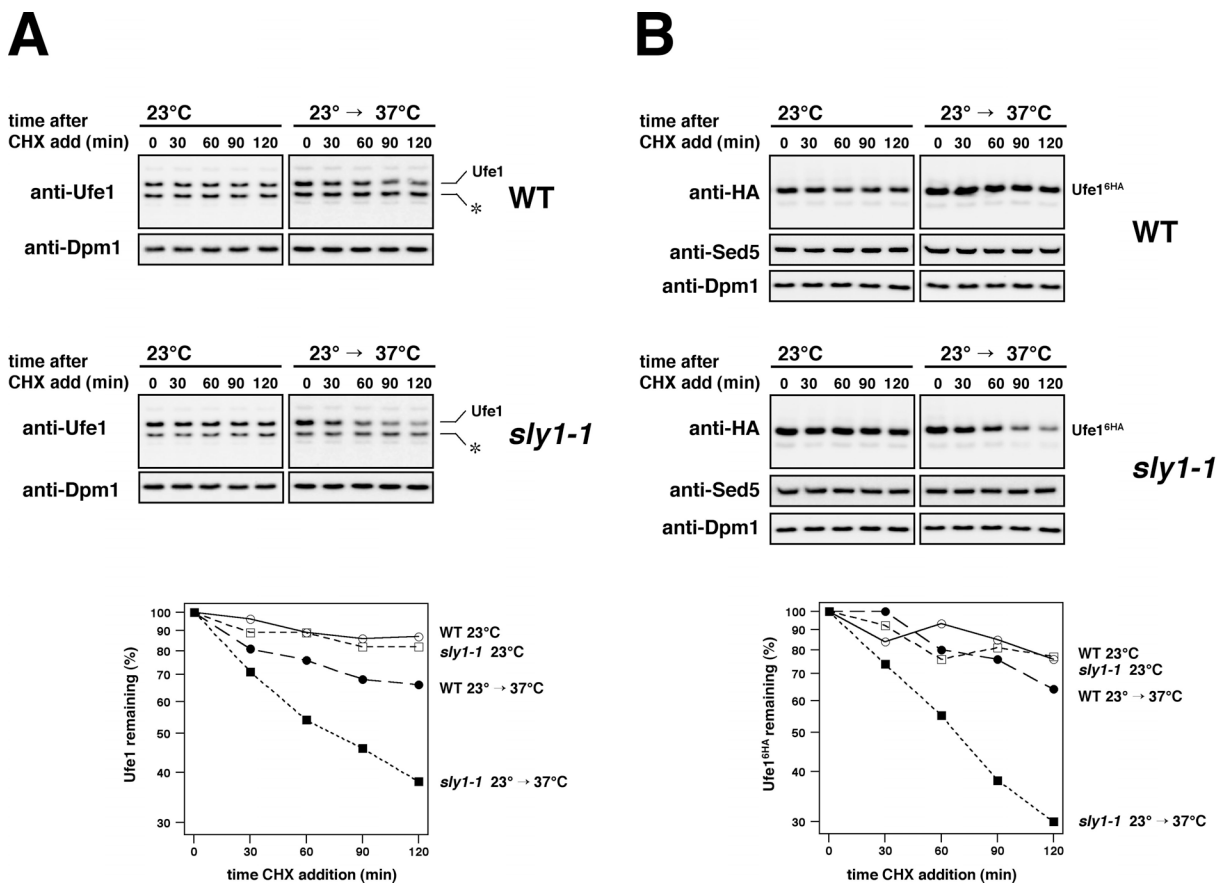


Figure 2-11. Ufe1 is nearly stable in WT cells but short-lived in a *sly1-1* mutant. (A) Cycloheximide chase experiment with WT (upper panel) and *sly1-1* cells (lower panel). Cells were grown in YPD to an OD₆₀₀ of 0.5 at 23°C and kept at this temperature or shifted to 37°C after addition of cycloheximide. At each indicated time point, the cellular level of Ufe1 was analyzed by anti-Ufe1 immunoblots. As a control, the blots were reprobed with an antibody against the stable ER-membrane protein Dpm1. The asterisk indicates a cross-reactive band. (B) Similar to (A) but with cells co-expressing C-terminally HA-tagged *UFE1* from a CEN plasmid under the control of its endogenous promoter. In addition, the blots were reprobed with an antibody against the Golgi SNARE Sed5. The graphs in (A) and (B) show the quantification of the decay of Ufe1 and Ufe1^{6HA}, respectively (time point zero was set as 100%).

Ufe1 at elevated temperatures suggests either that degradation may occur generally faster caused by a stress response or that Ufe1 turnover may be linked to physiological conditions, which proceeds faster at higher temperatures.

The moderate decay of the entire Ufe1 pool raised the question whether degradation might reflect a rather unspecific quality control mechanism to dispose misfolded Ufe1 molecules, or whether it might be part of an intrinsic regulation of the SNARE. Therefore, Ufe1 stability was studied under conditions where its function is expected to be compromised. Ufe1 is known to interact physically with Sly1, which belongs to the family of SM (Sec18/Munc1) proteins and is also essential (Dascher *et al.*, 1991; Yamaguchi *et al.*, 2002). In yeast 4 different SM proteins exist, which are all believed to assist in membrane fusion processes, yet their precise molecular function is still poorly understood. Ufe1 stability was examined in a temperature-sensitive mutant of *SLY1*. Interestingly, steady state levels of Ufe1 were strongly reduced in the *sly1-1* mutant when cells were incubated for a short period at the non-permissive temperature (data not shown). To analyze the half-life of Ufe1 in this mutant, a cycloheximide chase experiment was performed. When cycloheximide was added to *sly1-1* cells directly after they have been shifted to the restrictive temperature, Ufe1 levels were found to decline immediately, but not when cells were kept at the permissive temperature during the time course (Figure 2-11A, lower panel). Similar results were obtained for the half-life of Ufe1^{6HA}, indicating that the regulation of the epitope-tagged variant is unchanged (Figure 2-11B). Sly1 is known to interact also with another SNARE protein, Sed5 (Sogaard *et al.*, 1994; Yamaguchi *et al.*, 2002), which is implicated in protein sorting from the ER to the Golgi and represents the closest homolog to Ufe1. Notably, Sed5 is stable even at elevated temperatures, and its turnover is not altered in the *sly1-1* mutant (Figure 2-11B). Thus, the Sly1-dependent regulation of Ufe1 stability seems to be an intrinsic property of Ufe1 itself.

2.3.3. Ufe1 stability is directly linked to interaction with Sly1

Since Ufe1 is highly unstable in the temperature-sensitive *sly1-1* mutant, it was tempting to speculate that Sly1 binding to Ufe1 may directly influence its stability. Recent studies have mapped the interaction between Sly1 and its cognate SNARE partners (Bracher and Weissenhorn, 2002; Yamaguchi *et al.*, 2002). Both, Ufe1 and Sed5 interact with Sly1 via a short N-terminal stretch. Within this conserved binding motif, one phenylalanine residue (F) is crucial for binding (F10 in Sed5 and F9 in Ufe1) (Yamaguchi *et al.*, 2002). Sly1 itself makes contact with this phenylalanine residue by forming a hydrophobic binding pocket (Bracher and Weissenhorn, 2002). Therefore, reciprocal mutations in the binding interface of Ufe1 and Sly1 (Ufe1-F9A; Sly1-L137R and

Sly1-V156P) were generated to investigate the half-life of Ufe1 with respect to the interaction of Ufe1 with Sly1.

By performing yeast two-hybrid assays, both amino acid replacements within the binding pocket of Sly1 were confirmed to affect the interaction with Ufe1 especially at higher temperatures (Figure 2-12A, upper panel). Consistent with previous results (Yamaguchi *et al.*, 2002), the F9A mutation of Ufe1 similarly displayed only a weak interaction with Sly1 (Figure 2-12A, lower panel). The temperature-sensitive *sly1-1* mutant was also found to be reduced in its interaction with Ufe1 although the R266K exchange of the *sly1-1* allele is located outside the hydrophobic pocket. This may suggest that determinants outside the binding pocket of Sly1 are also important for interaction with Ufe1.

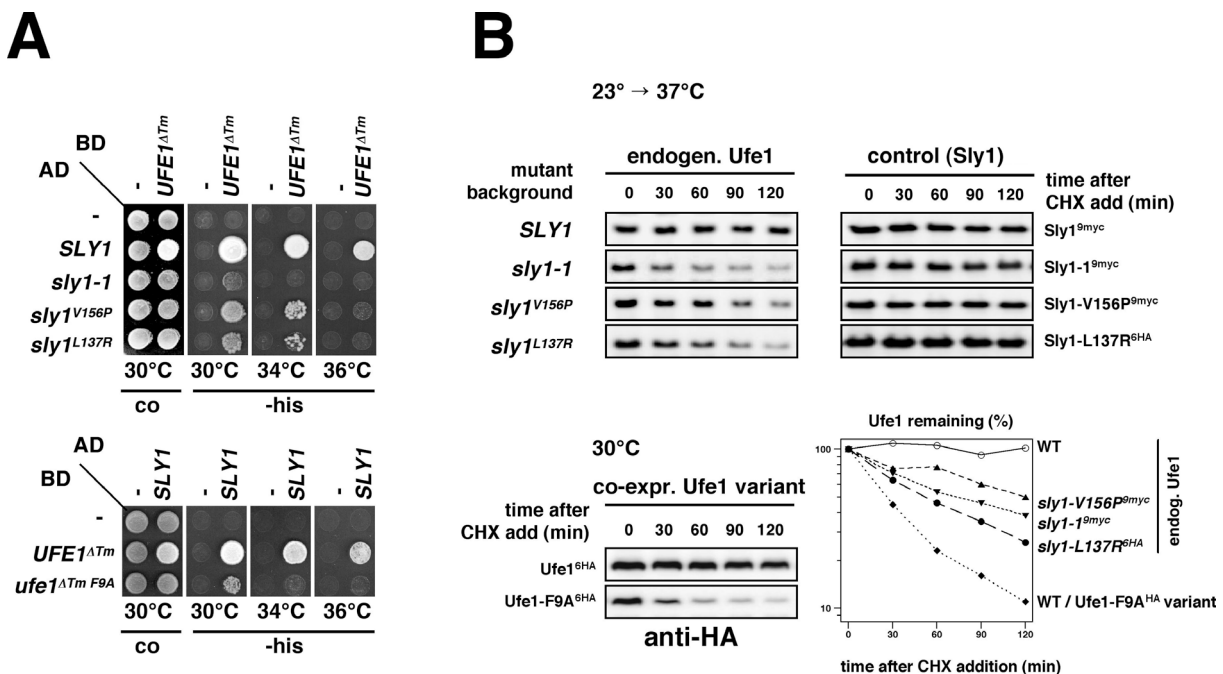


Figure 2-12. Stable interaction between Ufe1 and Sly1 is required to prevent Ufe1 degradation. (A) Yeast two-hybrid interaction of WT and mutant variants of *SLY1* and *UFE1*. Transformants were spotted onto SC–Leu⁻Trp⁻ plates as control (co) and SC–Leu⁻Trp⁻His⁻ (-his) plates to test for two-hybrid interaction and incubated for 2-3 days at different temperatures as indicated. Empty vectors are denoted as "-". **(B)** Upper panel: Cycloheximide chase experiments with Δ *sly1* cells expressing WT or mutant alleles of *SLY1* fused to C-terminal epitope-tags from a single copy plasmid under the control of the endogenous promoter. Cells were grown in YPD to an OD₆₀₀ of 0.5 and shifted to 37°C upon addition of cycloheximide. At each time point indicated, the cellular levels of Ufe1 and the respective Sly1 variant were analyzed with antibodies against Ufe1 (left), the myc- or HA-epitope (right), respectively. Lower panel: Cycloheximide chase at 30°C with WT cells co-expressing C-terminal HA-tagged variants of WT *UFE1* and *ufe1-F9A* from a CEN plasmid under the control of the *UFE1* promoter. The cellular levels of the epitope-tagged Ufe1 variants were analyzed by an anti-HA immunoblot. The graph shows the quantification of the decay of endogenous Ufe1 and co-expressed Ufe1-F9A^{6HA} in different strain backgrounds as indicated on the right side of the panel (time point zero was set as 100%).

To test the influence of the respective *sly1* mutants on the turnover of endogenous Ufe1, epitope-tagged variants of WT *SLY1* or the different mutant *sly1* alleles were expressed in $\Delta sly1$ cells and cycloheximide chases were performed. All mutants caused a significant destabilization of Ufe1 (Figure 2-12B, left panel), which correlates with the ability of the respective Sly1 variants to bind to Ufe1. To rule out the possibility that destabilization of Ufe1 might have been caused indirectly by a possible instability of the Sly1 mutants themselves, the turnover of the Sly1 variants was examined in addition. Immunoblots using antibodies against the respective epitope tags revealed that none of the Sly1 mutant proteins were found to be short-lived (Figure 2–12B, right panel).

Notably, the expression of *ufe1-F9A* is not able to complement the $\Delta ufe1$ deletion (data not shown), demonstrating that this mutation interferes with the essential function of Ufe1. Therefore, in order to investigate the influence of the F9A mutation on the stability of Ufe1, *ufe1-F9A* was expressed as an epitope-tagged variant in WT cells, which allows the detection of the mutant allele in the presence of the WT protein. Consistently, the Ufe1-F9A protein was also found to be highly unstable (Figure 2-12B, lower panel).

These results demonstrate that binding of Sly1 to Ufe1 is essential for Ufe1 stability. This may suggest that the balance between both proteins controls the regulation of Ufe1. Based on this assumption, overexpression of Ufe1 would also cause the degradation of Ufe1 molecules that exceed the amount of endogenous Sly1.

To test this idea, Ufe1 levels were raised step-wise, and steady state levels were examined. When expressed from a high copy plasmid using the endogenous Ufe1 promoter, steady state levels of Ufe1 were found to be significantly elevated compared to the expression from its chromosomal locus or a low copy plasmid. (Figure 2-13A, compare lane 3 with lane 1 and 2). However, only a marginal increase could be observed when Ufe1 was expressed from a high copy plasmid using the strong *GAL1-10* (Figure 2-13A, compare lane 4 with 3). In contrast, combined overexpression of *UFE1* and *SLY1* under these conditions led to a considerable further increase of Ufe1 levels (Figure 2-13A, compare lane 8 with 4). Conversely, endogenous Ufe1 levels were not affected by overexpressed *SLY1*, suggesting that under normal conditions Sly1 is not limited in binding to Ufe1 (Figure 2-13A, lane 9-12). These data suggest that overproduced Ufe1 is unstable due to a lack of the Sly1 binding partner. To confirm these data, the half-life of overproduced Ufe1 was examined in the absence or presence of equally overproduced Sly1. As shown in Figure 2-13B, step-wise overexpression of *UFE1* resulted in the instability of the protein, confirming that indeed the half-life of Ufe1 is altered when overproduced. As expected, the down-regulation could partially be overcome by co-expressing Sly1.

In conclusion, these data demonstrate that an imbalance between Ufe1 and Sly1 results in the rapid degradation of excessive Ufe1.

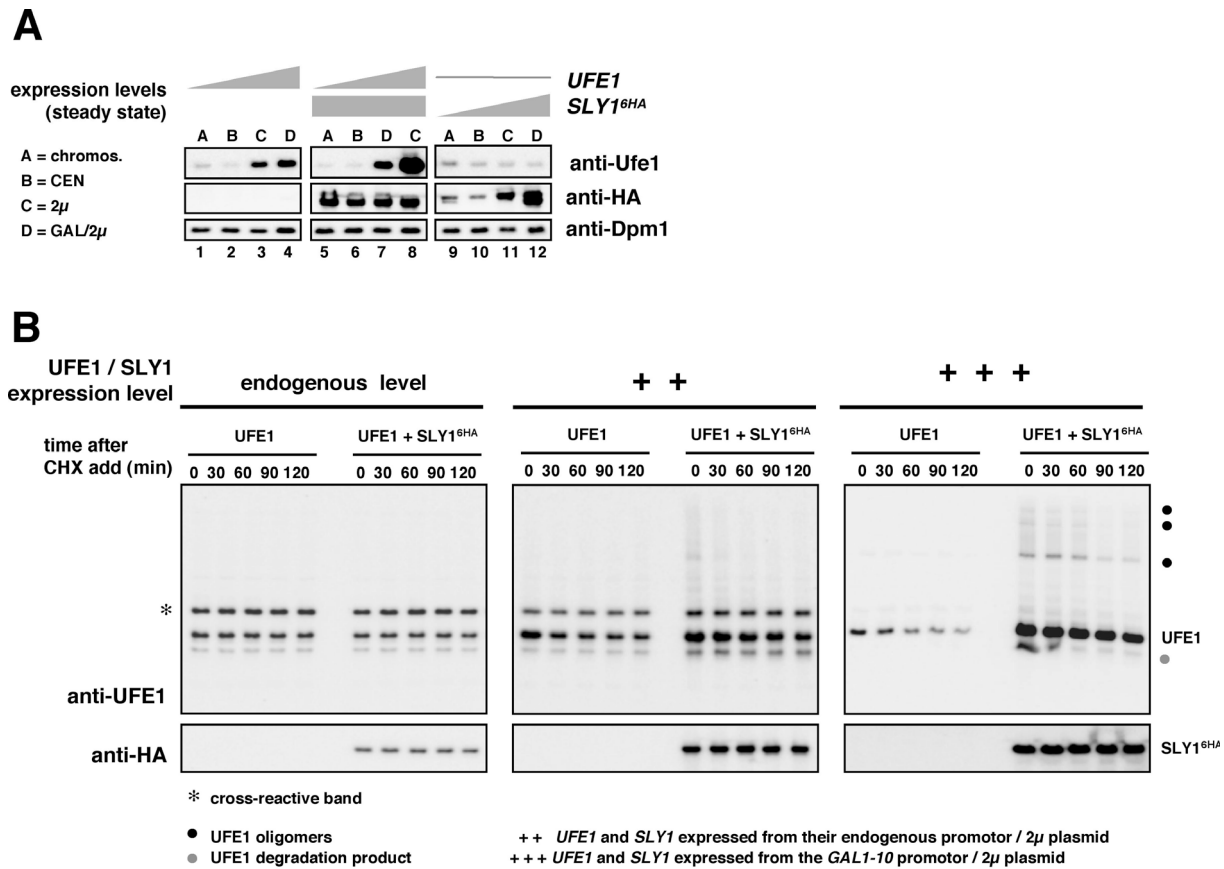


Figure 2-13. Overproduced Ufe1 is unstable but can be partially stabilized by concomitant overexpression of *SLY1*. (A) Left panel: Steady state levels of *UFE1* expressed in WT cells either from its chromosomal locus (lane A), from a CEN plasmid under the control of its own promoter (lane B), from a 2 μ plasmid under the control of its own promoter (lane C), or from a 2 μ plasmid under the control of the *GAL1-10* promoter (lane D). Middle panel: As before, but with concomitant overexpression of *SLY1^{6HA}* from a 2 μ plasmid under the control of the *GAL1-10* promoter. Right panel: *UFE1* expressed steadily from its chromosomal locus combined with *SLY1^{6HA}* expressed either from its chromosomal locus (lane A), from a CEN plasmid under the control of its own promoter (lane B), from a 2 μ plasmid under the control of its own promoter (lane C), or from a 2 μ plasmid under the control of the *GAL1-10* promoter (lane D). Cells were grown in SC media containing galactose to an OD₆₀₀ of 0.5 at 30°C and protein samples were prepared. Ufe1 and Sly1^{6HA} levels were analyzed by anti-Ufe1 and anti-HA-immunoblots, respectively. As a control, blots were reprobbed with an antibody against Dpm1. (B) Expression shut-off experiments with WT cells expressing either solely *UFE1* or *UFE1* in combination with *SLY1^{6HA}* at different expression levels as indicated. Cells were grown similar to (A); after adding cycloheximide (left and middle panel) or glucose and cycloheximide (right panel), aliquots were taken at time points indicated and analyzed by anti-Ufe1 and anti-HA immunoblots. Note that in case of overexpression from the *GAL1-10* promoter (denoted as “+++”), less protein sample was subjected to SDS-PAGE to avoid an overload of the gel. The asterisks denote cross-reactive bands. The gray filled circle indicates a degradation product of *UFE1* that co-migrates with the cross-reactive band seen in the left and middle panel. The black filled circles refer to possible SDS-resistant Ufe1 complexes, which might have been formed during the extract preparation.

2.3.4. Sly1-unengaged Ufe1 is degraded by the ubiquitin/proteasome system

To investigate whether the observed degradation of Ufe1 is mediated by the ubiquitin/proteasome system, several mutants defective in ERAD were introduced into the *sly1-1* background by crossing. As shown in Figure 2-14A, deletions of both E2 encoding genes, *UBC6* and *UBC7*, substantially stabilized Ufe1 in the *sly1-1* background, whereas a deletion of *UBC1*, which is also implicated in the degradation of certain ERAD substrates, did not considerably affect the turnover. Temperature-sensitive mutants of *CDC48* and of *PRE1*, encoding a proteasome subunit, influenced degradation of Ufe1 to a lesser but still significant extent. A minor stabilization effect could be observed for mutants of *UFD1* and *SHp1*, which are alternate substrate-recruiting factors of Cdc48. In contrast, deletion of *PEP4*, encoding a vacuolar protease, left Ufe1 turnover essentially unaffected. Although these mutants show varying degree of stabilization, these data suggest that Ufe1 down-regulation proceeds largely by ERAD involving the E2 enzymes Ubc6 and Ubc7, proteasomes, the Cdc48^{Ufd1/Npl4} complex and probably also the Cdc48^{Shp1} complex, which has been recently reported to play a subsidiary role in ubiquitin-dependent proteolysis (Schuberth *et al.*, 2004). The variations observed for the different mutants can be partially explained by the differences in the experimental setup: Whereas for the Ufe1 decay in deletion mutants a constant degradation rate was observed over the entire time course, temperature-sensitive alleles usually displayed a significant stabilization effect only after a lag phase. In contrast, the *sly1-1* allele-induced instability of Ufe1 starts without a delay when shifted to the non-permissive temperature (compare also Figure 2-11).

To conform these data, Ufe1 degradation was in addition studied in ERAD mutants expressing the Sly1 interaction-deficient *ufe1-F9A* mutant. ERAD mutants carrying complete deletions and co-expressing *ufe1-F9A^{6HA}* were examined at 30°C. As shown in Figure 2-14B, the double deletion mutant $\Delta ubc6 \Delta ubc7$ substantially stabilized the otherwise short-lived Ufe1-F9A^{6HA} variant. Moreover, also loss of other E2 enzymes (e.g. $\Delta ubc1$ and especially $\Delta ubc4 \Delta ubc5$) and of the vacuolar protease Pep4 affected the turnover of Ufe1-F9A^{6HA}. A contribution of Shp1 was not observed under these conditions. Temperature-sensitive strains expressing *ufe1-F9A^{6HA}* were incubated at the non-permissive temperature for 2 hours prior to the cycloheximide chase. Under these conditions, a strong stabilization effect for *ufd1-2* and *cdc48-6* could be detected as shown in Figure 2-15B (lower panel). Likewise, the proteasome mutant *pre1-1* stabilized the turnover robustly. The $\Delta shp1$ mutant displays also a temperature-sensitive growth phenotype and Ufe1-F9A^{6HA} degradation was slightly but significantly affected under this condition.

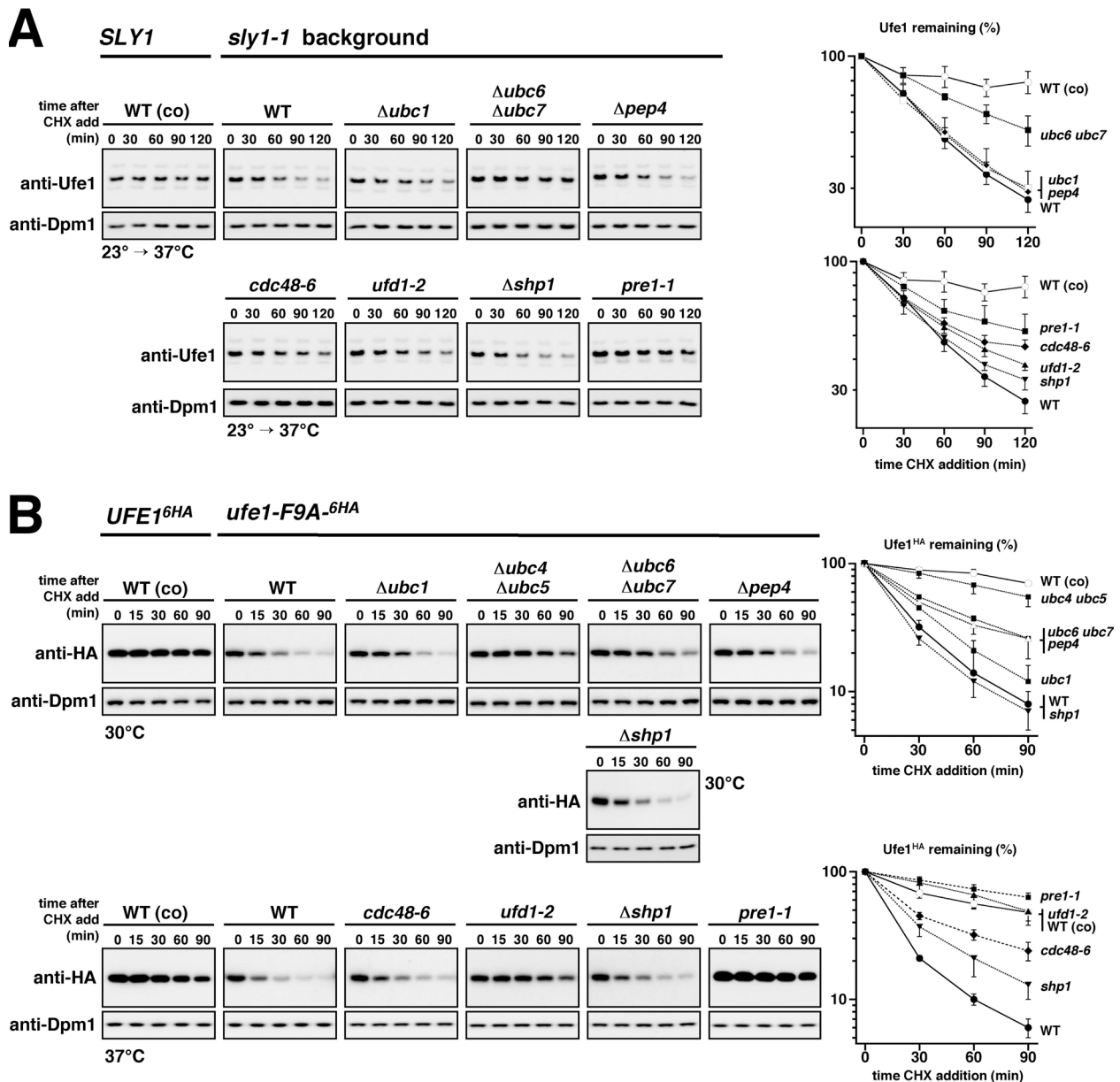


Figure 2-14. Unstable Ufe1 is degraded by ERAD. (A) Expression shut-off (cycloheximide chase) with WT, *sly1-1* cells and ERAD mutants in *sly1-1* background. Cells were grown in YPD to an OD_{600} of 0.5 at 23°C and shifted to 37°C upon addition of cycloheximide. Aliquots were taken at time points indicated and protein extracts were prepared. The protein level of Ufe1 was analyzed by anti-Ufe1 immunoblots. As a control blots were reprobed with an antibody against the stable ER membrane protein Dpm1. Shown is a representative experiment. The graphs present the quantification of the Ufe1 decay resulting from 3-4 independent experiments (symbols and bars represent the mean and the standard error) **(B)** Cycloheximide chase with WT cells and ERAD mutants co-expressing epitope-tagged WT *UFE1* or *ufe1-F9A* from the endogenous promoter. The experimental procedure was similar to (A) except that deletion mutants were grown to an OD_{600} of 0.6 at 30°C in SC media and kept at this temperature during the time course (upper panel), whereas conditional alleles were grown to an OD_{600} of 0.4 at 23°C, and then shifted for another 2 hours to 37°C before the expression shut-off was started (lower panel). The $\Delta shp1$ strain was analyzed at both temperatures, since it displays temperature sensitivity as well. The protein levels of the HA-tagged Ufe1 variants were analyzed by anti-HA immunoblots. Shown is a representative experiment. The graphs show the quantification of the Ufe1 decay resulting from 3-4 independent experiments (symbols and bars represent the mean and the standard error with the exception of $\Delta pep4$ and $\Delta shp1$ analyzed at 30° with $n = 2$; in this case the error bars represent the difference of the single measurements from the mean).

The data obtained by co-expressing *ufe1-F9A^{6HA}* in ERAD mutants were mostly consistent with the results obtained for endogenous Ufe1 in the *sly1-1* background. With both setups a contribution of Ubc6, Ubc7 and proteasomes could be demonstrated, indicating that Ufe1 is indeed degraded by the ubiquitin-proteasome system. Furthermore there is also evidence that the Cdc48^{Ufd1/Npl4} complex is implicated in Ufe1 turnover, as *ufd1-2*, *cdc48-6* as well as *npl4-1* (data not shown) substantially affect the degradation of Ufe1-F9A^{6HA}. To which extent Shp1 (presumably in complex with Cdc48) contributes to the turnover of Ufe1 remains to be solved, since Δ *shp1* displays only a stabilization effect at higher temperature. However, an involvement of Pep4 in degradation of Ufe1 was only observed for Ufe1-F9A^{6HA}, suggesting that a pool of this substrate might escape ERAD and is degraded within the vacuole.

To elucidate which E3 ligase participates in degradation of Ufe1, mutants of *RSP5*, *HRD1*, *DOA10/SSM4* and *TUL1* (Huibregtse *et al.*, 1995; Bays *et al.*, 2001; Swanson *et al.*, 2001; Reggiori and Pelham, 2002) were tested either in the *sly1-1* background or by expressing *ufe1-F9A^{6HA}*. However, no significant stabilization could be observed in any of the mutants examined (data not shown).

Together, these results reveal that a loss of functional Sly1 results in the instability of Ufe1 and that degradation proceeds largely by components of the ERAD pathway. Thus, it can be concluded (i) that one particular function of Sly1 is to act as a Ufe1-specific inhibitor of ERAD and (ii) that with respect to the essential function of Ufe1 as well as the inviability of the *ufe1-F9A* mutant, Sly1-binding to Ufe1 is essential for viability.

2.3.2. Function of the Sly1-dependent regulation of Ufe1 stability

2.3.2.1. Lack of Ufe1 regulation impairs viability

The finding that Sly1 prevents the proteasomal degradation of Ufe1 raised the question whether maintaining Ufe1 at constant levels reflects the crucial function of Sly1. According to this hypothesis, a block in Ufe1 degradation should result in the suppression of the temperature-sensitive phenotype of the *sly1-1* mutant.

To test this idea, several ERAD mutants in combination with the *sly1-1* allele were examined for their ability to grow at the non-permissive temperature of *sly1-1*. However, as shown in Figure 2-15, none of the double mutants tested were able to suppress the temperature sensitivity of *sly1-1*. In contrast, some of the double mutants, e.g. *pre1-1 sly1-1* or Δ *ubc1 sly1-1*, augmented the growth phenotype. This phenotype might in fact indicate that absence of any Ufe1 regulation by the simultaneous loss of Sly1 function and ERAD is detrimental for yeast growth. However, there is no clear correlation with Ufe1 degradation (e.g. *Ubc1* displays only a minor contribution in Ufe1 turnover; see Figure 2-14). Nonetheless, as the artificial up-regulation of Ufe1 in the absence of Sly1

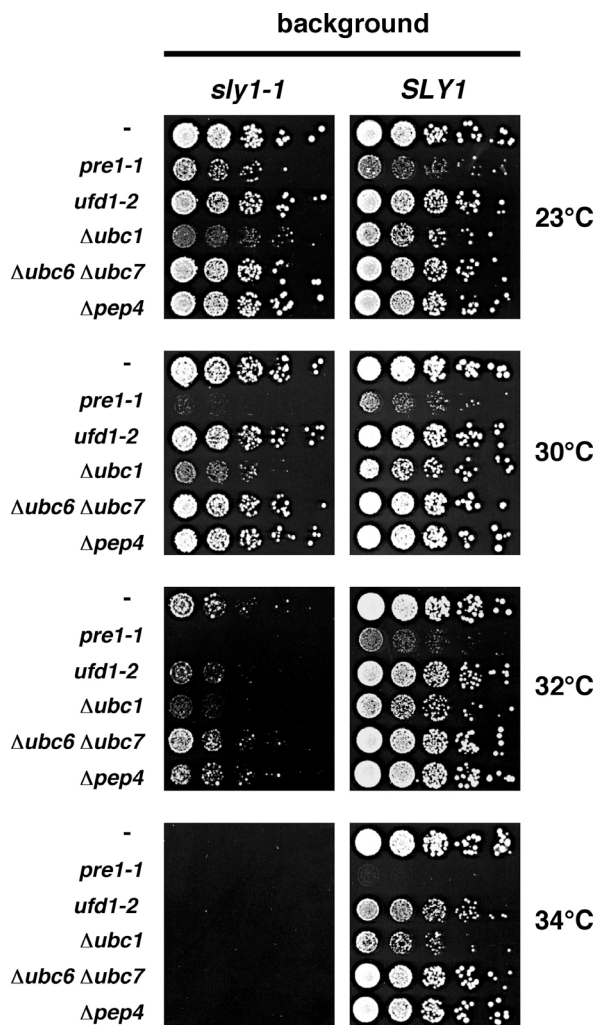


Figure 2-15. A restore of Ufe1 levels does not suppress the *sly1-1* temperature sensitive phenotype. WT cells and the following mutants *pre1-1*, $\Delta ubc1$, $\Delta ubc6 \Delta ubc7$, *ufd1-2* and $\Delta pep4$ were analyzed in the *sly1-1* and WT (*SLY1*) background. Cells were plated in 5-fold dilutions on full media (YPD) plates and incubated for 2-3 days at the temperature indicated.

setup, confirming that the growth defect is specific for *UFE1* overexpression.

In conclusion, these data demonstrate that Ufe1 levels have to be kept tightly regulated, and that this function is mediated by the presence of Sly1. Thus, excess of Ufe1 is detrimental to cellular growth as long as the balance between Ufe1 and Sly1 is not redressed by an up-regulation of Sly1.

is not sufficient to restore viability, Sly1 seems to provide further functions than its inhibitory role on ERAD of Ufe1. Indeed, the strict dependency on Sly1 suggests that an appropriate balance between Ufe1 and Sly1 seems to be important.

To assess this assumption, the cellular balance of Ufe1 and Sly1 was disturbed by overexpressing *UFE1* and *SLY1* either solely or in combination in WT cells (Figure 2-16). Whereas mild overexpression of *UFE1* did not significantly affect yeast growth, strong overexpression resulted in a considerable growth retardation, which was most pronounced at higher temperatures. Remarkably, concomitant overexpression of *SLY1* partially suppressed this phenotype. Interestingly, overexpression of *ufe1-F9A* was found to be less harmful to cells, and notably this mild phenotype could not be reverted by co-expression of *SLY1*, which is in agreement with the fact that the mutant allele is not able to bind Sly1. In contrast, similar overexpression of another ERAD substrate, *Deg1 SEC62^{FLAG}* (DSF), did not cause any significant growth retardation in this

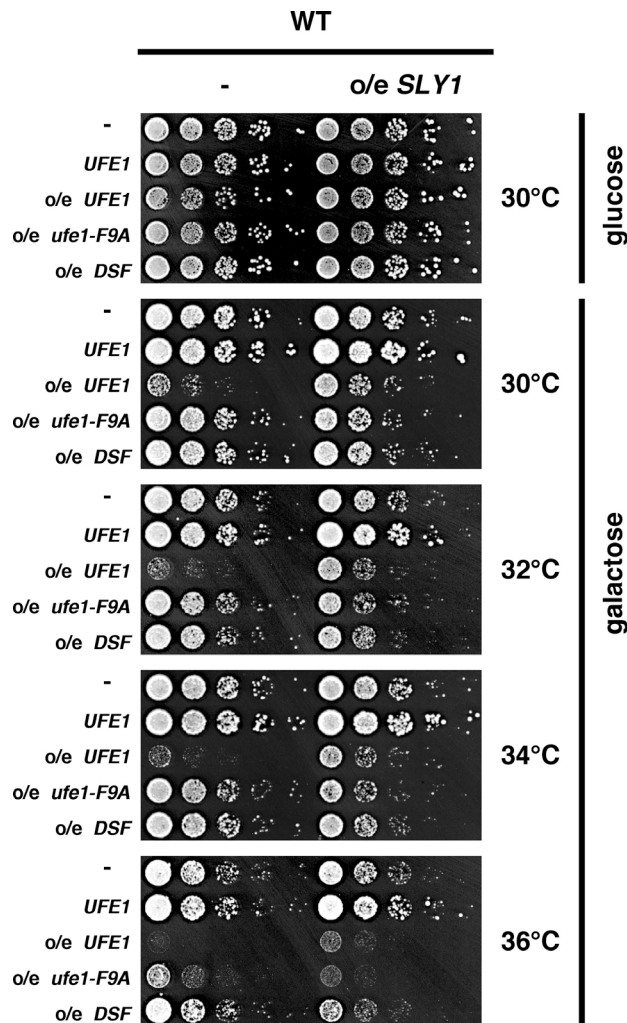


Figure 2-16. Imbalance between cellular levels of Ufe1 and Sly1 causes a slow growth defect. DF5 WT cells overexpressing different *UFE1* variants (left) or together with *SLY1* (right) were plated in 5-fold dilutions on synthetic media (SC) containing glucose (as a control) or galactose and incubated for 2-3 days at the temperatures indicated. Empty vectors are denoted as "-". Overexpression of the unrelated ERAD substrate ^{Deg1}*SEC62*^{FLAG} (*DSF*) was analyzed as negative control. All variants were strongly overexpressed from high copy 2μ plasmids under the control of the *GAL1-10* promoter except 'UFE1' (second row of each panel) that was mildly overexpressed from a 2μ plasmid using its own promoter.

2.3.2.2. Ufe1 competes with Sed5 for Sly1 interaction

Sly1 not only interacts with Ufe1 but also with the essential Golgi SNARE Sed5 (Yamaguchi *et al.*, 2002). Thus it appears conceivable that overproduced Ufe1 might interfere with the recruitment of Sly1 to Sed5, particularly since the cellular pool of Sly1 is rather limited (i.e. only 1-2 fold higher than that of Ufe1; data not shown). Furthermore, overexpression of the Sly1 interaction-deficient *ufe1-F9A* mutant displays only a slight growth defect in WT cells (Figure 2-17).

To investigate both Ufe1 and Sed5 concerning their requirements for Sly1, a genetic experiment was conducted with cells overexpressing either *UFE1*, or *SED5*, or both SNAREs combined using high-copy number plasmids that express the respective gene from the strong *GAL1-10* promoter (Figure 2-17). Overproduction of Ufe1 was found to result in a rather mild growth defect in the genome background used in this study (W303). For unknown reasons, overproduced Ufe1-F9A did not differ significantly from WT Ufe1 overproduction and caused a similar phenotype. Surprisingly, however,

overproduced Sed5 was strongly cytotoxic and almost no colonies could be detected even after several days. Intriguingly, when *UFE1* was co-expressed with *SED5*, the growth defect was slightly but significantly reduced. This effect was not observed when *ufe1-F9A* was co-expressed instead. In conclusion, these results suggest that Ufe1 and Sed5 might interfere with their respective functions when present in high amounts, presumably via their interaction with Sly1.

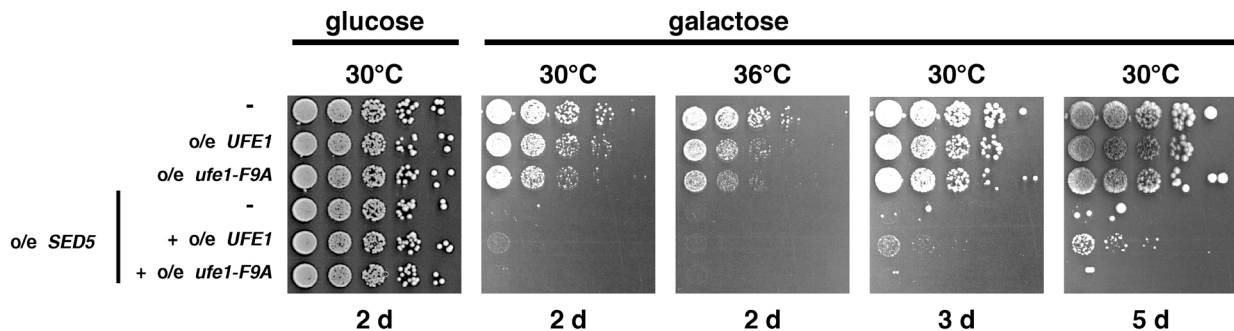


Figure 2-17. Overexpression of *SED5* is highly cytotoxic but can be partially suppressed by concomitant overexpression of *UFE1*. W303 WT cells overexpressing WT *SED5* solely or in combination with either *UFE1* or *ufe1-F9A* were plated in 5-fold dilutions on synthetic media (SC) containing glucose (as a control) or galactose and incubated at 30°C for several days as indicated. Empty vectors are denoted as "-". All variants were overexpressed from a high copy 2μ plasmid under the control of the *GAL1-10* promoter. The slow growth phenotype mediated by *UFE1* overexpression is weaker in W303 than in the DF5 background, and WT and mutant *UFE1* do not considerably differ concerning the growth defect.

2.3.2.3. Sly1 interacts genetically and physically with Cdc48 and Shp1

Besides its role in regulating the stability of Ufe1, it is attractive to speculate that Sly1 might also be required for the SNARE function of Ufe1 in membrane fusion. Support for this possibility comes from the finding that Ufe1-F9A results in a mild, but still significant, growth defect when overproduced in DF5 cells. Since this mutant shows only a weak binding to Sly1 (Figure 2-12A) it seems rather unlikely that the growth defect caused by Ufe1-F9A results from a competition with endogenous Sed5 as seen with overproduced WT Ufe1. In agreement with this notion, the Ufe1-F9A-mediated phenotype is not reverted by simultaneous overexpression of *SLY1* (see Figure 2-16). Thus, overproduced Ufe1-F9A may rather act as a dominant negative mutant in other processes, e.g. in the SNARE assembly of Ufe1 molecules and/or Ufe1-mediated membrane fusion process. Interestingly, when *ufe1-F9A* was overexpressed in mutants of *CDC48* and *SHP1*, the growth defect was found to be even more pronounced than in WT cells (Figure 2-18A). Moreover, when mutants of *CDC48* and *SHP1* were directly combined with a

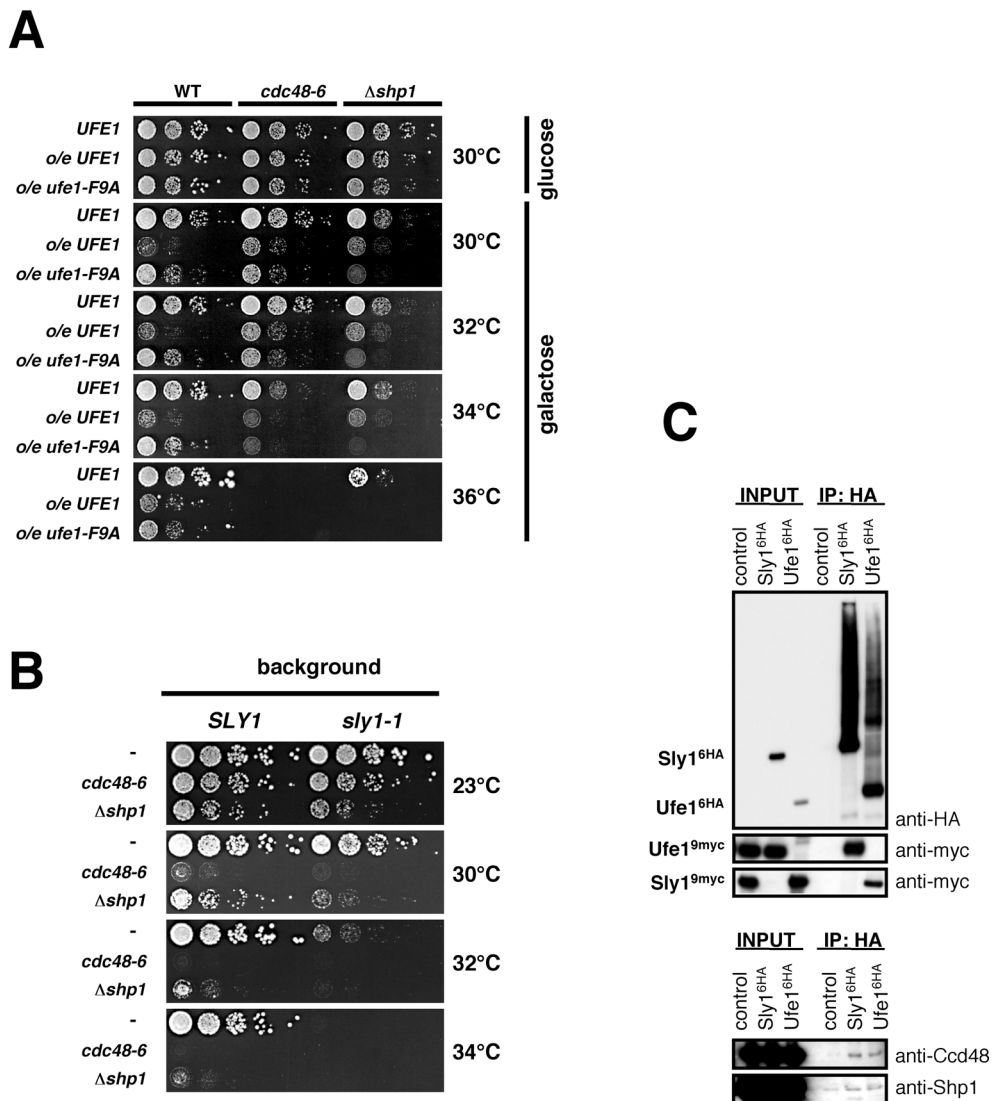


Figure 2-18. *SLY1* interacts genetically and physically with *CDC48* and *SHP1*. (A) Mutants of the Cdc48^{Shp1} complex are more sensitized toward overexpression of *ufe1-F9A* than WT cells. WT and mutant cells (DF5 background) overexpressing WT *UFE1* or *ufe1-F9A* were plated in 10-fold dilutions on synthetic media (SC) containing glucose (as a control) or galactose and incubated for 2-3 days at the temperatures indicated. All variants were strongly overexpressed from high copy 2 μ plasmids under the control of the *GAL1-10* promoter except '*UFE1*' (first row of each panel) that was moderately overexpressed from a 2 μ plasmid using its own promoter. (B) *sly1-1* displays a synthetic temperature sensitivity with mutants of the Cdc48^{Shp1} complex. The respective single and double mutants were plated in 5-fold dilutions on full media (YPD) and incubated for 1-2 days at the temperatures indicated. WT background (*SLY1*) is denoted as "-". (C) Ufe1 and Sly1 co-immunoprecipitate components of the Cdc48^{Shp1} complex. Whole cell lysates of cells expressing chromosomally respectively *UFE1*^{6HA} and *SLY1*^{9myc} or *UFE1*^{9myc} and *SLY1*^{6HA} were fractionated by ultra-centrifuging and microsomal fractions were solubilized in presence of 1% Triton X-100. After a second ultra-centrifugation step, the supernatant of the solubilized material was subjected to an anti-HA immunoprecipitation in presence of 0.3% Triton X-100. The input (1.5% of the soluble fraction used for the IP) and the immunoprecipitated material were analyzed by immunoblotting with an anti-HA antibody to visualize the efficiency of the IP. The immunoblot membrane were subsequently reprobbed with an anti-myc antibody to analyze the co-immunoprecipitation of Ufe1^{9myc} and Sly1^{9myc}, respectively (upper panels). In parallel, the immunoprecipitated material was examined for co-immunoprecipitation of components of the Cdc48^{Shp1} complex using Cdc48- and Shp1-specific antibodies (lower panels). Strains expressing respectively non-tagged *UFE1* or *SLY1* were used as controls.

deficiency in Sly1, the respective double mutants displayed an augmented temperature sensitivity (Figure 2-18B).

The observed genetic interaction suggests that Sly1, Cdc48 and Shp1 (probably in complex with Cdc48) act together on Ufe1. In order to examine the physical interaction between Sly1 and Cdc48^{Shp1}, co-immunoprecipitation experiments were performed. Microsomal fractions of strains expressing either chromosomally tagged *UFE1*^{6HA} and *SLY1*^{9myc} or *SLY1*^{6HA} and *UFE1*^{9myc}, respectively, were solubilized and subjected to anti-HA immunoprecipitations (IP). Reciprocal analysis of the IP material demonstrated that under these conditions Ufe1^{6HA} and Sly1^{6HA} are still efficiently bound to their cognate partners Sly1^{9myc} and Ufe1^{9myc}, respectively (Figure 18C, top panel). Ufe1 was reported to be associated with Cdc48 (Latterich *et al.*, 1995). Notably, analysis of the IP material with Cdc48- and Shp1-specific antibodies revealed that Cdc48 (and to a lesser extent Shp1) was weakly but specifically co-immunoprecipitated not only by Ufe1^{6HA} but also by Sly1^{6HA} (Figure 18C, bottom panel). Whether the interaction between Sly1^{6HA} and Cdc48 or Shp1, respectively, is direct or bridged via Ufe1 could not be resolved by this experiment. However, these data strongly suggest that Sly1 is associated with Ufe1 molecules being recruited to Cdc48 or the Cdc48^{Shp1} complex. As Cdc48 (presumably together with Shp1) has been assumed to operate in homotypic membrane fusion by disassembling Ufe1-SNARE complexes (Latterich *et al.*, 1995; Patel, S. K. *et al.*, 1998), the genetic and physical interaction shown here supports the view that Sly1 might be required not only for maintaining Ufe1 stability but also during the process of homotypic membrane fusion.

In conclusion, Sly1 seems to fulfill a dual function with respect to Ufe1: On one hand, Sly1 may regulate the stability of Ufe1 molecules. Since the cellular pool of Sly1 is rather limited, those Ufe1 SNAREs non-engaged with Sly1 are destined for degradation. As a consequence, the cellular pool and thus the activity of fusion processes mediated by Ufe1 seem to be indirectly controlled through this mechanism. On the other hand, Sly1 may be directly involved in the SNARE function of Ufe1, probably together with Cdc48 and Shp1, although the precise function remains to be resolved.

3. DISCUSSION

This study focused on two different aspects: firstly, the isolation of novel factors implicated in ER-associated degradation (ERAD), and secondly, the identification of novel, non-abnormal substrates regulated by ERAD. In addition, emphasis was placed on the mechanisms and the relevance of regulated degradation with respect to the cellular physiology.

3.1. Novel components of the ERAD pathway

Substrate recognition and ubiquitylation of proteins residing in the ER lumen or at the ER membrane were known to occur by components of a specific machinery referred to ER-associated degradation (ERAD). But how these substrates are relocated from the ER to the cytosol and delivered to the 26S proteasome has been remained enigmatic. This study identifies a number of novel factors implicated in the dislocation and proteasome targeting of several ERAD substrates: Relocation of luminal and membrane proteins of the ER was found to rely on the ubiquitin-selective chaperone Cdc48^{Ufd1/Npl4}. After retrotranslocation to the cytosol, the degradation of several substrates involves the action of the multiubiquitylation enzyme (E4) Ufd2 and of the soluble ubiquitin receptors Rad23 and Dsk2, which target substrates to the 26S proteasome. In addition, certain substrates may take a parallel route via the proteasome targeting factor Rpn10, which acts independently from Cdc48 and Ufd2. In the following, the action of these factors will be discussed in detail.

3.1.1. The Cdc48^{Ufd1/Npl4} complex promotes the relocation of ERAD substrates

The Cdc48^{Ufd1/Npl4} complex was previously shown to exhibit a pronounced specificity towards ubiquitin conjugates. In particular, it promotes the mobilization of the ubiquitylated, processed Spt23 transcription factor from the ER membrane in dependence of ATP (Rape *et al.*, 2001). This ability made Cdc48^{Ufd1/Npl4} likely to be also involved in the mobilization of ERAD substrates. Indeed, membrane as well as luminal substrates of ERAD were found to require all components of this complex for their efficient degradation (Figure 2–7). Furthermore, the ERAD substrate Ole1 was found to accumulate at the membrane in a *ufd1* mutant (Figure 2-6), consistent with the previous finding that a significant fraction of Cdc48^{Ufd1/Npl4} localizes to ER membranes (Rape *et al.*, 2001). In view of its ubiquitin-selectivity, it seems plausible that the Cdc48^{Ufd1/Npl4} complex operates downstream of the ubiquitin conjugation machinery and prior to proteasomal degradation as a general constituent of the ERAD machinery. Since the homohexameric, ring-shaped Cdc48 molecule was shown to undergo a dramatic rotational

outward movement upon ATP hydrolysis (Zhang *et al.*, 2000), the Cdc48^{Ufd1/Npl4} complex might act as ubiquitin-selective chaperone in untethering ubiquitylated substrates from non-modified partners. Thus, according to its function in ERAD, an attractive possibility would be that Cdc48^{Ufd1/Npl4} might segregate ubiquitylated ERAD substrates from the translocation channel. Similar results were discovered by other groups (Bays *et al.*, 2001; Ye *et al.*, 2001; Jarosch *et al.*, 2002; Rabinovich *et al.*, 2002).

But how does the chaperone ('segregase') cooperate with the ERAD machinery? It was reported that the activity of Cdc48^{Ufd1/Npl4} is sufficient to mobilize ERAD substrates into the cytosol (Jarosch *et al.*, 2002). However, the data of this study and others (Lee *et al.*, 2004) support a model, by which a successful membrane removal of ERAD substrate requires both Cdc48^{Ufd1/Npl4} and proteasome activity. According to this view, ubiquitylation, mobilization and degradation would be tightly physically and mechanistically coupled. Whereas an independently acting Cdc48^{Ufd1/Npl4} complex might result in the overflow of the cytosol with aberrant proteins, a coupled mechanism would ensure that substrates once trapped by the ERAD machinery would be efficiently targeted to the proteasome.

3.1.2. Ubiquitin-binding proteins escort ERAD substrates to proteasomes

A mechanistic coupling in ERAD was indeed recently shown by the discovery of a proteolytic pathway that includes Cdc48^{Ufd1/Npl4}, the multiubiquitylation enzyme (E4) Ufd2, and soluble ubiquitin receptors of the Rad23 family, which operates in proteasome targeting of proteolytic substrates (Richly *et al.*, 2005). Interestingly, all ubiquitin-binding factors of this pathway cooperate with each other by making contacts to their respective up- and downstream acting partners (Richly *et al.*, 2005; Figure 2-8D). Furthermore, interaction of all of these factors with ubiquitin-conjugates requires the presence of the respective upstream factors, indicating that substrates are handed over sequentially to their way to the proteasome (Richly *et al.*, 2005; Figure 2-8A - C). This escort pathway is not restricted to the turnover of cytosolic substrates but also participates in ERAD as demonstrated by this study.

3.1.2.1. The role of the multiubiquitylation enzyme (E4) Ufd2 in ERAD

Multiubiquitin chain assembly is often a processive and rapid reaction that does not rely on further factors. However, some reactions require the assistance of an E4 enzyme, probably since further attachment of ubiquitin moieties by the initiate E3 might be sterically hindered (Koegl *et al.*, 1999; Saeki *et al.*, 2004). This two-step reaction, e.g. mono- or oligo-ubiquitylation followed by E4-catalyzed multiubiquitylation, could offer another layer of control. In particular, this might be favorable to separate mono-ubiquitylation from subsequent multiubiquitylation reactions mediating distinct functions

as it has been assumed for the activation and degradation of certain transcription factors as for instance Spt23 (Hoppe *et al.*, 2000; Rape *et al.*, 2001; Richly *et al.*, 2005).

So far the only known E4 in yeast is Ufd2, which is able to recognize mono-ubiquitylated proteins and to elongate the ubiquitin chain by the addition of ubiquitin moieties (Koegl *et al.*, 1999). In view of a possible switch of function from mono- to multi-ubiquitylation, the participation of Ufd2 in ERAD was not anticipated, or at least a function for mono-ubiquitylation of ERAD substrates could not be addressed so far. However, deletion of *UFD2* was found to result in a prolonged half-life of several ERAD substrates by a factor of about 2 (Figure 2-9). Thus Ufd2 seems to be implicated in ERAD although the protein is not absolutely required. This might be due to a partial redundancy over other existing degradation pathways. Indeed, the double deletion mutant $\Delta ufd2 \Delta rpn10$ exhibits an almost complete block in the degradation of ^{Deg1}Sec62, but not of Hmg2 (Figure 2-9), indicating that certain substrates can take alternative degradation routes. However, Rpn10 was shown to act as a ubiquitin receptor in proteasomal targeting (Elsasser *et al.*, 2004; Verma *et al.*, 2004; see also below) and to bind preferentially to multi- but not oligo-ubiquitylated substrates (Richly *et al.*, 2005). Since Rpn10 seems to receive its substrates independent of Ufd2 (see below), apparently redundant

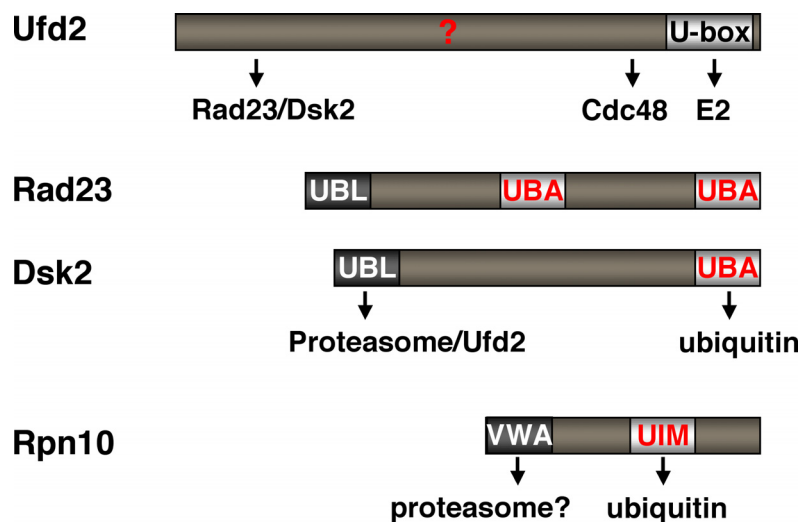


Figure 3-1. Interaction domains in the multiubiquitylation enzyme Ufd2 and the ubiquitin receptors Rad23, Dsk2, and Rpn10.

The Rad23 and Cdc48 interactions domains in Ufd2 have been mapped by yeast two-hybrid data (this study). The C-terminal U-box mediates binding to E2 analogous to the RING finger domain of E3 enzymes. The ubiquitin-binding motif has so far not been identified.

Ubiquitin receptors are assumed to shuttle substrates to the proteasome. Whereas binding to ubiquitin-conjugates is mediated by UBA and UIM domains (shown in light grey), association with the proteasome is mediated by the UBL domain of Rad23/Dsk2 and presumably by the VWA (van Willebrand A) domain of Rpn10, respectively (shown in dark grey). The UBL domain can also bind in a mutually exclusive manner to Ufd2.

multiubiquitylation mechanisms act during ERAD. However, this alternative route(s) might work less efficiently in chain elongation of oligo-ubiquitylated substrates, thereby explaining the prolonged half-life of ERAD substrates in the $\Delta ufd2$ mutant.

Besides its role in increasing the efficiency of ERAD, the Ufd2 pathway may provide another important function. Cdc48 and Ufd2 are able to form a ternary complex with substrates. Notably, *in vitro* studies demonstrated that in the presence of Cdc48, the reaction of the Ufd2-mediated chain elongation is restricted to the addition of only a few ubiquitin moieties. Nonetheless, the size of the multi-ubiquitin chain formed by this size-restricted catalysis is still sufficient for proteasome targeting (Richly *et al.*, 2005). Thus, the use of a limited multiubiquitin chain would prevent superfluous ubiquitylation reactions, which would not only be economical but also facilitate the disassembly of the ubiquitin chain at the proteasome. Therefore, the preferential use of the Ufd2 pathway by ERAD would also account for these advantages.

3.1.2.2. Alternate soluble ubiquitin receptors mediate proteasome targeting

Rad23 and its close relative Dsk2 were shown to bind ubiquitylated proteins via their UBA domain and to target them to the proteasome through association with their UBL motif via Rpn1 (Schauber *et al.*, 1998; Wilkinson, C. R. *et al.*, 2001; Chen, L. and Madura, 2002; Elsasser *et al.*, 2004; Verma *et al.*, 2004). Interestingly, the UBL motif of Rad23 is also engaged in binding to Ufd2, indicating that the interactions of Ufd2 with Rad23 and the proteasome are mutually exclusive (Kim *et al.*, 2004). In particular the detection of a ternary complex of Cdc48-Ufd2-Rad23 *in vivo* suggests that Rad23 (and presumably Dsk2) functions as proteasome targeting factors in the pathway downstream of Cdc48 and Ufd2 (Richly *et al.*, 2005). Consistently, integral membrane substrates tested in this study were found to be moderately stabilized in single mutants of *RAD23* and *DKS2* but were hardly degraded in the double mutant (Figure 2-9), underscoring that both proteins have overlapping functions in ERAD. Conversely, double mutants of either $\Delta ufd2 \Delta rad23$ or $\Delta ufd2 \Delta dsk2$ did not display any stronger defect in ERAD than the single $\Delta ufd2$ mutant, which confirms that Rad23 and Dsk2 act downstream of Ufd2 in the same pathway. This pathway seems to be used also for the degradation of luminal proteins (Medicherla *et al.*, 2004). Remarkably, multiubiquitin chains generated by size-restriction in the presence of Cdc48 and Ufd2 possess precisely the binding property needed for being collected by Rad23 and Dsk2 (Richly *et al.*, 2005). However, since degradation is significantly less affected by the lack of Ufd2 than by the simultaneous loss of Rad23 and Dsk2 (Figure 2-9), ERAD substrates might be partially collected by Rad23 and Dsk2 also independently of Ufd2.

Rpn10 binds ubiquitin conjugates via its UIM domain and was found to act as an alternative proteasome targeting factor (van Nocker *et al.*, 1996; Elsasser *et al.*, 2004; Verma *et al.*, 2004). Rpn10 also contributes to a certain extent to ERAD, since the combined block of the Rpn10 and the Ufd2 pathway results in a nearly complete stabilization of certain ERAD substrates (Figure 2-9; see also above). Due to the property of Rpn10 to bind preferentially to longer ubiquitin chains (Richly *et al.*, 2005), this ubiquitin receptor seems to function independently from the Cdc48/Ufd2 pathway generating size-restricted ubiquitin chains (see above). However, with respect to the weak degradation deficiency caused by the single $\Delta rpn10$ mutant compared with the strong defect observed in the double mutant $\Delta rad23 \Delta dsk2$, the degradation via Rpn10 seems to play only a subsidiary role in ERAD.

All together this study demonstrates that ERAD proceed by an escort pathway of several ubiquitin-binding factors acting downstream of ubiquitin conjugation (Figure 3-2). This pathway strongly depends on Cdc48^{Ufd1/Npl4} for mobilization of (oligo-) ubiquitylated substrates but employs in subsequent steps different partially redundant factors that are involved in further ubiquitylation events and proteasome targeting. Which route is taken might depend primarily on the nature of the substrates and on the E3 enzyme(s)

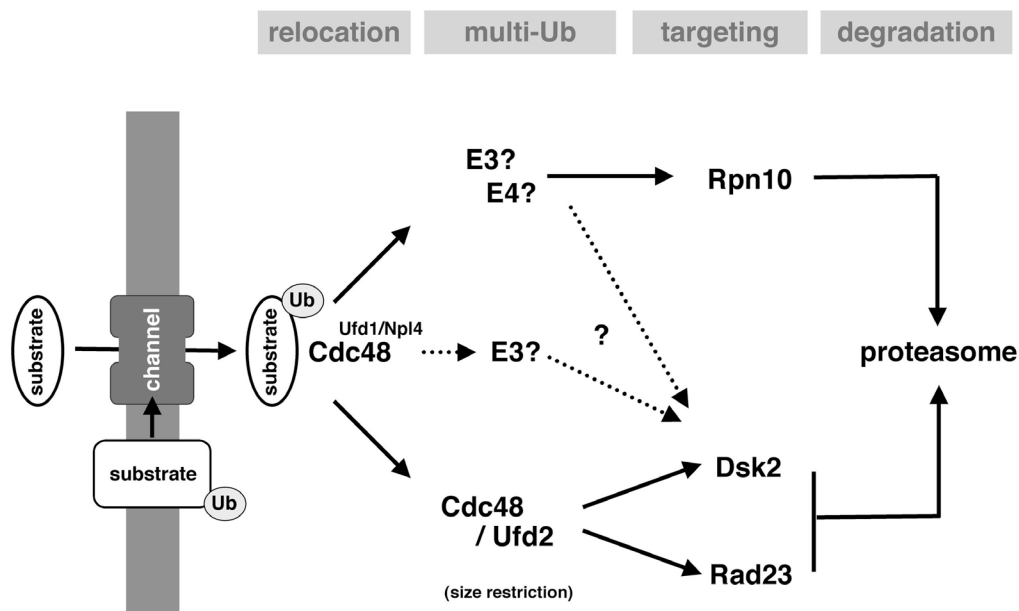


Figure 3-2. Model for substrate delivery to the proteasome by an escort pathway during ERAD.

Oligo-ubiquitylated substrates are recognized by Cdc48^{Ufd1/Npl4} at the cytosolic side of the dislocation channel and extracted upon ATP consumption. Subsequent multiubiquitylation by Ufd2 or other E3/E4 enzymes target them for proteasome delivery accomplished by the soluble ubiquitin receptors Rad23, Dsk2, or Rpn10. Multiubiquitylation mediated by Ufd2 in the presence of Cdc48 leads to the attachment of only a few ubiquitin molecules ('size restriction'), which are only recognized by Rad23 and Dsk2. Dashed lines indicate possible alternative routes between the parallel pathways.

involved in ubiquitin chain initiation. The guidance mechanism may ensure efficient degradation by coupling the events of multiubiquitylation and proteasome targeting. Furthermore, all ubiquitin-binding proteins may contribute to shield ubiquitin conjugates against the activity of ubiquitin hydrolases. However, the distinct factors apparently differ substantially concerning their binding properties: Ufd2 recognizes readily mono-ubiquitylated proteins, whereas Rad23 and Dsk2 preferentially bind to four or more ubiquitin moieties and Rpn10 even needs longer chains. Thus, ERAD may also take use of a loose 'ubiquitin number code' (Richly *et al.*, 2005), by which directionality may be provided.

3.2. Novel substrates of ERAD

Two novel substrates of ERAD could be identified by this study: the fatty acid desaturase Ole1 and the t-SNARE Ufe1, both implicated in essential cellular functions, i.e. fatty acid homeostasis and ER membrane fusion. Notably, both proteins do not represent abnormal proteins but are natural substrates of ERAD. Hence, ERAD of these substrates provides rather a function in regulation of physiological processes than a function in quality control.

3.2.1. Regulation of the fatty acid desaturase Ole1

3.2.1.1. Ole1 is a naturally short-lived protein and ERAD substrate

The fatty acid desaturase activity of Ole1 is exclusively regulated by adjusting the abundance of the ER protein Ole1, which takes place by a sophisticated regulon coined the OLE pathway. The expression of the *OLE1* gene is controlled via a negative feedback mechanism by UFAs (i.e. palmitoleic acid, 16:1 and oleic acid, 18:1), which are the products of the enzymatic reaction of the desaturase. Both transcription and mRNA decay are subject to this negative regulation (Choi *et al.*, 1996; Gonzalez, C. I. and Martin, 1996; Hoppe *et al.*, 2000). Thus, in order to ensure a rapid adaptation to cellular UFA requirements, Ole1 was assumed to be steadily turned over. Indeed, Ole1 was found to be short-lived *in vivo* (Figure 2-1) and to be degraded by ERAD (Figure 2-4). These findings substantiate the emerging view that ERAD is not restricted to quality control but also regulates the degradation of physiological substrates.

Interestingly, degradation of Ole1 resembles partially the pathway required for controlling its gene expression (see Figure 3-3): both the desaturase and the transcription factor Spt23 controlling the transcription of *OLE1* are mobilized by Cdc48^{Ufd1/Npl4} from the ER membrane (Figure 2-5; Rape *et al.*, 2001). Furthermore, degradation of both substrates involves E4 activity provided by Ufd2 and proteasome tar-

getting mediated by Rad23 and Dsk2 as well as Rpn10 (data not shown; Richly *et al.*, 2005). However, degradation of Spt23 is temporally and spatially separated from mono- or oligo-ubiquitylation at the ER membrane leading to its activation. Degradation of Spt23 is assumed to occur in the nucleus after the transcription of the *OLE1* gene has been initiated and may prevent hyperactivation of the OLE pathway (Richly *et al.*, 2005). Whether substrate ubiquitylation and segregation by Cdc48^{Ufd1/Npl4} result immediately in proteasomal degradation or in disassembly of oligomeric complexes may rely not only on the nature of the substrate but also on the mechanism of ubiquitylation (i.e. mono- or multiubiquitylation) and/or the requirement of accessory factors preventing the premature degradation.

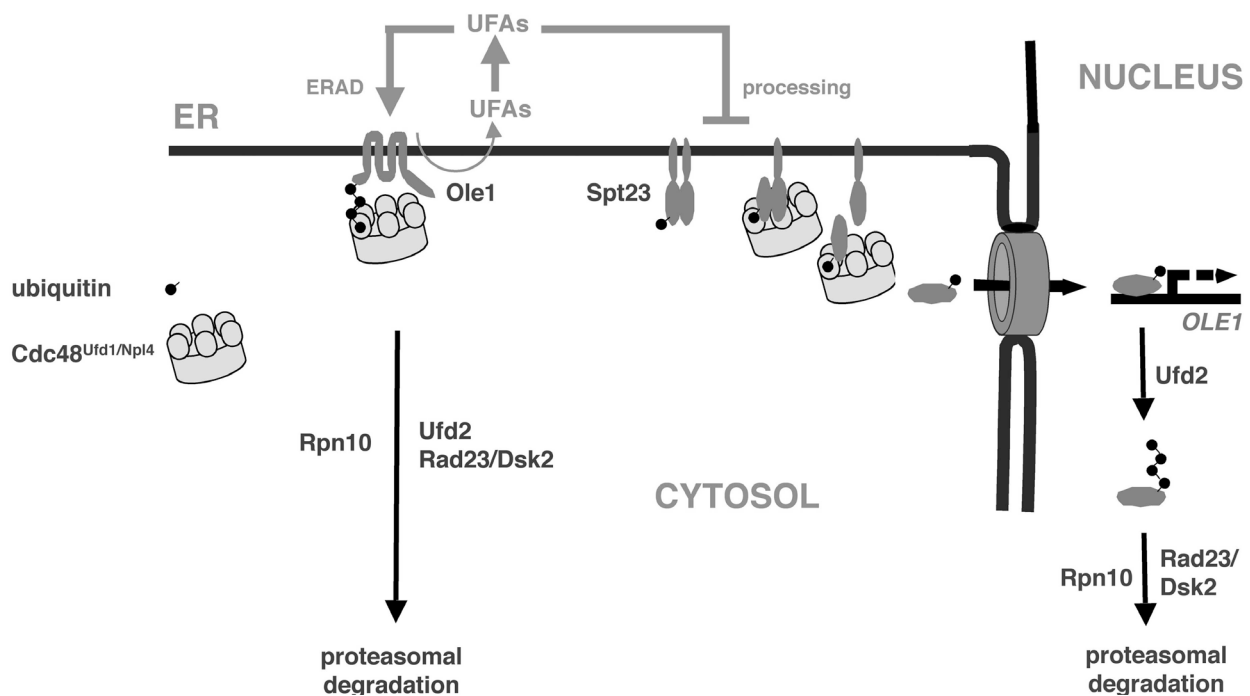


Figure 3-3. Proteolytic routes in the OLE pathway.

Upon ubiquitylation the fatty acid desaturase Ole1 is recognized by Cdc48^{Ufd1/Npl4} and extracted from the membrane. The transcription factor Spt23 is synthesized as a membrane-bound precursor (p120), which upon dimerization becomes ubiquitylated and subsequently processed by the 26S proteasome into the mature form (p90). Ubiquitylated, processed p90 is still bound to its uncleaved partner protein. Upon recognition by Cdc48^{Ufd1/Npl4}, p90 becomes mobilized and transported into the nucleus where it promotes the transcription of the *OLE1* gene. Both, Ole1 and processed Spt23 are multiubiquitylated and targeted to the 26S proteasome by similar pathways involving cytosolic and nuclear Ufd2 and Rad23/Dsk2, or Rpn10, respectively. Degradation of Spt23 probably takes place within the nucleus after the transcriptional activation of *OLE1*. Unsaturated fatty acids (UFAs) regulate both Ole1 degradation (positively) and Spt23 processing (negatively).

3.2.1.2. Ole1 turnover is regulated by unsaturated fatty acids

Besides the *OLE1* transcription and mRNA decay, degradation of Ole1 was also found to be subject to a negative feedback regulation by UFAs. Interestingly, depletion of UFAs or supplementation with saturated acids displayed a reciprocal effect. The rate of the turnover of Ole1 is modulated by a factor between 0.5 and 2 in the presence of palmitoleic acid (16:1) or its saturated counterpart palmitic acid (16:0), respectively (Figure 2-2 and data not shown). Such minor alterations in the degradation rate may still result in striking changes in the steady state levels of Ole1. Thus, the tight regulation of the entire OLE pathway highlights the importance of cellular homeostasis of fatty acids.

The control of the degradation of Ole1 by UFAs is reminiscent of the regulation of another yeast ERAD substrate, HMG CoA reductase (Hmg2). This enzyme plays a key role in setting the rate for the biogenesis of sterols and its derivatives and thus determines membrane composition along with Ole1 (for a review see Hampton, 1998). Interestingly, an intermediate of the mevalonate pathway, FPP (farnesyl pyrophosphate), which is produced downstream of the enzymatic reaction of Hmg2 and localizes to the ER membrane, stimulates the turnover of Hmg2. This indicates that a negative feedback mechanism exists for Hmg2 degradation analogous to Ole1 (Gardner and Hampton, 1999b). Hampton and colleagues demonstrated that entry of Hmg2 into the regulated degradation pathway requires the entire set of transmembrane domains and therefore referred to this structural property as 'distributed degron' (Gardner and Hampton, 1999a). According to this finding, they proposed a 'structural transition model', by which in the presence of FPP the normally stable protein Hmg2 undergoes structural changes within its transmembrane regions leading to its recognition as a quality control substrate by the ERAD machinery (Gardner *et al.*, 2001b).

It is tempting to speculate that Ole1 might be similarly regulated. However, one may pose the question what signal might be sensed by Ole1. Since exogenous fatty acids are taken up and incorporated into the phospholipid membrane (Bossie and Martin, 1989), UFAs might exert their regulatory effects either directly by interacting with the transmembrane domains of Ole1 or by changing the physical property of the membrane (i.e. fluidity, thickness). The fluidity of the lipid bilayer membrane is influenced by both the degree of saturation as well as the length of its fatty acid constituents. Thus, an enhanced fluidity may directly affect the diffusion of membrane proteins and thereby result in stochastically more frequent interactions between Ole1 and proteolytic factors (e.g. E3 ligases). Conversely, a reduced thickness of the membrane due to the incorporation of shorter fatty acids may affect the solvent exposure of membrane-buried residues within the transmembrane domains. This might induce a structural change of Ole1 leading to its recognition by ERAD similar to the 'structural transition model' proposed

by Hampton and colleagues. Intriguingly, Ole1 regulation is found to be more affected by shorter UFAs (i.e. 16:1 versus 18:1; Figure 2-2).

Besides the possibility that Ole1 functions as a direct sensor in the fatty acid composition of the ER membrane, other sensors might exist and contribute to Ole1 regulation. In particular, the processing of the ER membrane-anchored proteins Spt23 and Mga2 is similarly regulated by UFAs and thus requires also means of UFA sensing. Remarkably, degradation of Ole1 and its regulation by UFAs were found to be significantly affected in the $\Delta spt23 \Delta mga2$ mutant (Figure 2-3 and data not shown). This observation may give rise to the attractive hypothesis that Ole1 is directly associated with its transcription factors at the ER membrane and that UFA sensing is accomplished in a concerted manner through a multimeric signaling complex.

3.2.1.3. Implications of Ole1 on the fatty acid homeostasis

The importance of the homeostasis of fatty acid pools for the functional integrity and plasticity of the cellular vesicular system becomes evident by the depletion of endogenous unsaturated fatty acids (UFAs). A genetic screen in yeast for mutants with defects in mitochondrial distribution and morphology (*mdm* mutants) identified *MDM2* that encodes a fatty acid desaturase and is identical with *OLE1* (Stewart and Yaffe, 1991). The 2.5-fold decline of UFA levels associated with the temperature-sensitive *mdm2* allele correlates with a fragmentation of the reticular network of mitochondria and an accumulation of defective mitochondrial vesicles in the mother cell during cell division, which is reversible by supplementation with exogenous UFAs. Conversely, the excess of UFAs has also been found to be detrimental (Stukey *et al.*, 1990; Hoppe *et al.*, 2000). Thus, the intracellular UFA level has to be tightly controlled not only by the transcriptional activation of the *OLE1* gene by the OLE pathway but obviously also by regulating the turnover of the Ole1 protein by ERAD.

3.2.2 Regulation of the syntaxin SNARE Ufe1

The essential protein Ufe1 belongs to the family of syntaxin SNAREs and mediates the retrograde transport from the Golgi to the ER as well as homotypic membrane fusion of ER vesicles (Downing and Storms, 1996; Lewis *et al.*, 1997; Patel, S. K. *et al.*, 1998). Interestingly, whereas retrograde transport involves classical hetero-oligomeric SNARE complexes formed by one v-SNARE and three different t-SNAREs, homotypic membrane fusion requires the presence of Ufe1 molecules on both fusing vesicles, suggesting that Ufe1 forms homo-tetrameric complexes (Patel, S. K. *et al.*, 1998). Another significant difference in homotypic membrane fusion is the specific requirement for Cdc48 that is presumably engaged in disassembling Ufe1 SNARE complexes (Patel, S. K. *et al.*, 1998) similar to the function of Sec18^{Sec17} (NSF ^{α SNAP} in mammals). Cdc48 might

cooperate in this process together with its adaptor Shp1, analogous to mammalian p97, which works in conjunction with p47 in the reassembly of Golgi vesicles (Kondo *et al.*, 1997). In contrast to Ufe1 and Cdc48, Shp1 is not an essential protein, suggesting that either additional, redundant factors exist, or that the late step of homotypic membrane fusion (i.e. SNARE disassembly) is dispensable for viability. However, other factors that are directly involved in homotypic membrane fusion have not been identified in yeast so far. Previously, protein kinase C (Pkc1) was shown to be important for homotypic membrane fusion but the target of phosphorylation remains unknown. However, Ufe1 has been reported to be unstable in a *pkc1* mutant and to be turned over in a Ubc7-dependent manner, suggesting an involvement of ERAD (Lin, A. *et al.*, 2001).

The Sec1/Munc18 (SM) family member Sly1 is an essential, soluble hydrophilic protein and binds specifically to Ufe1 and the Golgi syntaxin Sed5 (Yamaguchi *et al.*, 2002). SM proteins were initially thought to function as negative SNARE regulators, since the vertebrate SM protein Munc18-1 binds to and stabilizes the so-called 'closed formation' of Syntaxin 1, in which the SNARE protein is incapable to assemble into *trans*-SNARE complexes (Dulubova *et al.*, 1999). However, various SM proteins were found to differ concerning the mode of interaction with their cognate SNARE partners. In fact, SM proteins seem to diverge with respect to their functions (Dulubova *et al.*, 2003). For instance, Sly1 fulfills a positive rather than negative function in ER to Golgi trafficking. The gain-of-function mutant *SLY1-20* was originally identified as a suppressor of the deletion of *YPT1* (suppressor of loss of *YPT1* function), which encodes a Rab GTPase involved in the early stage of vesicle tethering prior to SNARE assembly and membrane fusion (Dascher *et al.*, 1991; Ossig *et al.*, 1991). Besides its possible role in vesicle docking, Sly1 seems to be implicated in later stages of membrane fusion, i.e. assembly of Sed5 into Golgi *trans*-SNARE complexes (Kosodo *et al.*, 2002; Peng, R. and Gallwitz, 2002) and disassembly of *cis*-SNARE complexes mediated by Sec18^{Sec17} (Kosodo *et al.*, 2003). Very recent results have demonstrated that Sly1 is also involved in the Ufe1-mediated retrograde transport (Li *et al.*, 2005), indicating that Sly1 might also be required in other membrane transport processes. However, whether Sly1 also takes part in the Ufe1-mediated homotypic ER membrane fusion could not be addressed so far. Likewise, the molecular mechanism by which Sly1 contributes to membrane fusion remains obscure.

3.2.2.1. Sly1 protects Ufe1 from degradation

The previously reported requirement of protein kinase C for the stability of Ufe1 suggested that Ufe1 might be proteolytically regulated in response to environmental stimuli or during the cell cycle (Lin, A. *et al.*, 2001). The results presented here indicate that a cellular pool of Ufe1 is indeed constitutively ubiquitylated (Figure 2-10), however,

the majority of Ufe1 appears to be rather stable in WT cells. In contrast, Ufe1 is highly unstable in the conditional *sly1-1* mutant at its non-permissive temperature (Figure 2-11). Such a pronounced destabilization effect was not observed with a *pkc1-2* allele with the strain background used in this study (data not shown). Ufe1 was known to interact with Sly1 via a short stretch at its N-terminus and the phenylalanine residue at position 9 is crucial for this association (Yamaguchi *et al.*, 2002). Binding to this phenylalanine residue of Ufe1 is mediated by a hydrophobic pocket of Sly1 (Bracher and Weissenhorn, 2002). The generation of reciprocal mutations in the interaction face demonstrated that a stable interaction is necessary to confer Ufe1 stability (Figure 2-12), suggesting that Sly1 prevents degradation directly through binding to Ufe1. This was further confirmed by overproducing Ufe1. Whereas an excess of Ufe1 is ultimately degraded, simultaneous overexpression of *SLY1* significantly stabilized the overproduced levels of Ufe1 (Figure 2-13). By introducing ERAD mutants into *sly1-1* cells or by transforming a short-lived Sly1 interaction-deficient *ufe1* variant into WT cells, it could be demonstrated that turnover of destabilized Ufe1 proceeds largely by ERAD (Figure 2-14). Thus, one essential role of Sly1 in Ufe1-mediated membrane fusion is to regulate the stability of Ufe1 by preventing its breakdown through ERAD. This function is an intrinsic property of Ufe1 since Sed5 was not found to be destabilized in *sly1-1* cells in accordance with previous findings (Peng, R. and Gallwitz, 2002).

Remarkably, a similar stabilizing function has been reported for another SM protein. In cells lacking the non-essential SM protein Vps45, the corresponding SNARE protein Tlg2 is degraded by the 26S proteasome. Blocking proteasomal activity restored levels of Tlg2 but stabilized Tlg2 is non-functional and unable to bind to its cognate SNARE partners (Bryant and James, 2001). Thus, stabilization of Tlg2 seems to be not the only crucial function of Vps45 and a chaperone-like activity was proposed for this SM protein (Bryant and James, 2001). According to this, a similar requirement of Sly1 for Ufe1 besides its stabilization could also be assumed (see below).

One possibility by which the degradation of a proteolytic target can be regulated through a partner protein is to mask an internal degradation signal. This type of regulated proteolysis is found for example for the yeast MAT $\alpha 2$ repressor. The degradation signal within the Deg1 sequence of $\alpha 2$ overlaps with a binding motif for its partner protein **a1**. Thus, in the presence of **a1** the degron is not recognized by the E2/E3 enzymes and $\alpha 2$ is not degraded (Johnson, P. R. *et al.*, 1998). To assess whether a similar mechanism might be employed for the regulated degradation of Ufe1, different variants were generated by fusing N-terminal parts of Ufe1 to the stable ER protein Sec62. Certain fusion proteins were indeed found to be degraded in the absence of Sly1, indicating that a transferable degron in Ufe1 seems to exist (data not shown). However, the very N-terminal stretch carrying primarily the Sly1 interaction motif was not sufficient to con-

fer instability. Thus, Sly1 binding is supposed to prevent ERAD by another mechanism, for example by avoiding access through steric hindrance or by affecting the folding of Ufe1.

3.2.2.2. Sly1 availability balances the cellular pool of Ufe1

The strict regulation of Ufe1 through its binding to Sly1 suggests that Ufe1 levels have to be properly balanced within the cell. Indeed, when Ufe1 was stabilized in *sly1-1* by blocking proteasomal activity, the temperature sensitivity of the mutant was found to be augmented (Figure 2-15). In accordance with this finding, strong overexpression of *UFE1* caused a growth defect, which was partially reversible by concomitant overexpression of *SLY1* (Figure 2-16). This suggests that not the absolute amount of Ufe1 but the balance between Ufe1 and Sly1 might be important for cellular homeostasis.

This idea raised the question which cellular functions might be impaired by a surplus of Ufe1. The finding that overexpression of a Sly1 interaction-deficient *ufe1* mutant is less toxic than WT *UFE1* suggested that overexpression might affect specific cellular functions that particularly rely on Sly1. Thus, an excess of Ufe1 might result in the titration of the available cellular pool of Sly1 that normally is engaged with other partners, e.g. Sed5, which is also essential for viability. Reciprocally, overproduced Sed5 would be equally expected to interfere with the essential functions of Ufe1. Indeed, overexpression of *SED5* caused an even stronger cytotoxic effect (Figure 2-17), probably since Sed5 is intrinsically stable and cannot be proteolytically down-regulated contrary to Ufe1. Intriguingly, concomitant overexpression of *UFE1* but not of the Sly1 interaction-deficient *ufe1* mutant reduced the growth defect caused by the surplus of Sed5 (Figure 2-17). Likewise, the Sed5-mediated cytotoxicity could be compensated directly by overexpression of *SLY1* (data not shown). Since both SNAREs reside in different compartment – Ufe1 in the ER, Sed5 in the Golgi apparatus – it is unlikely that they interact directly with each other. Instead the attractive possibility could be envisaged that Ufe1 and Sed5 might communicate via a competition for available cellular pools of Sly1. This would provide an elegant mechanism by which both SNARE proteins and their respective vesicle fusion processes could be reciprocally regulated. However, whereas superfluous Ufe1 is disposed by ERAD, a similar mechanism does not seem to exist for Sed5.

Interestingly, Sly1 was found to be associated more tightly with Sed5 than with Ufe1 when examined by co-immunoprecipitations (data not shown) in agreement with previous findings (Yamaguchi *et al.*, 2002). This may suggest that under normal growth conditions the Sly1-dependent function of Sed5 (anterograde transport) may dominate over the Sly1-dependent function of Ufe1 (retrograde transport and homotypic fusion). Based on this assumption, an upregulation of Ufe1 and Sly1, or a downregulation of

Sed5 might result in a balance shift towards the Ufe1-mediated functions. Such a mechanism would ensure to coordinate the need for an increase in ER vesicle fusion under particular conditions, e.g. during/after mitosis, karyogamy, or sporulation. Intriguingly, Ufe1 and Sed5 were indeed found to be reciprocally regulated on the transcriptional level during sporulation (Chu *et al.*, 1998).

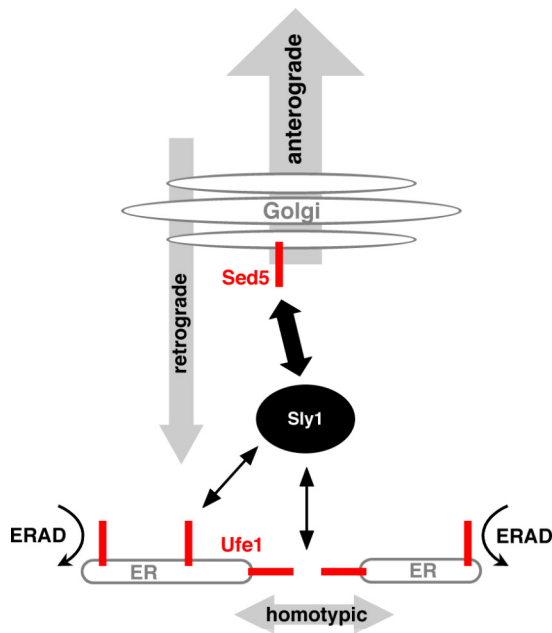


Figure 3-4. Hypothetical model for reciprocal regulation of Ufe1- and Sed5-mediated membrane fusion by the availability of Sly1.

Sed5 and Ufe1 may compete for cellular pools of Sly1 to mediate their respective functions, i.e. anterograde transport and retrograde transport/homotypic membrane fusion, respectively. The thickness of black arrows indicates the respective strength of the interaction between Sed5 or Ufe1 with Sly1, and the thickness of the grey arrows indicate the resulting activity of the respective transport pathways. Non-engaged (free) Ufe1 is turned over by ERAD.

3.2.2.3. A putative function of Sly1 in homotypic membrane fusion

The requirement of Sly1 for the stability of Ufe1 suggests that it may act in a chaperone-like manner by avoiding an unfavorable fold through its binding and thereby preventing the degradation of the SNARE protein. However, albeit Sed5-mediated transport also relies on Sly1, the stability of Sed5 is not regulated by the SM protein, suggesting that Sly1 may provide additional functions. It was therefore attractive to speculate that Sly1 might be also directly involved in the Ufe1-mediated processes of retrograde transport or homotypic membrane fusion (Lewis *et al.*, 1997; Patel, S. K. *et al.*, 1998). Indeed, a requirement of Sly1 for the Sec18-dependent retrograde transport has been reported recently (Li *et al.*, 2005). Conversely, homotypic membrane fusion involves Cdc48 (Latterich *et al.*, 1995; Patel, S. and Latterich, 1998). According to this, the observation of the synthetic temperature sensitivity of *sly1-1 cdc48-6* and *sly1-1 Δshp1* double mutants (Figure 2-18B) suspected Sly1 also to participate in ER homotypic membrane fusion. Furthermore, *cdc48-6* and *Δshp1* cells were found to be sensitized towards an excess of Sly1-unengaged Ufe1, which may act as dominant negative mutant in fusion (Figure 2-18A). Finally, Cdc48 and Shp1 were also found to be physically associated with Sly1 *in vivo* (Figure 2-18C). It remains to be clarified whether Sly1 interacts with the

single components or the assembled Cdc48^{Shp1} complex and whether this interaction is direct or bridged by Ufe1. Nonetheless it is tempting to speculate that Sly1 might be still bound to *cis*-SNARE complexes of Ufe1 and to assist in the late stage of membrane fusion.

Support for this notion comes from recent genetic data linking *SLY1* to *SEC18* and the finding that the Sec18-dependent disassembly of Golgi SNAREs is retarded in *sly1-1* cells (Kosodo *et al.*, 2002). The mammalian NSF^{αSNAP} complex has been shown to be sufficient to disassemble ternary SNARE complexes *in vitro*. However, Sly1 might still participate at this stage *in vivo*, e.g. by maintaining a favorable fold of the SNARE or by facilitating the recruitment of the disassembling ATPases (i.e. Sec18^{Sec17}, Cdc48^{Shp1}) to the SNARE complex.

3.2.2.4. Does Ufe1 ubiquitylation provides a link to SNARE disassembly?

Cdc48^{Ufd1/Npl4} has been primarily linked to ubiquitin/proteasome proteolysis. Conversely, p97^{p47} was originally assumed to mediate ubiquitin-independent functions. However, p47 and its yeast homolog Shp1 have recently been shown to bind to ubiquitylated proteins via their ubiquitin-associated (UBA) domains (Meyer *et al.*, 2002; Hartmann-Petersen *et al.*, 2004; Schuberth *et al.*, 2004). This and other findings revealed a functional link of ubiquitylation also to membrane fusion (for a review see Meyer, 2005). Still, neither the targets nor the function of ubiquitylation could be identified so far. However, the observation that Ufe1 (this study) and certain other SNARE proteins (Peng, J. *et al.*, 2003) are modified by ubiquitin gives rise to the attractive possibility that one function of ubiquitylation might be to target SNAREs in order to become specifically recruited to p97^{p47} and Cdc48^{Shp1}, respectively.

Interestingly, whereas Ufe1 was found *in vivo* to be partially associated with Cdc48 and Shp1 as judged by co-immunoprecipitation, no interaction could be demonstrated by yeast two-hybrid assays (data not shown). Furthermore, no specific interaction was detected between recombinant proteins, i.e. GST-Shp1 and Ufe1 (data not shown). These findings suggest that recruitment of Ufe1 by Cdc48^{Shp1} may either rely on the localization of Ufe1 to the membrane or require additional factors and/or modifications, for example ubiquitylation. Remarkably, ubiquitylated Ufe1 was found to be predominantly modified by only a few ubiquitin moieties in WT cells (Figure 2-10B). This finding may suggest a specific function for this type of ubiquitylation (e.g. in protein-protein interaction) besides the proteasome targeting role during ERAD, which requires exclusively longer chains. Cdc48 is assumed to act specifically on ubiquitylated substrates in order to segregate a modified protein from its non-modified partner(s). Interestingly, whereas *cis*-SNARE complexes disassembled by NSF/Sec18 are usually hetero-oligomers, Ufe1 SNARE complexes seem to exist as homo-oligomers. However,

a dissimilarity between the homomeric SNARE proteins could be accomplished by tagging only one specific Ufe1 molecule with ubiquitin. It may be possible that this distinction between the single SNARE partners may be required to allow the successful segregation of the Ufe1 SNARE complexes by Cdc48^{Shp1}.

3.3. General implication of ERAD in regulatory pathways

The growing number of native (i.e. not aberrantly folded) substrates emphasizes the view that ERAD is not solely a protein quality pathway involved in the elimination of misfolded or misassembled proteins of the ER. Contrary, ERAD seems to be implicated in different cellular pathways being mostly essential for viability. What might be the advantage of having this elaborate process? It might be the coupling of signal emitting, transducing and receiving directly at the place of action. As Hmg2 is the rate-limiting enzyme in the mevalonate pathway and able to sense the amount of produced sterols by its transmembrane domains (Hampton, 2002), the fatty acid desaturase Ole1 apparently employs a related mechanism to discern the content of unsaturated fatty acids (UFAs). The SNARE protein Ufe1 is regulated by the availability of its partner Sly1. Thus, all different pathways are able to regulate their activity by a direct feedback loop, and the surplus of the respective crucial factor is subject to degradation.

Intriguingly, despite the fact that these ERAD substrates do not represent abnormal proteins, the way by which they are degraded resembles the hallmarks of quality control. This surveillance mechanism utilizes primarily parameters that discriminate the folding state, the exposure of hydrophobic patches or the failure of protein-protein interactions in a long time scale. This is in contrast to the fast and temporally precise mechanisms used in signaling cascades such as phosphorylation (Laney and Hochstrasser, 1999). Hmg2 for instance is assumed to alter the conformation of its transmembrane domains upon high concentrations of the mevalonate intermediate FPP. Thus it enters the quality control pathway by changing its structure that now is recognized by Hrd1/Hrd3 (Hampton, 2002). It is very likely that Ole1 is regulated in a similar way since its four transmembrane domains are the most suitable candidates for sensing the UFA content within the membrane. Finally, the interaction of Sly1 with Ufe1 may prevent an unfavorable folding state of the SNARE protein that might tend to aggregate in isolation and thus be recognized by ERAD. Hence, regulated ERAD might have evolved from the ancient mechanism of protein quality control, as its substrates seem to adopt the characteristics of misfolded proteins in a controlled manner.

4. MATERIALS AND METHODS

The subsequent microbiological, molecular biological and biochemical are based on standard techniques (Sambrock *et al.*, 1989; Asubel *et al.*, 1994) or follow the manufacturers' instructions. When protocols have been modified, detailed information is provided. For all methods described, de-ionized sterile water, sterile solutions and sterile flasks were used.

Unless otherwise noted, chemicals and reagents (pro analysis grade) were purchased from Amersham-Pharmacia, Applied Biosystems, Biomol, Biorad, Difco, Fluka, Invitrogen, Kodak, Merck, New England Bioloabs, Promega, Roth, Roche, Riedel de Haen, Serva, or Sigma.

4.1. Computer-based analyses

For database researches (sequence search and comparison, literature research) electronic services were used provided by *Saccharomyces Genome Database* (<http://www.yeastgenome.org/>) and *National Center for Biotechnology Information* (<http://www.ncbi.nlm.nih.gov/>). DNA and protein sequence analyses (DNA restriction enzyme maps, DNA sequencing analyses, DNA primer design, protein sequence comparison) were done with *DNA-Star* (DNA Star Inc.). Chemiluminescence signals of immunoblots were detected by a CCD camera (LAS 1000, Fujifilm) and processed with the software programs *Image Reader LAS 1000 V1.1* (Fujifilm), *Image Gauge V3.01* (Fujifilm), and *Adobe Photoshop* (Adobe Systems Inc.). Autoradiography was detected by a phosphorimager (BAS 2500, Fujifilm) using the software *Image Reader BAS 2500 V1.4E* (Fujifilm). For the presentation of texts, tables and figures, software programs of the *Microsoft Office* packet (Microsoft Corp.) were used. For graph presentations and curve fits *Kaleidagraph* (Synergy software) was used.

4.2. Mikrobiological and genetic techniques

4.2.1. *E. coli* techniques

E. coli strains

XL1-Blue: hsd R17 rec A1 end A1 gyrA46 thi-1 sup E44 relA1 lac
[F' pro AB lacI^qZΔM15 Tn10 (Tet^r)] (Stratagene)
BL21 (DE3)/RIL: B F⁻ ompT hsdS(rB⁻ mB⁻) dcm+ Tet^r galλ (DE3) EndA
Hte [argU ileY leuW Cam^r] (Stratagene)

E. coli vectors

pet28a-c (Novagen)
pQE30 (Qiagen)
pGEX-4T1-3 (Amersham)

E. coli media

LB-medium (agar plates): 1% Trypton (Difco)
0,5% yeast extract (Difco)
1% NaCl
(1,5% agar)
sterilized by autoclaving

Cultivation and storage of *E.coli*

Liquid cultures were grown in LB media shaking at 200 rpm at 37°C except for protein expression (23° or 30°C). Cultures on agar plates were incubated at 37°C. For the selection of transformed bacteria, the following antibiotics were added to the media: ampicillin (50 µg/ml), chloramphenicol (24 µg/ml) or kanamycin (30 µg/ml). The culture density was determined by measuring the absorbance at a wavelength of 600 nm (OD₆₀₀). Cultures on solid media were stored at 4°C up to 7 days. For long-term storages, stationary cultures were frozen in 15% (v/v) glycerol solutions at –80°C.

Preparation of competent bacteria

E.coli vectors were transformed into competent cells either with calcium chloride or with electroporation for yielding higher efficiencies. For the preparation of competent cells, 1 l liquid LB medium was inoculated with 10 ml of an overnight culture derived from a single *E.coli* colony and grown to an OD₆₀₀ of 0.6-0.8 at 37°C. After chilling the culture flask in ice-cold water for 1 h, cells were harvested by centrifugation (5 min, 5000 g, 4°C). All following steps were performed with prechilled sterile materials and solutions at 4°C. For the preparation of chemically competent cells, sedimented cells were carefully resuspended in 200 ml MgCl₂ solution (100mM). The resuspended cells were pelleted by centrifugation, resuspended in 400 ml CaCl₂ solution (100mM) and after incubation of in ice-cold water for 20 min pelleted again. Finally, the competent cells were resuspended in 20 ml 100 mM CaCl₂ solution containing 10% (v/v) glycerol and stored in 100 µl aliquots at –80°C. For the preparation of electrocompetent bacteria, sedimented cells were washed once with 1 l water and once with 0,5 l water containing 10% (v/v) glycerol. After the last centrifugation step, cells were resuspended in 3 ml 10% (v/v) glycerol and stored in 100 µl aliquots at –80°C.

Transformation of plasmid DNA into bacteria cells

Competent cells were thawed on ice. For chemical transformation, 50 µl competent cells were mixed with 10 ng plasmid DNA and incubated on ice for 40 min. A heat shock was performed at 42°C for 20-90 s. Subsequently, the cell suspension was incubated on ice for 2 min and after adding 1 ml LB medium without antibiotics incubated on a shaker at 37° for 1 h. After recovery, transformed cells were selected by streaking out the cell suspension on LB agar plates containing the respective antibiotic(s) and incubated over night at 37°.

For electroporation, 25 µl competent cells were mixed with 10 ng plasmid DNA or 2 µl ligation sample dialyzed against water. The suspension was electroporated in a pre-chilled cuvette (0.1 cm electrode gap) with a pulse of 1.8 kV and 25 µF at a resistance of 200 Ω. After adding 1 ml LB medium without antibiotics, the suspension was transferred into a 12 ml polystyrene tube and incubated on a shaker at 37° for 1 h. Selection of transformants was carried out on antibiotic-containing LB agar plates over night at 37°.

Expression of proteins in *E.coli*

For the expression of recombinant proteins exclusively, the *E.coli* strain BL21(DE3)/RIL was used. Liquid LB medium was inoculated at a dilution of 1:100 with an overnight culture of a freshly transformed colony. The culture was incubated at either 23° or 37° depending on the expression construct and expression of the protein was induced by addition of IPTG (0.1-1 mM final concentration) at an an OD₆₀₀ of 0.6. Cells were harvested after 3-6 h after IPTG addition, and samples were taken before and after induction and analyzed for protein expression by SDS PAGE and coomassie staining. For purification of the expressed protein, cells were harvested by centrifugation (10 min, 5000 g, 4°C), washed in ice-cold PBS containing protease inhibitors and stored after shock freezing in liquid nitrogen at –80°C.

4.2.2. *S.cerevisiae* techniques

S.cerevisiae strains

Unless otherwise indicated all strains are isogenic to DF5. Mutant alleles from other strain backgrounds were introduced into DF5 by repetitive mating and tetrad dissection.

For the *pGAL1-10*-mediated overexpression experiments with *SED5*, the W303 wildtype strain (*ade2-1*, *his3Δ200*, *leu2-3,2-112*, *trp1-1(am)*, *ura3-52*; source: Kim Nasmyth) was used, which is better suited for growth on galactose-containing medium, especially in combination with cellular stress.

For Yeast-Two-Hybrid assays, the strain PJ69-4a was used:

MAT α , *trp901-*, *leu2-3,112*, *ura3-53*, *his3-200*, *gal4*, *gal80*, *GAL1::HIS3*, *GAL2-ADE2*, *met2::GAL7-lacZ* (James *et al.*, 1996)

Table 4-1: yeast strains

<i>S. cerevisiae</i> DF5 derivatives	genotype	source
DF5 diploid wt	<i>Y0001 his3Δ200, leu2-3,2-112, lys2-801, trp1-1(am), ura3-52</i>	Finley <i>et al.</i> , 1987
haploid wt	<i>Y0002 MATα</i> , derived from Y0001 by sporulation	
haploid wt	<i>Y0003 MATα</i> , derived from Y0001 by sporulation	
<i>ufd1-2</i>	<i>Y0473 ufd1-2</i>	Hoppe <i>et al.</i> , 2000
<i>pre1-1</i>	<i>Y0484 pre1::TRP1, pTX49pre1-1</i>	Mayer <i>et al.</i> , 1998
Δ <i>ubc6</i> Δ <i>ubc7</i>	<i>Y0571 MATα, ubc6::HIS3, ubc7::HIS3</i>	Mayer <i>et al.</i> , 1998
Δ <i>rpn10</i>	<i>Y0581 MATα, rpn10::HIS3</i>	Kögl <i>et al.</i> , 1999
Δ <i>ufd2</i>	<i>Y0598 MATα, ufd2::LEU2</i>	Johnson <i>et al.</i> , 1995
Δ <i>ufd2</i> Δ <i>rpn10</i>	<i>Y0598 ufd2::LEU2, rpn10::HIS3</i>	Kögl <i>et al.</i> , 1999
<i>cdc48-6</i>	<i>Y0649 cdc48-6</i>	Kai-Uwe Fröhlich
Δ <i>spt23</i> Δ <i>mga2</i>	<i>Y0749 spt23::hisG, mga2::LEU2</i>	Hoppe <i>et al.</i> , 2000
<i>ole1</i>	<i>Y0778 ole1::LEU2</i>	Hoppe <i>et al.</i> , 2000
<i>npl4-1</i>	<i>Y0801 npl4-1</i>	DeHoratious and Silver, 1996
Δ <i>shp1</i>	<i>Y0843 MATα, shp1::kanMX</i>	Braun <i>et al.</i> , 2002
Δ <i>cue1</i>	<i>Y0885 MATα, cue1::HIS3</i>	Biederer <i>et al.</i> , 1997
Δ <i>hrd1</i>	<i>Y0886 MATα, hrd1::TRP1</i>	Friedlander <i>et al.</i> , 2000
Δ <i>rad23</i>	<i>Y1043 MATα, rad23::kanMX</i>	Richly <i>et al.</i> , 2005
Δ <i>ufd2</i> Δ <i>rad23</i>	<i>Y1101 ufd2::LEU2, rad23::kanMX</i>	Richly <i>et al.</i> , 2005
Δ <i>dsk2</i>	- <i>MATα, dsk2::kanMX</i>	Richly <i>et al.</i> , 2005
Δ <i>rad23</i> Δ <i>dsk2</i>	- <i>MATα, rad23::kanMX, dsk2::kanMX</i>	Richly <i>et al.</i> , 2005
Δ <i>ufd2</i> Δ <i>dsk2</i>	- <i>MATα, ufd2::LEU2, dsk2::kanMX</i>	Richly <i>et al.</i> , 2005
<i>prc1-1</i>	<i>SGY001 MATα, prc1-1</i>	this study
<i>prc1-1 ufd1-2</i>	<i>SGY002 MATα, prc1-1, ufd1-2</i>	this study
<i>prc1-1 npl4-1</i>	<i>SGY003 MATα, prc1-1, npl4-1</i>	this study
<i>UFE1</i>	<i>SGY017 MATα, ufe1::kanMX, pUFE1-UFE1 (CEN/URA3)</i>	this study
<i>UFE1^{6HA}</i>	<i>SGY068 MATα, ufe1::UFE1^{6HA}::TRP1</i>	this study
<i>UFE1^{9myc}</i>	<i>SGY072 MATα, ufe1::UFE1^{9myc}::TRP1</i>	this study
<i>sly1-1 cdc48-6</i>	<i>SGY147 MATα, sly1::kanMX, pSLY1-sly1-1 (CEN/URA3), cdc48-6</i>	this study
<i>sly1-1 ufd1-2</i>	<i>SGY149 MATα, sly1::kanMX, pSLY1-sly1-1 (CEN/URA3), ufd1-2</i>	this study
<i>SLY1^{6HA}</i>	<i>SGY170 MATα, sly1::sly1^{6HA}::TRP1</i>	this study
<i>SLY1</i>	<i>SGY179 MATα, sly1::kanMX, pSLY1-SLY1 (CEN/URA3)</i>	this study
<i>sly1-1</i>	<i>SGY180 MATα, sly1::kanMX, pSLY1-sly1-1 (CEN/URA3)</i>	this study

Table 4-1: yeast strains (continued)

S. cerevisiae DF5 derivatives		genotype	source
<i>sly1-1 Δubc1</i>	SGY184	<i>MATα, sly1::kanMX, pSLY1-sly1-1 (CEN/URA3), ubc1::HIS3</i>	this study
<i>sly1-1 Δubc6 Δubc7</i>	SGY186	<i>MATα, sly1::kanMX, pSLY1-sly1-1 (CEN/URA3), ubc6::HIS3, ubc7::HIS3</i>	this study
<i>sly1-1 Δshp1</i>	SGY191	<i>MATα, sly1::kanMX, pSLY1-sly1-1 (CEN/URA3), shp1::kanMX</i>	this study
<i>sly1-1 pre1-1</i>	SGY325	<i>MATα, sly1::kanMX, pSLY1-sly1-1 (CEN/URA3)</i>	this study
<i>sly1-1 Δpep4</i>	SGY336	<i>MATα, sly1::kanMX, pSLY1-sly1-1 (CEN/URA3), pep4::HIS3</i>	this study
<i>UFE1^{6HA} SLY1^{9myc}</i>	SGY340	<i>MATα, ufe1::UFE1^{6HA}::TRP1, sly1::SLY1^{9myc}::TRP1</i>	this study
<i>UFE1^{9myc} SLY1^{6HA}</i>	SGY342	<i>MATα, ufe1::UFE1^{9myc}::TRP1, sly1::SLY1^{6HA}::TRP1</i>	this study
<i>UFE1^{6HA}</i>	SGY380	<i>MATα, ufe1::kanMX, pUFE1-UFE1^{6HA} (CEN/LEU2)</i>	this study
<i>sly1-1^{9myc}</i>	SGY381	<i>MATα, sly1::kanMX, pSLY1-sly1-1^{9myc} (CEN/LEU2)</i>	this study
<i>sly1-V156P^{9myc}</i>	SGY382	<i>MATα, sly1::kanMX, pSLY1-sly1-V156P^{9myc} (CEN/LEU2)</i>	this study
<i>sly1-L137R^{6HA}</i>	SGY383	<i>MATα, sly1::kanMX, pSLY1-sly1-L137R^{6HA} (CEN/LEU2)</i>	this study
<i>SLY1^{9myc}</i>	SGY384	<i>MATα, sly1::kanMX, pSLY1-SLY1^{9myc} (CEN/LEU2)</i>	this study
other S. cerevisiae strains			
<i>cim5-1</i>	Y0355	<i>MATα, cim5-1, ura3-52, leu2Δ1, his3Δ200</i>	Carl Mann
<i>sec61-R2</i>	Y1015	<i>MATα, sec61::HIS3, ade2-1, can-100, his3-11,15, leu2-3, trp1Δ1, ura3-3, pSEC61-sec61-R2, pUPRE-lacZ (pMZ11)</i>	Zhou and Schekman, 1999

S.cerevisiae vectors

CEN plasmids: pYCplac33 (*URA3*), pYCplac22 (*TRP1*), pYCplac111 (*LEU2*)
 2μ plasmids: pYEplac195 (*URA3*), pYEplac112 (*TRP1*), pYEplac181 (*LEU2*)
 integrative plasmids: YIplac211 (*URA3*), pYIplac204 (*TRP1*), pYIplac128 (*LEU2*)
 (Gietz and Sugino, 1988)

Yeast-Two-Hybrid vectors: pGAD-C1-3, pGBD-C1-3 (James *et al.*, 1996)

S.cerevisiae plasmids

The *OLE1* ORF was amplified from a cDNA library and cloned into *YIplac211* containing three N-terminal myc-tags (3myc). Expression was driven by the *GAL1-10* promoter. The *ole1-AA* mutant expressing the physiologically inactive desaturase was constructed by site-directed mutagenesis exchanging the two conserved, essential histidine residues with alanine (H161A and H166A; see Figure 1B). Both constructs were inserted into the *URA* locus of *ura3-52* strains by linearizing the vectors with *EcoRI*. The protein ^{Deg1}SEC62 expressed from a *GAL1-10* promoter is analogous to the ^{Deg1}SEC62^{FLAG} construct described previously (Mayer *et al.*, 1998), except that it has a FLAG tag N-terminal of SEC62 (^{Deg1}-FLAG^{SEC62}). The ^{6myc}HMG2 construct (*pRH244*) was a gift by R. Hampton. The *prc1-1* construct (*pRS306-prc1-1*) used for the expression of CPY* was obtained by T.Sommer and was originally described by D.Wolf. It was inserted into the *PRC1* locus by linearizing the vector with *BglII*. Myc-tagged ubiquitin was expressed from a 2μ plasmid (YE96) under the control of copper promoter obtained by M.Hochstrasser. The plasmid expressing Ub-ProbGal (Bachmair and Varshavsky, 1989) was a gift by A. Varshavsky. Plasmids expressing *UFE1*, *SLY1*, and *SED5* were cloned by PCR amplification of genomic DNA. For examination of expression at the endogenous level, the respective ORF was cloned with its 5'UTR usually covering the upstream sequence until the

next stop codon. However, for the expression of *UFE1* the upstream 247 bp sequence has been shown to be sufficient for appropriate expression (Lewis *et al.*, 1997) and, hence, was used for cloning *pUFE1-UFE16HA* and *pUFE1-ufe1-F9A^{BHA}*. C-terminal epitope-tagged variants of *UFE1* and *SLY1* were cloned by genomic PCR with chromosomally tagged strains.

***S.cerevisiae* media and solutions**

YPD / YPGal (agar plates):	1%	(10 g/l)	yeast extract (Difco)
	2%	(20 g/l)	bacto-peptone (Difco)
	2%	(20 g/l)	D-(+)-glucose or galactose
	(2%	(20 g/l)	agar)
			sterilized by autoclaving

YPD G418 plates After autoclaving, YPD medium including 2% agar was left at room temperature until cooled to 50°C. Just prior to pouring, G418 (geneticine disulphate; Sigma) was added as powder (final concentration 200 mg/l).

YPD oleic acid plates: as above, but instead oleic acid (Sigma) was mixed with an equal volume of Nonidet P40 (NP40) and added to the medium prior to pouring to a final concentration of 0.2% (v/v) each.

SC-media/plates:	0.67%	(6,7 g/l)	yeast nitrogen base (Difco)
	0.2%	(2 g/l)	drop out amino acid mix (according to the requirements)
	2%	(20 g/l)	carbon source (glucose, raffinose, or galactose)
	(2%	(20 g/l)	agar)

SC-5'FOA plates:	0.67%	(6,7 g/l)	yeast nitrogen base (Difco)
	0.2%	(2 g/l)	drop out amino acid mix (according to the requirements)
	3%	(30 g/l)	adenine
	3%	(30 g/l)	uracil
	2%	(20 g/l)	carbon source (glucose, raffinose, or galactose) solved in 500 ml water
	2%	20 g/l	agar / 500 ml water, autoclaved

After medium and molten agar were mixed and left until cooled to 50°C, 1 g 5'FOA was added (final concentration 1 g/l) and stirred up to complete dissolving prior to pouring.

drop out amino acid mix:	20	mg	Ade, Ura, Trp, His; 30 mg Arg, Tyr, Leu, Lys
	50	mg	Phe
	100	mg	Glu, Asp
	150	mg	Val
	200	mg	Thr
	400	mg	Ser

Sporulation medium:	2% (w/v)	potassium acetate (in sterile water)
---------------------	----------	--------------------------------------

SORB:	100 mM	LiOAc
	10 mM	Tris-HCl, pH 8.0
	1 mM	EDTA, pH 8.0
	1 M	sorbitol
		sterilized by filtration

PEG:	100 mM	LiOAc
	10 mM	Tris-HCl, pH 8.0
	1 mM	EDTA, pH 8.0
	40 % (w/v)	PEG-3350
		sterilized by filtration, stored at 4°C
Zymolase 20T solution:	0.9 M	sorbitol
	0.1 M	Tris-HCl, pH 8.0
	0.1 M	EDTA, pH 8.0
	50 mM	DTT (add freshly)
	0.5 mg/ml	zymolase 20T (ICN Biochemicals)

Cultivation and storage of *S.cerevisiae*

Liquid starter cultures were usually inoculated with a single yeast colony from strains freshly streaked on plates and grew at 30°C in a shaking incubator over night or for 2 days (temperature sensitive strains at 23°C). The main culture was inoculated with the starter culture at a dilution of 1:100 – 1:1000, and growth was carried out in a shaking incubator at 150-250 rpm (depending on the volume of the culture) until the culture had reached the mid-log phase growth ($1-5 \times 10^7$ cells/ml). The culture density was determined by measuring the absorbance at a wavelength of 600 nm (OD_{600}). An OD_{600} of 1 is equal to 1.5×10^7 cells/ml. Cultures on solid media were stored at 4°C up to 1-2 months. For long-term storages, stationary cultures were frozen in 15% (v/v) glycerol solutions at –80°C.

Preparation of competent yeast cells

For transformation by the lithium acetate method, competent yeast cells were prepared as follows: 50 ml of a mid-log phase growing culture was harvested by centrifugation (500 *g*, 5 min, room temperature), washed once with 1/5 volume sterile water, once with 1/10 volume SORB solution and resuspended in 360 μ l SORB solution. After adding of 40 μ l carrier DNA (salmon sperm DNA, 10 mg/ml, Invitrogen), competent cells were stored in 50 μ l aliquots at –80°C.

Transformation of yeast cells

For transformation ~ 0.2 μ g of circular or ~ 2 μ g linearized plasmid DNA (or PCR products) were mixed with 10 μ l or 50 μ l competent cells, respectively. After adding 6 volumes of PEG solution, the cell suspension was incubated at 30°C for 30 min. Subsequently, DMSO (final concentration 10%) was added and a heat shock performed at 42°C for 15 min. After that, cells were sedimented by centrifugation (400 *g* for 3 min at room temperature) and resuspended in 100 μ l sterile water. Selection of transformants was carried out on the respective SC medium plates for 2-3 days at 30°C (or room temperature in case of temperature sensitive strains). When the antibiotic G418 was used for selection, transformed cells were incubated for 3-12 hours in liquid YPD medium before they were streaked out onto plates containing G418. If necessary, transformants were replica-plated on G418 containing YPD plates to dissect true positive transformants from false-positive clones expressing the G418/Kan resistance marker only transiently.

Genomic integration by homologous recombination

For the stable integration of a plasmid-encoded gene (integrative transformation), the ORF was cloned together with the respective promoter (endogenous, conditional, or constitutive) and a yeast terminator (usually 200 bp of the sequence 3' downstream from the stop codon of *ADH1*) into the multiple cloning site of integrative vectors of the YIplac series (Gietz and Sugino, 1988). These vectors contain no autonomous replication (*ARS/CEN*) elements, thus only stably integrated vectors are propagated in yeast. In addition, integrative vectors encode selectable mark-

ers conferring auxotrophy for nutrients, which after transformation and stable integration into the chromosomal locus can complement mutant alleles. To increase the efficiency of the integration event, vectors are usually linearized by introducing double strand breaks within the auxotrophy marker gene with the help of restriction enzymes (i.e. *EcoRV*, *StuI*). After transforming into yeast cells, the free DNA ends of the marker gene on the linearized plasmid recombine with the homologous DNA sequences at the endogenous locus of the marker gene and enable the vector to integrate. This results in the duplication of the auxotrophy marker and the insertion of the gene of interest in between on the chromosomal locus.

A similar strategy was applied for the replacement of the endogenous locus by mutant alleles (transplacement). This method was used for the replacement of the *PRC1* locus encoding the vacuolar protease carboxypeptidase Y (CPY) by the *prc1-1* allele carrying a point mutation, which results in the expression of the mutant unstable variant CPY*. In this case, the integrative plasmid harbors the *prc1-1* allele besides the *URA3* gene as a selectable marker. But contrary to the method described above, homologous recombination is not targeted to the marker gene but to the *PRC1* locus by linearizing the integrative plasmid within the *prc1-1* allele with the restriction enzyme *BglII*. Recombinant cells were selected by their ability to grow in the absence of Ura within the medium, revealing that the *URA3* marker and the *prc1-1* allele have been inserted into the *PRC1* locus ('pop-in'). Subsequently, cells were selected on a second recombination event that resembles in principle a reversion of the first one, by which the *URA3* marker and parts of the *PRC1/prc1-1* gene have been lost ('pop-out'). This type of recombination event is monitored by negative selection in presence of the pyrimidine analogue 5'FOA (5'-fluoroorotic acid), which results in a toxic intermediate only when *URA3* is expressed. Since the second recombination event can take place at any position within the *PRC1/prc1-1* locus, recombinants can be screened for being *URA3* negative but still harboring the point mutation of the *prc1-1* allele. This was accomplished by isolation of the *PRC1* locus via PCR of genomic DNA combined with restriction analysis of the PCR product with *BstXI*, which yields an additional cleavage product for the *prc1-1* encoded sequence.

The insertion of gene deletions or epitope tags on chromosomes was accomplished by a PCR strategy (Longtine *et al.*, 1998; Knop *et al.*, 1999). Besides the sequences for amplification of the PRC cassette, the oligonucleotides contain the flanking sequences of the target gene to allow homologous recombination within the endogenous locus. For gene deletions, usually 50 bp of the promoter sequence 3' of the start ATG (S3 primer), and 50 bp of the terminator sequence 5' of the stop codon (S2 primer), respectively, serve as complementary sequences to the target gene. For the insertion of C-terminal epitope tags, the S3 primer contains 50 bp 3' of the stop codon instead. The PCR cassette includes the respective tag with the *ADH1* terminator as well as a marker gene for selection with promoter and terminator. After amplification of the cassette, the PRC product was precipitated with ethanol and transformed into competent yeast cells. Recombination occurs alike the insertion of integrative plasmids. In the case of epitope tag insertion, the endogenous stop codon of the endogenous target gene is replaced by the epitope sequence enclosing a separate stop codon. The recombination event was analyzed either by PCR, immunological methods, or tetrad dissection of spores derived from diploid transformants.

Mating type analysis of haploid strains

For the analysis of the mating type, the tester strains RC634a and RC75-7 α were used for growth assays. These strains are hypersensitive to the pheromone secreted by the opposite mating type strain. 75 μ l of an aqueous cell suspension of each tester strain was mixed with 7.5 ml of a molten 1% (w/v) agar solution that has been cooled down to 45°C, and poured on YPD plates as top agar. Strains to be analyzed were replica plated on the a- and α -tester top agar plates. After 1-2 days of incubation, the tester strains were grown densely within the top agar

unless the colonies of the replica-plated strain displayed the opposite mating type. In this case, halos appeared around the colonies according to the hypersensitivity of the tester strain against the secreted pheromone. Diploid cells do not secrete any mating type pheromones, therefore no halo formation is seen with both mating type tester strains.

Mating of haploid *S.cerevisiae* strains

Haploid strains of opposite mating types ($MATa$, $MAT\alpha$) grown to mid-log growth phase were mixed together by spotting 10 μ l of each on a pre-warmed YPD plate. After incubation at 30°C for 3-4 h, mated yeast cells (zygotes) became distinguishable from haploid cells by their specific morphology ('mexican hut': a polar lobe with a bud in the middle). Zygotes were isolated by a micromanipulator (Singer MSM Systems). Alternatively, when the original haploid strains display different auxotrophy markers, cells were streaked after mating onto the respective selection plates to select diploid cells.

Sporulation and tetrad analysis of diploid *S.cerevisiae* strains

Diploid cells of a stationary culture (500 μ l) were harvested by centrifugation (500 g, 3 min), washed 4-5 times with sterile water and resuspended in 5 ml sporulation medium. After incubation on a shaker at 23°C for 3 days, 10 μ l sporulated cells were mixed with 10 μ l zymolase-20T solution and digested at 23°C for 10 min. The spores of the sporulated cells (asci) were dissected in tetrads by the use of a micromanipulator (Singer MSM Systems). Germination and growth of the spores were carried out on non-selective YPD plates for 2-3 days. Subsequently, tetrads were analyzed genotypically by replica plating on selection plates and/or incubating at the permissive and non-permissive temperatures.

Analysis of protein-protein interactions with the Two-hybrid-system

Proteins being analyzed by two-hybrid interaction assays were fused at their N-terminus to the DNA-binding and activation domain of the Gal4 protein by cloning the respective full-length or truncated ORFs into *pGAD424* and *pGBD* vectors, respectively. Various combinations of 'bait' and 'prey' plasmids were transformed into PJ69-7A cells (James *et al.*, 1996) and were plated on SC-Leu-Trp plates. Transformants were streaked onto SC-Leu-Trp-His and SC-Leu-Trp-Ade plates. A successful interaction of bait and prey results in the reconstitution of the Gal4 transcription activator and thus the expression of reporter genes under the control of Gal4 (i.e. *HIS3*, *ADE2*) and allow yeast cells to grow on the respective selection media.

Phenotype analysis by growth tests

To analyze the phenotype (e.g. temperature sensitivity) of yeast strains, serial dilutions of yeast cultures were spotted onto YPD plates and incubated at different temperatures for several days. This method allows comparing colony growth and formation of cells from different strains spotted at equal numbers and gives more reliable results than streaking out a single colony. Yeast cultures grown in YP or selective media to mid-log growth phase were diluted with sterile water to an OD_{600} of 0.1 that is equal to 1.5×10^6 cells. With this starter dilution, 4-5 following dilutions were prepared in a ratio of 1:5 or 1:10 (five- or ten-fold dilution) usually in 96-well microtiter plate. The cell suspension dilutions were plated onto YP or selection plates by the use of a stamp with a pin array corresponding to the grid of the 96-well plate (either 48 or 96 pins). The stamp was briefly dipped into the wells, taken out quickly to avoid losing the cell suspension drops on the pins, put onto the medium plate and left there for 20-30 s to ensure that the cell suspension drops are efficiently come off the pins. The amount of cell suspension put onto the plate by this method equals a volume of 3 μ l.

Promoter shut-off and cycloheximide chase experiments

To determine the stability of proteins either the transcription of the particular gene was selectively turned off by using a repressible promoter (shut-off experiments), or the total cellular translation was blocked by addition of the translation inhibitor cycloheximide (cycloheximide chase), or both approaches were combined (expression shut-off experiment). By this method, any *de novo* protein synthesis is blocked that allows studying exclusively the decay of the given protein in a time course experiment.

For expression shut-off experiments, usually the gene of interest was fused to the inducible *GAL1-10* promoter, which is only active in presence of galactose but repressed in presence of glucose in the medium. Strains of the DF5 background require being adapted to galactose as carbon source. Usually they were let grown on raffinose/galactose plates (both 2% w/v) before they were inoculated in only galactose-containing liquid medium (in presence of raffinose the *GAL1-10* promoter is de-repressed but still not active). Starter cultures under these conditions need several days to grow to saturation. For preparation of the main culture, usually 25 ml YPGal or SC-Gal medium (2% v/w galactose) was inoculated with 100 μ l or 300 μ l of a saturated starter culture grown in the respective medium (in the case of yeast strains displaying a substantially prolonged cell cycle even at 23°C, the inoculation volume was accordingly increased). After 12-15 h shaking at 23°C, the culture was grown to mid -log growth phase ($OD_{600} = 0.5$). Whereas yeast strains without any temperature sensitivity were incubated at 30°C for 1-2 h, temperature sensitive mutants were shifted to the non-permissive temperature (usually 37°C) for 2-3 h prior to the start of the shut-off experiment (except when the protein stability of Ufe1 was examined in strains carrying *slp1* mutant alleles; in this case cells were shifted to 37°C directly at the beginning of the kinetic). The time course was started by sedimenting the cells (500 g, 5 min, 23°C) and resuspending them in YPD containing 0.5 mg/ml cycloheximide in an appropriate volume corresponding to $OD_{600} = 1$. After taking the zero point sample (normally 1 ml corresponding to 3×10^6 cells) cultivation was continued and further samples were harvested at the time-points indicated. Note that in order to avoid a dilution effect the same volume but not the same cell number compared to the zero point sample was taken (even when cells momentarily continue to divide, the amount of the given protein does not increase due to the transcriptional and translational block). Proteins extracts were performed by NaOH lysis and TCA precipitation as described (Knop *et al.*, 1999) and analyzed by immunoblots.

For studying the turnover of proteins encoded by genes under the control of the endogenous or the constitutive *ADH1* promoter, cycloheximide chase experiments were performed. For preparation of the main culture, usually 25 ml YPD or selective medium containing glucose (2% v/w) was inoculated with 25 μ l or 100 μ l of a saturated starter culture grown in the respective medium. Translational arrest was induced by adding cycloheximide to the medium to a final concentration of 0.5 mg/ml. Cell lysis and sample preparation were done as described above.

Pulse chase assays

Metabolic labeling of cells with radioactive [³⁵S]-methionin allows studying the decay of exclusively *de novo* synthesized proteins during the pulse period and thus to determine directly the half-life of a protein. This method was applied for studying the turnover of the ERAD substrate CPY*.

To induce efficiently the expression of the *PRC1* gene encoding the vacuolar protease CPY or its mutant variant CPY* (by the mutant allele *prc1-1*), late-log phase cells were starved for nitrogen following the protocol modified from M.Knop (see Finger *et al.*, 1993):

labeling medium:	6.7	g/l	yeast nitrogen base w/o (NH ₄) ₂ SO ₄ w/o amino acids
	20	g/l	glucose
	2	g/l	drop out mix, pH adjusted to 6.0; sterilized by filtration
	25	μCi	[³⁵ S]-methionine (Amersham-Pharmacia)/per OD ₆₀₀ .cells added separately
chase medium:			as labeling medium but with:
	6 mg/ml		methionine (40 mM)
	2 mg/ml		BSA (fraction V, Sigma)

Synthetic medium (10 ml) was inoculated with a saturated starter culture resulting in an OD₆₀₀ = 0.4 and was let grown for 5-6 h at the respective temperature. Cells grown to an OD₆₀₀ = 2.0-2.8 (corresponding to a cell amount of 10 OD₆₀₀) were sedimented (500 g at 23°C for 5 min) and carefully washed 3 times with labeling medium (without radioactive [³⁵S]-methionine). After the final wash step cells were resuspended in labeling medium corresponding to an OD₆₀₀ = 10 and incubated at the respective temperature for 1 h. Subsequently, cells were metabolically labeled by adding 25 μCi [³⁵S]-methionine per 1 OD₆₀₀. After 15 min the chase was initiated by adding an equal volume of pre-warmed chase medium. Samples corresponding to 2 OD₆₀₀ were taken at time-points indicated and cell pellets frozen in liquid nitrogen. Proteins extracts were performed by NaOH lysis and TCA precipitation and subjected to immunoprecipitation under denaturing conditions with an antibody against CPY. Finally, samples were analyzed by SDS-PAGE and autoradiography (see 4.4.3.).

4.3. Molecular biological methods

General buffers and solutions

TE buffer	10	mM	Tris-HCl, pH 8.0
	1	mM	EDTA
			sterilized by autoclaving
TBE buffer 5x stock	90	mM	Tris
	90	mM	boric acid
	2.5	mM	EDTA, pH 8.0
			sterilized by autoclaving
DNA loading buffer 10x	0.5%	(w/v)	SDS
	0.25%	(w/v)	bromophenol blue or orange G
	0.25%	(v/v)	glycerol
	25	mM	EDTA, pH 8.0

4.3.1. Isolation of DNA

Isolation of plasmid DNA from *E.coli*

LB medium (usually 4 ml) containing the appropriate antibiotic was inoculated with a single *E.coli* colony harboring the DNA plasmid of interest and shaken for 8-14 h at 37°C. Plasmids were isolated using kits from the companies Qiagen (plasmid mini kit) or Macherey-Nagel (nucleospin plasmid quick pure) according to the manufacturers' instructions.

Isolation of plasmid DNA from *S.cerevisiae*

Breaking buffer	2%	(v/v)	Triton X-100
	1%	(v/v)	SDS
	100	mM	NaCl
	10	mM	Tris-HCl, pH 8.0
	1	mM	EDTA, pH 8.0

Plasmid DNA was released from a yeast transformant along with chromosomal DNA by a rapid isolation protocol for direct propagation in *E.coli*. A yeast culture (1.5 ml) grown to saturation was transferred to a microcentrifuge tube and spun 5 s at high speed at room temperature. The sedimented cells were resuspended in 200 μ l breaking buffer. After adding of 0.3 g acid-washed glass beads (~ 200 μ l volume; \varnothing 425-600 μ m; Sigma) and 200 μ l phenol/chloroform/isoamyl alcohol (24:24:1 v/v/v; Roth) cells were lysed by vortexing 2 min at highest speed. Centrifugation at high speed for 5 min at room temperature yielded an aqueous phase containing the DNA, of which 0.5 μ l were used for transformation of *E.coli* for plasmid propagation.

Isolation of chromosomal DNA from *S.cerevisiae*

Chromosomal yeast DNA was isolated as template for the amplification of yeast genes via PCR. Cells from a saturated yeast culture (10 ml) were sedimented by centrifugation (1500 g, 5 min, 23°C), washed once in 0.5 ml water and resuspended in 200 μ l breaking buffer. After adding of 0.3 g acid-washed glass beads (~ 200 μ l volume; \varnothing 425-600 μ m; Sigma) and 200 μ l phenol/chloroform/isoamyl alcohol (24:24:1 v/v/v; Roth) cells were lysed by vortexing 3 min at highest speed. The lysate was mixed with 200 μ l TE buffer, centrifuged for 5 min at high speed at 23°C and the aqueous layer transferred to a microcentrifuge tube. DNA was precipitated by adding 1 ml ethanol (100%) and centrifugation at high speed for 3 min at 23°C. The pellet was resuspended in 0.4 ml TE buffer. RNA contaminants were eliminated by adding 30 μ l of DNase-free RNase A (1 mg/ml) and incubated for 5 min at 37°C. Afterwards, DNA was precipitated by adding 10 μ l of ammonium acetate (4 M) and 1 ml ethanol (100%), briefly centrifuged and the pellet resuspended in 100 μ l TE buffer. The yield of the DNA isolation was estimated by analytical restriction digestion and visualizing of the fragments on an agarose gel.

Precipitation of DNA

For ethanol precipitation 1/10 volume sodium acetate (3 M, pH 4.8) and 2.5 volume ethanol were added to the DNA solution and incubated at -20°C for 30 min. Subsequently, the DNA solution was centrifuged at 16000 g at 4°C for 20 min. The DNA pellet was washed once with 0.5 ml 70% ethanol. After centrifugation the DNA was air-dried and resuspended in an appropriated volume of TE buffer or sterile water.

Determination of DNA concentration in solution

The DNA concentration was photometrically determined by measuring the absorbance at a wavelength of 260 nm (OD_{260}). An $OD_{260} = 1$ equals a concentration of 50 μ g/ml double-stranded DNA.

4.3.2. Molecular cloning methods

Restriction digestion of DNA

The sequence-specific cleavage of DNA with restriction enzymes was performed according to standard protocols (Sambrook *et al.*, 1989) and the instructions of the manufacturer (NEB). Usually, 5-10 units restriction enzyme was used for the digestion of 1 μ g DNA. Reaction sam-

ples were incubated in the appropriate buffer at recommended temperature for 30-60 min or >2 h for analytical and preparative purposes, respectively. To avoid the recirculation of linearized vectors the 5' end of vector DNA was dephosphorylated by adding 5-10 units shrimp alkaline phosphatase (Roche) and incubating at 37°C for 30 min. Subsequently, the alkaline phosphatase was heat-inactivated at 70°C for 15 min.

Separation of DNA fragments by gel electrophoresis

For analytical and preparative isolation DNA fragments were electrophoretically separated on 0.8 - 2% agarose gels containing ethidium bromide (final concentration 0.5 µg/ml). DNA samples were mixed with 6x DNA loading buffer and electrophoretically separated at 100 volts in TBE buffer. DNA fragments could be visualized by the intercalation of ethidium bromide into DNA by using a UV transilluminator (324 nm). The size of the fragments was estimated by standard size markers (1 kb DNA ladder, Invitrogen).

Isolation of DNA fragments from agarose gels

After gel electrophoresis the DNA fragment was isolated by excising the respective piece of agarose using a razor blade. The DNA was extracted from the agarose block using kits of the companies Qiagen (QIAExII, QIAquick gel extraction kit) or Macherey-Nagel (nucleospin extract II) according to the manufacturers' instructions and eluted with an appropriated volume of elution buffer (10 mM Tris-HCl, pH 8.5).

Ligation of DNA fragment

The respective amounts of isolated DNA fragments ('insert') and linearized vectors were estimated on an ethidium bromide-containing agarose gel viewed with UV light. For the ligation reaction a ratio of 1:3 – 1:10 of vector to insert was used. The reaction sample (10 µl) usually contained ~ 100 ng of vector DNA and 10 units T4 DNA ligase (NEB). The reaction was performed either at 23°C for 1 h or at 16°C for 4-20 h. In case of transformation of *E.coli* via electroporation, the ligation sample was dialyzed against de-ionized water for 15 min using a nitrocellulose filter (pore size: 0.05 µm, Millipore).

Sequencing of DNA

DNA sequencing reactions were carried out by the institute with an Abi-Prism 377 sequencer. Sample preparations and sequencing reactions were performed with the DYEnamic ET terminator cycle sequencing kit according to the manufacturers' instructions (Amersham-Pharmacia). The sample usually contained 0.5 µg plasmid DNA and 5 pmol primer.

4.3.3. Polymerase chain reaction (PCR)

The PCR method was applied for cloning of plasmid constructs, for amplification of PCR cassettes for chromosomal epitope-tagging or gene disruptions, or for analysis of recombination events after chromosomal integration into yeast strains.

PCR reactions were usually performed in a volume of 50 µl with 50 ng plasmid DNA or 0.2 µg genomic DNA, 0.6 µM of the respective forward and reverse oligonucleotide primers, 1.75 µl deoxynucleotide mix (each 10 mM, NEB) and 0.2-5 units DNA polymerase (Pfu turbo, Stratagene, a mixture of 4:1 taq/vent polymerase, NEB, or for analytical purpose taq polymerase only) in the respective PCR buffer (Pfu turbo, Stratagene; Thermopol buffer, NEB). For amplification a PCR Mastercycler (Eppendorf) was used. The reaction profile was adjusted according to the quantity and quality of the template DNA, the length and G/C content of the oligonucleotides and the length of the amplified sequence. If necessary, the temperatures for primer annealing and

primer extension have been optimized. In general, the following program was used, in which the polymerase was added after the initial denaturation step:

initial denaturation	94°C	3	min
10 amplification cycles	94°C	30	s
	46°C	30	s
	68°C	120	s
25 amplification cycles	94°C	30	s
	54°C	30	s
	68°C	120	s
+20 s / cycle			
final extension	68°C	10	min
cooling	4°C		

For the verification of chromosomal integration events (e.g. gene disruptions), usually the colony PCR method was applied: Cells from a single yeast colony (approximately of a pinhead size) were resuspended in 20 μ l NaOH (20 mM), to which a spatula tip of acid-washed glass beads (\varnothing 425-600 nm, Sigma) was added, and shaken in a thermomixer at 100°C at maximum speed for 5 min. After brief centrifugation (15 s) 4 μ l of the supernatant was used as template DNA for the PCR reaction carried out in a volume of 50 μ l with 0.6 μ M of the respective forward and reward oligonucleotide primers, 1.75 μ l deoxynucleotide mix (each 10 mM, NEB) and 2 units taq polymerase in thermopol buffer (NEB) with the following program in a Mastercycler (Eppendorf):

initial denaturation	94°C	5	min
30 amplification cycles	94°C	30	s
	55°C	30	s
	68°C	60	s
final extension	68°C	5	min
cooling	4°C		

4.3.4. Site-directed mutagenesis

For the insertion of point mutations, a PCR-based strategy was developed according to the QuickChange method (Stratagene). This method uses two complementary oligonucleotide primers with the codon to be mutated in the middle flanked by 15 additional base pairs each corresponding to the target sequence. The reaction was performed in a volume of 25 μ l with 50 ng plasmid DNA as template, 62.5 ng of each primer, 0.625 μ l deoxynucleotide mix (each 10 mM, NEB) and 5 units Pfu turbo (Stratagene) in Pfu turbo buffer (Stratagene) with the following program in a Mastercycler (Eppendorf):

initial denaturation	94°C	30	s
19 amplification cycles	94°C	30	s
	55°C	60	s
	68°C	2	min / 1 kb plasmid
final extension	68°C	5	min
cooling	4°C		

The PCR results in the amplification of both strains of the total plasmid that immediately anneal. To eliminate the template DNA, the reaction was subsequently digested with *DpnI* at 37°C for 1-2 h. This restriction enzyme cleaves specifically methylated template DNA. After dialysis the PCR product can directly be used for transformation. The efficiency of the PCR amplification and *DpnI* digestion was estimated by comparing the number of clones with a sample having been incubated either without primers in the PCR reaction (negative control) or without enzyme in the digestion step (positive control). The mutagenesis was verified by DNA sequencing usually of 2-6 clones.

4.4. Protein and biochemical methods

4.4.1. Preparation of cell extracts and microsomal fractions

Preparation of denatured yeast extracts

For examination of post-translational modifications and cellular protein levels denatured protein extracts were prepared in order to avoid proteolysis during the lysis procedure. Usually, 1 ml of mid-log phase yeast cells corresponding to an $OD_{600} = 1$ were harvested by centrifugation and resuspended in 1 ml ice-cold water. Subsequently, 150 μ l 1.85 M NaOH, 7.5% β -mercaptoethanol was added and placed on ice for 15 min. Then 150 μ l 55% trichloroacetic acid (TCA, w/v) was added and the mixture was incubated for 10 min on ice. The cells were pelleted (20000 g at 4° for 20 min) and the supernatant removed. After a second brief centrifugation and the removal of residual traces of TCA, the pellet was resuspended in 50 μ l HU sample buffer (200 mM phosphate buffer, pH 6.8, 8 M urea, 5% w/v SDS, 1 mM EDTA, 1.5% v/v DTT, bromophenol blue).

Preparation of native yeast extracts

Native proteins extracts were usually prepared for microsome preparations and immunoprecipitations under native conditions. Yeast cells of mid-log phase culture were harvested by centrifugation and washed once with ice-cold PBS (Tris-HCl, pH 7.4, 150 mM NaCl). The cell pellet was resuspended in 200-400 μ l lysis buffer per cell amount corresponding to 100 OD_{600} in a 15 ml Falcon tube (lysis buffer: PBS containing protease inhibitors: *complete mix*, Roche; 20 mM NEM, 5 mM benzamidine, 6 μ g/ml antipain, 6 μ g/ml leupeptin, 4.5 μ g/ml aprotinin, 5 μ g/ml trypsin inhibitor, 5 μ g/ml pepstatin, 6 μ g/ml chymostatin, all purchased from Sigma; 4 mM pefablock, Roche). After adding an equal volume of acid-washed glass beads (\varnothing 425-600 μ m, Sigma) the cells were lysed by vortexing 4-5 times for 30 s. The cell lysate was collected by centrifugation through a small hole in the tube made with a 23 gauge syringe. After transferring the lysate into a microcentrifuge tube, the cell debris was removed by pelleting at 720 g at 4°C for 5 min. The supernatant (whole cell extract) contains the soluble fraction (including cytosolic and nuclear proteins) as well as microsomes from the nuclear envelope, the ER and other organelles. Proteins normally residing in the lumen of organelles might have been partially leaked off into the soluble fraction due to the partial disruption of membrane-enclosed compartments by the glass bead lysis.

Preparation of microsomal fractions

For crude separation of microsomes from the soluble phase, whole cells extracts were fractionated by high spin centrifugation at 20,000 g according to standard techniques (Rape *et al.*, 2001). For a refined fractionation, whole cell extracts were subjected to ultracentrifugation with 100.000 g at 4°C for 1 h (Optima™ Max Ultracentrifuge, Beckmann). Subsequently, the microsomal fraction containing also small membrane vesicles was solubilized in presence of 1% Triton X-100 constantly rotating on a falcon roller for 60-90 min at 4°C. Afterwards, non-solubilized material was removed by a second ultracentrifugation step. For immunoprecipitations (see below), the solubilized protein fraction was usually diluted with lysis buffer resulting in a final concentration of Triton x-100 below 0.4%.

Determination of protein concentration solution

Protein concentrations were determined by using the Bradford method (BioRad protein assay; BioRad) and compared to a BSA standard dilution series by measuring the OD_{595} .

4.4.2. Immunoprecipitation

Immunoprecipitation under denaturing conditions

For examination of post-translational modifications and metabolically [³⁵S]-pulsed proteins, whole cell extracts were subjected to immunoprecipitations under denaturing conditions. Cell amounts corresponding to 2-3 OD₆₀₀ were lysed by NaOH/β-mercaptoethanol and proteins were precipitated by TCA addition (see 4.2.1.). Subsequently, the protein pellet was resolved in a modified HU buffer containing less SDS and no reducing agents (200 mM phosphate buffer, pH 6.8, 8 M urea, 1% w/v SDS, 1 mM EDTA) and incubated at 65°C for 30-60 min. After removal of the unsolved material by centrifugation (16000 g at 23°C for 15 min), the protein solution was diluted in lysis buffer (see 4.2.1.) resulting in a final concentration of SDS below 0.05%. Occasionally, Nonidet P40 or Triton X-100 was added to a final concentration of 0.1% to avoid un-specific binding. Immunoprecipitation was carried out with 25 μl slurry anti-HA IgG (3F10, Roche) coupled to agarose beads or 2 μg anti-CPY IgG (A-6248, Invitrogen-Molecular Probes) bound to proteinG sepharose constantly rotating on a falcon roller for 90-180 min at 4°C. Un-specific bound material was removed by 4-5 wash steps with lysis buffer containing detergent in a centrifuge using spin columns (MoBiTec). Usually, a final wash step was performed with lysis buffer without detergent. The specific bound material was eluted from the column by adding 50 μl 1% SDS, incubating at 65°C for 15 min shaking on a thermomixer and subsequent centrifugation at high speed for 30 s. The eluate was concentrated in a speed vac and resuspended in 25-50 μl HU sample buffer (200 mM phosphate buffer, pH 6.8, 8 M urea, 5% w/v SDS, 1 mM EDTA, 1.5% v/v DTT, bromophenol blue).

Immunoprecipitation under native conditions

For examination of protein-protein interactions whole cell extracts or solubilized membrane fractions (see 4.2.1.) were subjected to immunoprecipitations under native conditions. After glass bead lysis and preparation of extracts, Nonidet P40 or Triton X-100 was added to a final concentration of 0.1-0.4% to avoid un-specific binding. Immunoprecipitation was carried out with 25 μl slurry anti-HA IgG (3F10, Roche) or anti-myc IgG (9E10, Santa Cruz) coupled to agarose beads constantly rotating on a falcon roller for 90-180 min at 4°C. Unspecific bound material was removed by 4-5 wash steps with lysis buffer containing detergent in a centrifuge using spin columns (MoBiTec). Usually, a final wash step was performed with lysis buffer without detergent. The specific bound material was eluted from the column by adding 50 μl 1% SDS, incubating at 65°C for 15 min shaking on a thermomixer and subsequent centrifugation at high speed for 30 s. The eluate was concentrated in a speed vac and resuspended in 25-50 μl HU sample buffer (200 mM phosphate buffer, pH 6.8, 8 M urea, 5% w/v SDS, 1 mM EDTA, 1.5% v/v DTT, bromophenol blue).

4.4.3. Gel electrophoresis and immunoblot techniques

SDS polyacrylamide gel electrophoresis (SDS-PAGE)

For the standard separation of proteins under denaturing conditions SDS-PAGE was performed using a discontinuous buffer system (Laemmli, 1970) in *mighty small* or *tall* electrophoresis chambers (Hoefler) or similar chambers made by the institute. The percentage of the resolving gels varied between 10 and 15% acrylamide, depending on the desired resolution range. The stacking gel was usually made of 4% acrylamide. The accurate composition is listed below. Electrophoresis was carried out at a constant current of 15-15 mA in 25 mM Tris base, 250 mM glycine, 0.1% SDS.

Table 4-2: Laemmli SDS-PAGE gels

% acrylamide	resolving gel			stacking gel
	10%	12%	15%	4%
H ₂ O [ml]	4.0	3.3	2.3	1.7
30% acrylamide/ 0.8% bis-acrylamide [ml]	3.3	4	5	1.7
1.5 M Tris-HCl, pH 8.8 [ml]	2.5	2.5	2.5	-
1 M Tris-HCl, pH 6.8 [ml]	-	-	-	1.25
10% SDS [μ l]	100	100	100	100
10% ammonium peroxodisulfate [μ l]	50	50	50	50
TEMED [μ l]	4	4	4	4

The separation of the SNARE protein Ufe1 required a gel system with a higher resolution (SNARE proteins generally tend to 'smear'). Therefore, usually tricine gels (Schagger and von Jagow, 1987) were used, which were originally developed for the resolution of especially small polypeptides but which are also applicable for proteins up to 100 kD. The percentage of the resolving gels was either 6.5% or 8.5%. The pH of the stacking and resolving gel is actually set by the cathode buffer (0.1 M Tris base, 0.1 M tricine, 0.1% SDS) and the anode buffer (0.2 M Tris-HCl, pH 8.9). Electrophoresis was carried out at a constant current of 15-20 mA at 4°C.

Table 4-3: Tricine SDS-PAGE gels

% acrylamide	resolving gel		stacking gel
	6.5%	8.5%	4%
H ₂ O [ml]	4.0	2.7	3.85
30% acrylamide/ 0.8% bis-acrylamide [ml]	2.1	2.8	0.85
3 M Tris-HCl, pH 8.45 [ml]	3.33	3.33	1.55
87% glycerol [ml]	1.15	1.15	-
10% ammonium peroxodisulfate [μ l]	100	100	75
TEMED [μ l]	6	6	10

Alternatively, 4-12% gradient Bis-Tris PAGE pre-cast (Invitrogen) or self-poured gels were applied, which allow a high resolution over large range of different sized proteins (10-200 kD) and do not require a stacking gel. Electrophoresis was carried out at a constant voltage of 140 V in MOPS buffer (50 mM 3-N-Morpholinopropane sulfonic acid, 50 mM Tris base, 3.5 mM SDS, 1 mM EDTA).

Coomassie staining of protein gels

After electrophoresis, SDS-PAGE gels were stained with a Coomassie solution (0.1% Coomassie Brilliant Blue R-250, 20% methanol, 10% acetic acid) for 30-60 min and destained by incubation in fixing solution (20% methanol, 10% acetic acid) until unspecific stain was removed.

Autoradiography

After electrophoresis, SDS-PAGE gels were incubated for 15 min in fixing solution (20% methanol, 10% acetic acid) followed by 15 min incubation in amplifier solution (Amplify™ fluorographic reagent, Amersham-Pharmacia) to increase the detection efficiency. Subsequently, gels were dried on a 3MM whatman paper in a slab gel dryer (GD2000, Hoefer) and exposed to a phosphorimager plate. Autoradiography was detected by a phosphorimager (BAS 2500, Fujifilm) using the software *Image Reader BAS 2500 V1.4E* (Fujifilm).

Immunoblotting

After proteins were resolved by SDS-PAGE they were transferred to a polyvinylidene fluorid (PVDF) membrane (Immobilon P, Millipore) in a tank blot system in 250 mM Tris base, 1.92 M glycine, 0.1% SDS, 20% methanol) at a constant voltage at 70 V for 60-120 min preferentially at 4°C. The PVDF membrane was blocked with TBST-milk (25 mM Tris-HCl, pH 7.5, 137 mM NaCl, 2.6 mM KCl, 0.1% v/v Tween 20, 5% w/v low fat milk powder) at least for 20 min, followed by the incubation with the primary antibody in the same buffer for 90 min at 23°C or overnight at 4°C. Subsequently, the blot membrane was washed 4 times at least for 10 min in TBST and afterward incubated with the secondary antibody coupled to horseradish peroxidase (Dianova) at a dilution of 1:5000 in TBST-milk for 60-90 min. The blot membrane was washed as before and detection was carried out as described in the protocol for the chemiluminescence kit (ECL or ECL plus, Amersham) followed by exposure to ECL hyperfilm (Amersham) or to a CCD camera (LAS, Fuji).

Digitalized images acquired by a CCD (charged-coupled device) camera were processed and quantified with the software programs *Image Reader LAS 1000 V1.1* and *Image Gauge V3.01* (Fujifilm), respectively. For detection of chemiluminescence signals with the *Image Reader* program, the iris of the lens (URF 20L, Fuji) was set at 0.85, and signal exposure was done in the precision mode with dark frame subtraction and flat frame correction usually for 2-10 min depending on the signal intensity (longer exposure times were not used due to the time-dependent decay of the chemiluminescence intensity). Optionally, the binning mode (2x2) was used to increase the signal intensity when a lower image resolution was tolerable. For quantification of the relative intensity of the chemiluminescence with the *Image Gauge* program, all specific signals reflecting the protein at the expected size as well as the typical high molecular weight 'smear' (most probably ubiquitylated species) were used for determination of the AU (area under curve) values, from which the background was subtracted. The background subtraction is accomplished by the software program irrespective of the area size; only in cases when the signal:noise ratio was substantially low, the background area was individually adapted.

Table 4-4: antibodies used in this study

antibody	clone, source	dilutions in TBST milk
commercial primary antibodies:		
monoclonal anti-c-myc	9E10 sc-40, Santa Cruz	1:2000
polyclonal anti-c-myc	A-14 sc-789, Santa Cruz	1:2000 – 1:5000
monoclonal anti-HA	F-7 sc-7392, Santa Cruz	1:2000
monoclonal anti-FLAG	M2, Sigma	1:10000
monoclonal anti-Dpm1	Invitrogen-Molecular Probes	1:5000
monoclonal anti-CPY	A-6248, Invitrogen-Molecular Probes	
non-commercial primary antibodies:		
polyclonal anti-Ufe1 serum	6His-Ufe1 Δ Sn Δ Tm, this study	1:10000 – 1:50000
polyclonal anti-Ufe1 aff. purif.	6His-Ufe1 Δ Sn Δ Tm, this study	1:2000
polyclonal anti-Sed5 aff. purif.	Gallwitz lab	1:10000
polyclonal anti-Cdc48 aff. purif.	GST-Cdc48, Jentsch lab	1:10000 – 1:20000
polyclonal anti-Shp1 aff. purif.	GST-Shp1, Jentsch lab	1:10000 – 1:20000
commercial secondary antibodies:		
HRP-coupled anti-rabbit IgG (H+L)	Dianova	1:5000
HRP-coupled anti-mouse IgG (H+L)	Dianova	1:5000

For the generation of anti-Ufe1 specific polyclonal antibodies, the *UFE1* ORF was cloned without the terminal 709-1041 bp encoding the SNARE and the transmembrane domain and recombinantly expressed in bacteria. The recombinant fusion protein His₆-Ufe1ΔSnΔTm was affinity purified under denaturing conditions and subsequently dialyzed against PBS (see 4.4.4.). For the immunization, 250 μg of the purified protein solved 750 μl PBS was mixed with an equal volume of Freud adjuvant (TiterMax complete, Sigma) to a homogeneous emulsion and injected at different positions subcutaneously into the rabbit. The first immunization was followed by two boosts with an equal amount of protein emulsified in Freud adjuvant incomplete by intervals of 6 and 2 weeks, respectively (Sigma). 10 days after the second boost the rabbit was bled. The serum (200 ml) was recovered by first incubating at 37°C for 1 h and then at 4°C for 16 h, followed by centrifugation (20000 g, 4°C). The serum was stored at -80°C prior to affinity purification or used directly for immunoblots.

4.4.4. Purification of recombinant proteins

Purification of recombinant proteins from *E.coli*

Recombinant Ufe1 proteins were employed for raising polyclonal antibodies and GST pulldown experiments. For bacterial expression the *UFE1* ORF was cloned without the terminal 709-1041 bp encoding the SNARE and the transmembrane domain to increase the expression affinity. The respective constructs were expressed in *E.coli* (BL21 pRIL) and the recombinant proteins subsequently affinity purified by their introduced tags (His₆ or GST-epitope).

For the purification of His₆-Ufe1ΔSnΔTm, 1 l bacteria culture of an OD₆₀₀ of 3 was harvested by centrifugation and the pellet was resuspended in 40 ml denaturing lysis buffer (100 mM NaH₂PO₄, 10 mM Tris base, 8 M urea, pH 8.0). Cell lysis was performed by repetitively freezing and thawing the cell suspension and the bacterial DNA was sheared by pressing the lysate several times through a 23 gauge syringe. After removal of the cell debris by centrifugation (20000 g, 23°C, 60 min), the supernatant was incubated with 2 ml slurry of a 50% NiNTA agarose solution (Qiagen) with gentle agitation for 2 h at 23°C. Bound material was washed 5 times with wash buffer (100 mM NaH₂PO₄, 10 mM Tris base, 8 M urea, pH 6.3) and subsequently eluted in fractions with elution buffer (100 mM NaH₂PO₄, 10 mM Tris base, 8 M urea, pH 5.9; 100 mM NaH₂PO₄, 10 mM Tris base, 8 M urea, pH 4.5). The elution of the recombinant proteins was monitored by measuring the protein concentration and by SDS-PAGE. Positive fractions were pooled and step-wise dialyzed against PBS (Tris-HCl, pH 7.4, 150 mM NaCl).

For the purification of GST-Ufe1ΔSnΔTm, 2 l bacteria culture of an OD₆₀₀ of 2.5 were harvested by centrifugation and the pellet was resuspended in 50 ml ice-cold PBS buffer containing protease inhibitors (6 μg/ml antipain, 6 μg/ml leupeptin, 4.5 μg/ml aprotinin, 5 μg/ml trypsin inhibitor, 5 μg/ml pepstatin, 6 μg/ml chymostatin, all purchased from Sigma; 4 mM pefablock, Roche). Cell lysis was performed with an Emulsiflex C5 cell disruptor. Subsequently, Triton X-100 was added to a final concentration of 1% and the cell lysate was incubated at 4° for 30 min. After removal of the non-solubilized material by centrifugation (20000 g, 23°C, 30 min), the lysate was incubated with 6 ml slurry of 50% glutathione sepharose solution (Amersham-Pharmacia) with gentle agitation for 2-3 h at 4°C. Material bound to the glutathione resin was washed 3 times with PBS and thereafter eluted in fractions with elution buffer (PBS containing 300 mM NaCl, 0.1% Triton X-100 and 10 mM glutathione). The elution of the recombinant proteins was monitored by measuring the protein concentration and by SDS-PAGE.

Affinity purification of polyclonal antibodies

For the purification of the polyclonal antibody raised against His₆-Ufe1ΔSnΔTm, the serum (see

4.4.3.) was immunoaffinity chromatography purified. The purification included two successive columns. As an unrelated antigen, whole cell lysate of BL21 cells, in which GST was expressed, was coupled to a pre-column, whereas purified recombinant GST-Ufe1 Δ Sn Δ Tm was used as specific antigen for the main column. For covalent binding, CnBr sepharose 4CLB (Amersham-Pharmacia) was used as matrix for the columns. The respective antigens were first dialyzed against coupling buffer (100 mM NaHCO₃ pH 8.3, 0.5 M NaCl) and subsequently coupled onto CnBr sepharose. Free binding sites were blocked with glycine (0.2 M glycine, pH 8.0). Both columns were prepared by several wash steps (6 volumes 100 mM NaAc pH 4.0, 0.5 M NaCl; 3 volumes PBS; 3 volumes PBS, 1% SDS; denaturation at 65° for 40 min; 2 volumes PBS, 1% SDS; pre-column only: 6 volumes PBS, 1% Triton X-100; main column only: 3 volumes PBS, 1% Triton X-100; 3 volumes PBS, 1% Triton X-100, 1% BSA). After washing, both columns were connected with each other and the serum was applied and passed 3 times over both columns. Subsequently, the columns were washed with 2 volumes PBS, and after disconnecting the main column was washed with 6 volumes PBS, 1% Triton X-100 and 6 volumes PBS. Specifically bound IgGs were eluted in fractions first with glycine buffer (0.2 M glycine pH 2.5, 1 mM EGTA) and immediately neutralized with 1 M Tris-HCl, pH 8.0. High affinity-bound IgGs were eluted with guanidinium hydrochloride buffer (4 M GnHCl, pH 7.0). Positive fractions of both eluates were pooled and dialyzed against PBS. After addition of glycerol to a final concentration of 50%, the purified IgGs were stored at -80°C.

5. REFERENCES

- Ahner, A. and J. L. Brodsky (2004). Checkpoints in ER-associated degradation: excuse me, which way to the proteasome? *Trends Cell Biol* **14**(9): 474-8.
- Asubel, F. M., R. Brent, R. E. Kingston, D. D. Moore, J. G. Seidman, J. A. Smitz and K. Struhl (editors) (1987). Current protocols in molecular biology. Greene publishing associates, New York.
- Baboshina, O. V. and A. L. Haas (1996). Novel multiubiquitin chain linkages catalyzed by the conjugating enzymes E2EPF and RAD6 are recognized by 26 S proteasome subunit 5. *J Biol Chem* **271**(5): 2823-31.
- Babst, M., D. J. Katzmann, E. J. Estepa-Sabal, T. Meerloo and S. D. Emr (2002a). Escrt-III: an endosome-associated heterooligomeric protein complex required for mvb sorting. *Dev Cell* **3**(2): 271-82.
- Babst, M., D. J. Katzmann, W. B. Snyder, B. Wendland and S. D. Emr (2002b). Endosome-associated complex, ESCRT-II, recruits transport machinery for protein sorting at the multivesicular body. *Dev Cell* **3**(2): 283-9.
- Bachmair, A. and A. Varshavsky (1989). The degradation signal in a short-lived protein. *Cell* **56**(6): 1019-32.
- Bays, N. W., R. G. Gardner, L. P. Seelig, C. A. Joazeiro and R. Y. Hampton (2001). Hrd1p/Der3p is a membrane-anchored ubiquitin ligase required for ER-associated degradation. *Nat Cell Biol* **3**(1): 24-9.
- Biederer, T., C. Volkwein and T. Sommer (1996). Degradation of subunits of the Sec61p complex, an integral component of the ER membrane, by the ubiquitin-proteasome pathway. *Embo J* **15**(9): 2069-76.
- Biederer, T., C. Volkwein and T. Sommer (1997). Role of Cue1p in ubiquitination and degradation at the ER surface. *Science* **278**(5344): 1806-9.
- Blom, D., C. Hirsch, P. Stern, D. Tortorella and H. L. Ploegh (2004). A glycosylated type I membrane protein becomes cytosolic when peptide: N-glycanase is compromised. *Embo J* **23**(3): 650-8.
- Bossie, M. A. and C. E. Martin (1989). Nutritional regulation of yeast delta-9 fatty acid desaturase activity. *J Bacteriol* **171**(12): 6409-13.
- Bracher, A. and W. Weissenhorn (2002). Structural basis for the Golgi membrane recruitment of Sly1p by Sed5p. *Embo J* **21**(22): 6114-24.
- Braun, S., K. Matuschewski, M. Rape, S. Thoms and S. Jentsch (2002). Role of the ubiquitin-selective CDC48(UFD1/NPL4) chaperone (segregase) in ERAD of OLE1 and other substrates. *Embo J* **21**(4): 615-21.
- Brower, C. S., S. Sato, C. Tomomori-Sato, T. Kamura, A. Pause, R. Stearman, R. D. Klausner, S. Malik, W. S. Lane, I. Sorokina, *et al.* (2002). Mammalian mediator subunit mMED8 is an Elongin BC-interacting protein that can assemble with Cul2 and Rbx1 to reconstitute a ubiquitin ligase. *Proc Natl Acad Sci U S A* **99**(16): 10353-8.

- Bryant, N. J. and D. E. James (2001). Vps45p stabilizes the syntaxin homologue Tlg2p and positively regulates SNARE complex formation. *Embo J* **20**(13): 3380-8.
- Caldwell, S. R., K. J. Hill and A. A. Cooper (2001). Degradation of endoplasmic reticulum (ER) quality control substrates requires transport between the ER and Golgi. *J Biol Chem* **276**(26): 23296-303.
- Chau, V., J. W. Tobias, A. Bachmair, D. Marriott, D. J. Ecker, D. K. Gonda and A. Varshavsky (1989). A multiubiquitin chain is confined to specific lysine in a targeted short-lived protein. *Science* **243**(4898): 1576-83.
- Chen, L. and K. Madura (2002). Rad23 promotes the targeting of proteolytic substrates to the proteasome. *Mol Cell Biol* **22**(13): 4902-13.
- Chen, P., P. Johnson, T. Sommer, S. Jentsch and M. Hochstrasser (1993). Multiple ubiquitin-conjugating enzymes participate in the in vivo degradation of the yeast MAT alpha 2 repressor. *Cell* **74**(2): 357-69.
- Choi, J. Y., J. Stuke, S. Y. Hwang and C. E. Martin (1996). Regulatory elements that control transcription activation and unsaturated fatty acid-mediated repression of the *Saccharomyces cerevisiae* OLE1 gene. *J Biol Chem* **271**(7): 3581-9.
- Chu, S., J. DeRisi, M. Eisen, J. Mulholland, D. Botstein, P. O. Brown and I. Herskowitz (1998). The transcriptional program of sporulation in budding yeast. *Science* **282**(5389): 699-705.
- Dascher, C., R. Ossig, D. Gallwitz and H. D. Schmitt (1991). Identification and structure of four yeast genes (SLY) that are able to suppress the functional loss of YPT1, a member of the RAS superfamily. *Mol Cell Biol* **11**(2): 872-85.
- DeHoratius, C. and P. A. Silver (1996). Nuclear transport defects and nuclear envelope alterations are associated with mutation of the *Saccharomyces cerevisiae* NPL4 gene. *Mol Biol Cell* **7**(11): 1835-55.
- DeLaBarre, B. and A. T. Brunger (2003). Complete structure of p97/valosin-containing protein reveals communication between nucleotide domains. *Nat Struct Biol* **10**(10): 856-63.
- Deng, L., C. Wang, E. Spencer, L. Yang, A. Braun, J. You, C. Slaughter, C. Pickart and Z. J. Chen (2000). Activation of the I κ B kinase complex by TRAF6 requires a dimeric ubiquitin-conjugating enzyme complex and a unique polyubiquitin chain. *Cell* **103**(2): 351-61.
- Deveraux, Q., V. Ustrell, C. Pickart and M. Rechsteiner (1994). A 26 S protease subunit that binds ubiquitin conjugates. *J Biol Chem* **269**(10): 7059-61.
- Downing, T. A. and R. K. Storms (1996). Molecular analysis of UFE1, a *Saccharomyces cerevisiae* gene essential for spore formation and vegetative growth. *Curr Genet* **30**(5): 396-403.
- Dreveny, I., H. Kondo, K. Uchiyama, A. Shaw, X. Zhang and P. S. Freemont (2004). Structural basis of the interaction between the AAA ATPase p97/VCP and its adaptor protein p47. *Embo J* **23**(5): 1030-9.
- Dulubova, I., S. Sugita, S. Hill, M. Hosaka, I. Fernandez, T. C. Sudhof and J. Rizo (1999). A conformational switch in syntaxin during exocytosis: role of munc18. *Embo J* **18**(16): 4372-82.

- Dulubova, I., T. Yamaguchi, D. Arac, H. Li, I. Huryeva, S. W. Min, J. Rizo and T. C. Sudhof (2003). Convergence and divergence in the mechanism of SNARE binding by Sec1/Munc18-like proteins. *Proc Natl Acad Sci U S A* **100**(1): 32-7.
- Ellgaard, L. and A. Helenius (2003). Quality control in the endoplasmic reticulum. *Nat Rev Mol Cell Biol* **4**(3): 181-91.
- Elsasser, S., D. Chandler-Militello, B. Muller, J. Hanna and D. Finley (2004). Rad23 and Rpn10 serve as alternative ubiquitin receptors for the proteasome. *J Biol Chem* **279**(26): 26817-22.
- Fan, C. M. and T. Maniatis (1991). Generation of p50 subunit of NF-kappa B by processing of p105 through an ATP-dependent pathway. *Nature* **354**(6352): 395-8.
- Feldman, R. M., C. C. Correll, K. B. Kaplan and R. J. Deshaies (1997). A complex of Cdc4p, Skp1p, and Cdc53p/cullin catalyzes ubiquitination of the phosphorylated CDK inhibitor Sic1p. *Cell* **91**(2): 221-30.
- Finger, A., M. Knop and D. H. Wolf (1993). Analysis of two mutated vacuolar proteins reveals a degradation pathway in the endoplasmic reticulum or a related compartment of yeast. *Eur J Biochem* **218**(2): 565-74.
- Finley, D., B. Bartel and A. Varshavsky (1989). The tails of ubiquitin precursors are ribosomal proteins whose fusion to ubiquitin facilitates ribosome biogenesis. *Nature* **338**(6214): 394-401.
- Finley, D., E. Ozkaynak and A. Varshavsky (1987). The yeast polyubiquitin gene is essential for resistance to high temperatures, starvation, and other stresses. *Cell* **48**(6): 1035-46.
- Finley, D., S. Sadis, B. P. Monia, P. Boucher, D. J. Ecker, S. T. Crooke and V. Chau (1994). Inhibition of proteolysis and cell cycle progression in a multiubiquitination-deficient yeast mutant. *Mol Cell Biol* **14**(8): 5501-9.
- Friedlander, R., E. Jarosch, J. Urban, C. Volkwein and T. Sommer (2000). A regulatory link between ER-associated protein degradation and the unfolded-protein response. *Nat Cell Biol* **2**(7): 379-84.
- Gardner, R. G. and R. Y. Hampton (1999a). A 'distributed degron' allows regulated entry into the ER degradation pathway. *Embo J* **18**(21): 5994-6004.
- Gardner, R. G. and R. Y. Hampton (1999b). A highly conserved signal controls degradation of 3-hydroxy-3-methylglutaryl-coenzyme A (HMG-CoA) reductase in eukaryotes. *J Biol Chem* **274**(44): 31671-8.
- Gardner, R. G., H. Shan, S. P. Matsuda and R. Y. Hampton (2001a). An oxysterol-derived positive signal for 3-hydroxy-3-methylglutaryl-CoA reductase degradation in yeast. *J Biol Chem* **276**(12): 8681-94.
- Gardner, R. G., A. G. Shearer and R. Y. Hampton (2001b). In vivo action of the HRD ubiquitin ligase complex: mechanisms of endoplasmic reticulum quality control and sterol regulation. *Mol Cell Biol* **21**(13): 4276-91.
- Ghislain, M., R. J. Dohmen, F. Levy and A. Varshavsky (1996). Cdc48p interacts with Ufd3p, a WD repeat protein required for ubiquitin-mediated proteolysis in *Saccharomyces cerevisiae*. *Embo J* **15**(18): 4884-99.

- Ghislain, M., A. Udvardy and C. Mann (1993). *S. cerevisiae* 26S protease mutants arrest cell division in G2/metaphase. *Nature* **366**(6453): 358-62.
- Gietz, R. D. and A. Sugino (1988). New yeast-*Escherichia coli* shuttle vectors constructed with in vitro mutagenized yeast genes lacking six-base pair restriction sites. *Gene* **74**(2): 527-34.
- Glickman, M. H., D. M. Rubin, O. Coux, I. Wefes, G. Pfeifer, Z. Cjeka, W. Baumeister, V. A. Fried and D. Finley (1998). A subcomplex of the proteasome regulatory particle required for ubiquitin-conjugate degradation and related to the COP9-signalosome and eIF3. *Cell* **94**(5): 615-23.
- Goldknopf, I. L. and H. Busch (1977). Isopeptide linkage between nonhistone and histone 2A polypeptides of chromosomal conjugate-protein A24. *Proc Natl Acad Sci U S A* **74**(3): 864-8.
- Gonzalez, C. I. and C. E. Martin (1996). Fatty acid-responsive control of mRNA stability. Unsaturated fatty acid-induced degradation of the *Saccharomyces OLE1* transcript. *J Biol Chem* **271**(42): 25801-9.
- Gonzalez, F., A. Delahodde, T. Kodadek and S. A. Johnston (2002). Recruitment of a 19S proteasome subcomplex to an activated promoter. *Science* **296**(5567): 548-50.
- Groll, M., M. Bajorek, A. Kohler, L. Moroder, D. M. Rubin, R. Huber, M. H. Glickman and D. Finley (2000). A gated channel into the proteasome core particle. *Nat Struct Biol* **7**(11): 1062-7.
- Groll, M., L. Ditzel, J. Lowe, D. Stock, M. Bochtler, H. D. Bartunik and R. Huber (1997). Structure of 20S proteasome from yeast at 2.4 Å resolution. *Nature* **386**(6624): 463-71.
- Hampton, R. Y. (1998). Genetic analysis of hydroxymethylglutaryl-coenzyme A reductase regulated degradation. *Curr Opin Lipidol* **9**(2): 93-7.
- Hampton, R. Y. (2002). ER-associated degradation in protein quality control and cellular regulation. *Curr Opin Cell Biol* **14**(4): 476-82.
- Hartmann-Petersen, R., M. Wallace, K. Hofmann, G. Koch, A. H. Johnsen, K. B. Hendil and C. Gordon (2004). The Ubx2 and Ubx3 cofactors direct Cdc48 activity to proteolytic and nonproteolytic ubiquitin-dependent processes. *Curr Biol* **14**(9): 824-8.
- Haynes, C. M., S. Caldwell and A. A. Cooper (2002). An HRD/DER-independent ER quality control mechanism involves Rsp5p-dependent ubiquitination and ER-Golgi transport. *J Cell Biol* **158**(1): 91-101.
- Helliwell, S. B., S. Losko and C. A. Kaiser (2001). Components of a ubiquitin ligase complex specify polyubiquitination and intracellular trafficking of the general amino acid permease. *J Cell Biol* **153**(4): 649-62.
- Hetzer, M., H. H. Meyer, T. C. Walther, D. Bilbao-Cortes, G. Warren and I. W. Mattaj (2001). Distinct AAA-ATPase p97 complexes function in discrete steps of nuclear assembly. *Nat Cell Biol* **3**(12): 1086-91.
- Hicke, L. and R. Dunn (2003). Regulation of membrane protein transport by ubiquitin and ubiquitin-binding proteins. *Annu Rev Cell Dev Biol* **19**: 141-72.
- Hirsch, C., E. Jarosch, T. Sommer and D. H. Wolf (2004). Endoplasmic reticulum-associated protein degradation--one model fits all? *Biochim Biophys Acta* **1695**(1-3): 215-23.

- Hitchcock, A. L., H. Krebber, S. Fietze, A. Lin, M. Latterich and P. A. Silver (2001). The conserved npl4 protein complex mediates proteasome-dependent membrane-bound transcription factor activation. *Mol Biol Cell* **12**(10): 3226-41.
- Hoege, C., B. Pfander, G. L. Moldovan, G. Pyrowolakis and S. Jentsch (2002). RAD6-dependent DNA repair is linked to modification of PCNA by ubiquitin and SUMO. *Nature* **419**(6903): 135-41.
- Hofmann, K. and L. Falquet (2001). A ubiquitin-interacting motif conserved in components of the proteasomal and lysosomal protein degradation systems. *Trends Biochem Sci* **26**(6): 347-50.
- Hoppe, T., G. Cassata, J. M. Barral, W. Springer, A. H. Hutagalung, H. F. Epstein and R. Baumeister (2004). Regulation of the myosin-directed chaperone UNC-45 by a novel E3/E4-multiubiquitylation complex in *C. elegans*. *Cell* **118**(3): 337-49.
- Hoppe, T., K. Matuschewski, M. Rape, S. Schlenker, H. D. Ulrich and S. Jentsch (2000). Activation of a membrane-bound transcription factor by regulated ubiquitin/proteasome-dependent processing. *Cell* **102**(5): 577-86.
- Huibregtse, J. M., M. Scheffner, S. Beaudenon and P. M. Howley (1995). A family of proteins structurally and functionally related to the E6-AP ubiquitin-protein ligase. *Proc Natl Acad Sci U S A* **92**(7): 2563-7.
- Huibregtse, J. M., J. C. Yang and S. L. Beaudenon (1997). The large subunit of RNA polymerase II is a substrate of the Rsp5 ubiquitin-protein ligase. *Proc Natl Acad Sci U S A* **94**(8): 3656-61.
- Imai, Y., M. Soda, S. Hatakeyama, T. Akagi, T. Hashikawa, K. I. Nakayama and R. Takahashi (2002). CHIP is associated with Parkin, a gene responsible for familial Parkinson's disease, and enhances its ubiquitin ligase activity. *Mol Cell* **10**(1): 55-67.
- James, P., J. Halladay and E. A. Craig (1996). Genomic libraries and a host strain designed for highly efficient two-hybrid selection in yeast. *Genetics* **144**(4): 1425-36.
- Jarosch, E., C. Taxis, C. Volkwein, J. Bordallo, D. Finley, D. H. Wolf and T. Sommer (2002). Protein dislocation from the ER requires polyubiquitination and the AAA-ATPase Cdc48. *Nat Cell Biol* **4**(2): 134-9.
- Jentsch, S. (1992). The ubiquitin-conjugation system. *Annu Rev Genet* **26**: 179-207.
- Jentsch, S., J. P. McGrath and A. Varshavsky (1987). The yeast DNA repair gene RAD6 encodes a ubiquitin-conjugating enzyme. *Nature* **329**(6135): 131-4.
- Jentsch, S. and G. Pyrowolakis (2000). Ubiquitin and its kin: how close are the family ties? *Trends Cell Biol* **10**(8): 335-42.
- Jenuwein, T. and C. D. Allis (2001). Translating the histone code. *Science* **293**(5532): 1074-80.
- Johnson, E. S. and G. Blobel (1997). Ubc9p is the conjugating enzyme for the ubiquitin-like protein Smt3p. *J Biol Chem* **272**(43): 26799-802.
- Johnson, E. S., P. C. Ma, I. M. Ota and A. Varshavsky (1995). A proteolytic pathway that recognizes ubiquitin as a degradation signal. *J Biol Chem* **270**(29): 17442-56.

- Johnson, P. R., R. Swanson, L. Rakhilina and M. Hochstrasser (1998). Degradation signal masking by heterodimerization of MAT α 2 and MAT α 1 blocks their mutual destruction by the ubiquitin-proteasome pathway. *Cell* **94**(2): 217-27.
- Jungmann, J., H. A. Reins, C. Schobert and S. Jentsch (1993). Resistance to cadmium mediated by ubiquitin-dependent proteolysis. *Nature* **361**(6410): 369-71.
- Katzmann, D. J., M. Babst and S. D. Emr (2001). Ubiquitin-dependent sorting into the multivesicular body pathway requires the function of a conserved endosomal protein sorting complex, ESCRT-I. *Cell* **106**(2): 145-55.
- Kim, I., K. Mi and H. Rao (2004). Multiple interactions of rad23 suggest a mechanism for ubiquitylated substrate delivery important in proteolysis. *Mol Biol Cell* **15**(7): 3357-65.
- Kisselev, A. F., T. N. Akopian, K. M. Woo and A. L. Goldberg (1999). The sizes of peptides generated from protein by mammalian 26 and 20 S proteasomes. Implications for understanding the degradative mechanism and antigen presentation. *J Biol Chem* **274**(6): 3363-71.
- Knop, M., A. Finger, T. Braun, K. Hellmuth and D. H. Wolf (1996). Der1, a novel protein specifically required for endoplasmic reticulum degradation in yeast. *Embo J* **15**(4): 753-63.
- Knop, M., K. Siegers, G. Pereira, W. Zachariae, B. Winsor, K. Nasmyth and E. Schiebel (1999). Epitope tagging of yeast genes using a PCR-based strategy: more tags and improved practical routines. *Yeast* **15**(10B): 963-72.
- Koegl, M., T. Hoppe, S. Schlenker, H. D. Ulrich, T. U. Mayer and S. Jentsch (1999). A novel ubiquitination factor, E4, is involved in multiubiquitin chain assembly. *Cell* **96**(5): 635-44.
- Kondo, H., C. Rabouille, R. Newman, T. P. Levine, D. Pappin, P. Freemont and G. Warren (1997). p47 is a cofactor for p97-mediated membrane fusion. *Nature* **388**(6637): 75-8.
- Kosodo, Y., Y. Noda, H. Adachi and K. Yoda (2002). Binding of Sly1 to Sed5 enhances formation of the yeast early Golgi SNARE complex. *J Cell Sci* **115**(Pt 18): 3683-91.
- Kosodo, Y., Y. Noda, H. Adachi and K. Yoda (2003). Cooperation of Sly1/SM-family protein and sec18/NSF of *Saccharomyces cerevisiae* in disassembly of cis-SNARE membrane-protein complexes. *Biosci Biotechnol Biochem* **67**(2): 448-50.
- Laemmli, U. K. (1970). Cleavage of structural proteins during the assembly of the head of bacteriophage T4. *Nature* **227**(5259): 680-5.
- Lam, Y. A., T. G. Lawson, M. Velayutham, J. L. Zweier and C. M. Pickart (2002). A proteasomal ATPase subunit recognizes the polyubiquitin degradation signal. *Nature* **416**(6882): 763-7.
- Lambertson, D., L. Chen and K. Madura (2003). Investigating the importance of proteasome-interaction for Rad23 function. *Curr Genet* **42**(4): 199-208.
- Lander, E. S., L. M. Linton, B. Birren, C. Nusbaum, M. C. Zody, J. Baldwin, K. Devon, K. Dewar, M. Doyle, W. FitzHugh, *et al.* (2001). Initial sequencing and analysis of the human genome. *Nature* **409**(6822): 860-921.
- Laney, J. D. and M. Hochstrasser (1999). Substrate targeting in the ubiquitin system. *Cell* **97**(4): 427-30.

- Latterich, M., K. U. Frohlich and R. Schekman (1995). Membrane fusion and the cell cycle: Cdc48p participates in the fusion of ER membranes. *Cell* **82**(6): 885-93.
- Lee, R. J., C. W. Liu, C. Harty, A. A. McCracken, M. Latterich, K. Romisch, G. N. DeMartino, P. J. Thomas and J. L. Brodsky (2004). Uncoupling retro-translocation and degradation in the ER-associated degradation of a soluble protein. *Embo J* **23**(11): 2206-15.
- Lewis, M. J., J. C. Rayner and H. R. Pelham (1997). A novel SNARE complex implicated in vesicle fusion with the endoplasmic reticulum. *Embo J* **16**(11): 3017-24.
- Li, Y., D. Gallwitz and R. Peng (2005). Structure-based Functional Analysis Reveals a Role for the SM Protein Sly1p in Retrograde Transport to the Endoplasmic Reticulum. *Mol Biol Cell*.
- Liakopoulos, D., G. Doenges, K. Matuschewski and S. Jentsch (1998). A novel protein modification pathway related to the ubiquitin system. *Embo J* **17**(8): 2208-14.
- Lilley, B. N. and H. L. Ploegh (2004). A membrane protein required for dislocation of misfolded proteins from the ER. *Nature* **429**(6994): 834-40.
- Lin, A., S. Patel and M. Latterich (2001). Regulation of organelle membrane fusion by Pkc1p. *Traffic* **2**(10): 698-704.
- Lin, L. and M. Kobayashi (2003). Stability of the Rel homology domain is critical for generation of NF-kappa B p50 subunit. *J Biol Chem* **278**(34): 31479-85.
- Longtine, M. S., A. McKenzie, 3rd, D. J. Demarini, N. G. Shah, A. Wach, A. Brachat, P. Philippsen and J. R. Pringle (1998). Additional modules for versatile and economical PCR-based gene deletion and modification in *Saccharomyces cerevisiae*. *Yeast* **14**(10): 953-61.
- Mayer, T. U., T. Braun and S. Jentsch (1998). Role of the proteasome in membrane extraction of a short-lived ER-transmembrane protein. *Embo J* **17**(12): 3251-7.
- McDonough, V. M., J. E. Stuke and C. E. Martin (1992). Specificity of unsaturated fatty acid-regulated expression of the *Saccharomyces cerevisiae* OLE1 gene. *J Biol Chem* **267**(9): 5931-6.
- McGrath, J. P., S. Jentsch and A. Varshavsky (1991). UBA 1: an essential yeast gene encoding ubiquitin-activating enzyme. *Embo J* **10**(1): 227-36.
- Medicherla, B., Z. Kostova, A. Schaefer and D. H. Wolf (2004). A genomic screen identifies Dsk2p and Rad23p as essential components of ER-associated degradation. *EMBO Rep* **5**(7): 692-7.
- Menetret, J. F., A. Neuhof, D. G. Morgan, K. Plath, M. Radermacher, T. A. Rapoport and C. W. Akey (2000). The structure of ribosome-channel complexes engaged in protein translocation. *Mol Cell* **6**(5): 1219-32.
- Meyer, H. H. (2005). Golgi reassembly after mitosis: The AAA family meets the ubiquitin family. *Biochim Biophys Acta* **1744**(2): 108-19.
- Meyer, H. H., H. Kondo and G. Warren (1998). The p47 co-factor regulates the ATPase activity of the membrane fusion protein, p97. *FEBS Lett* **437**(3): 255-7.

- Meyer, H. H., J. G. Shorter, J. Seemann, D. Pappin and G. Warren (2000). A complex of mammalian ufd1 and npl4 links the AAA-ATPase, p97, to ubiquitin and nuclear transport pathways. *Embo J* **19**(10): 2181-92.
- Meyer, H. H., Y. Wang and G. Warren (2002). Direct binding of ubiquitin conjugates by the mammalian p97 adaptor complexes, p47 and Ufd1-Npl4. *Embo J* **21**(21): 5645-52.
- Morris, J. R. and E. Solomon (2004). BRCA1 : BARD1 induces the formation of conjugated ubiquitin structures, dependent on K6 of ubiquitin, in cells during DNA replication and repair. *Hum Mol Genet* **13**(8): 807-17.
- Morris, M. C., P. Kaiser, S. Rudyak, C. Baskerville, M. H. Watson and S. I. Reed (2003). Cks1-dependent proteasome recruitment and activation of CDC20 transcription in budding yeast. *Nature* **423**(6943): 1009-13.
- Muratani, M. and W. P. Tansey (2003). How the ubiquitin-proteasome system controls transcription. *Nat Rev Mol Cell Biol* **4**(3): 192-201.
- Neupert, W. and M. Brunner (2002). The protein import motor of mitochondria. *Nat Rev Mol Cell Biol* **3**(8): 555-65.
- Nishikawa, H., S. Ooka, K. Sato, K. Arima, J. Okamoto, R. E. Klevit, M. Fukuda and T. Ohta (2004). Mass spectrometric and mutational analyses reveal Lys-6-linked polyubiquitin chains catalyzed by BRCA1-BARD1 ubiquitin ligase. *J Biol Chem* **279**(6): 3916-24.
- Osley, M. A. (2004). H2B ubiquitylation: the end is in sight. *Biochim Biophys Acta* **1677**(1-3): 74-8.
- Ossig, R., C. Dascher, H. H. Trepte, H. D. Schmitt and D. Gallwitz (1991). The yeast SLY gene products, suppressors of defects in the essential GTP-binding Ypt1 protein, may act in endoplasmic reticulum-to-Golgi transport. *Mol Cell Biol* **11**(6): 2980-93.
- Palombella, V. J., O. J. Rando, A. L. Goldberg and T. Maniatis (1994). The ubiquitin-proteasome pathway is required for processing the NF-kappa B1 precursor protein and the activation of NF-kappa B. *Cell* **78**(5): 773-85.
- Patel, S. and M. Latterich (1998). The AAA team: related ATPases with diverse functions. *Trends Cell Biol* **8**(2): 65-71.
- Patel, S. K., F. E. Indig, N. Olivieri, N. D. Levine and M. Latterich (1998). Organelle membrane fusion: a novel function for the syntaxin homolog Ufe1p in ER membrane fusion. *Cell* **92**(5): 611-20.
- Peng, J., D. Schwartz, J. E. Elias, C. C. Thoreen, D. Cheng, G. Marsischky, J. Roelofs, D. Finley and S. P. Gygi (2003). A proteomics approach to understanding protein ubiquitination. *Nat Biotechnol* **21**(8): 921-6.
- Peng, R. and D. Gallwitz (2002). Sly1 protein bound to Golgi syntaxin Sed5p allows assembly and contributes to specificity of SNARE fusion complexes. *J Cell Biol* **157**(4): 645-55.
- Petroski, M. D. and R. J. Deshaies (2005). Function and regulation of cullin-RING ubiquitin ligases. *Nat Rev Mol Cell Biol* **6**(1): 9-20.
- Pickart, C. M. (2001). Mechanisms underlying ubiquitination. *Annu Rev Biochem* **70**: 503-33.

- Pickart, C. M. and R. E. Cohen (2004). Proteasomes and their kin: proteases in the machine age. *Nat Rev Mol Cell Biol* **5**(3): 177-87.
- Pickart, C. M. and D. Fushman (2004). Polyubiquitin chains: polymeric protein signals. *Curr Opin Chem Biol* **8**(6): 610-6.
- Pilon, M., R. Schekman and K. Romisch (1997). Sec61p mediates export of a misfolded secretory protein from the endoplasmic reticulum to the cytosol for degradation. *Embo J* **16**(15): 4540-8.
- Plemper, R. K., S. Bohmler, J. Bordallo, T. Sommer and D. H. Wolf (1997). Mutant analysis links the translocon and BiP to retrograde protein transport for ER degradation. *Nature* **388**(6645): 891-5.
- Rabinovich, E., A. Kerem, K. U. Frohlich, N. Diamant and S. Bar-Nun (2002). AAA-ATPase p97/Cdc48p, a cytosolic chaperone required for endoplasmic reticulum-associated protein degradation. *Mol Cell Biol* **22**(2): 626-34.
- Rabouille, C., H. Kondo, R. Newman, N. Hui, P. Freemont and G. Warren (1998). Syntaxin 5 is a common component of the NSF- and p97-mediated reassembly pathways of Golgi cisternae from mitotic Golgi fragments in vitro. *Cell* **92**(5): 603-10.
- Rape, M., T. Hoppe, I. Gorr, M. Kalocay, H. Richly and S. Jentsch (2001). Mobilization of processed, membrane-tethered SPT23 transcription factor by CDC48(UFD1/NPL4), a ubiquitin-selective chaperone. *Cell* **107**(5): 667-77.
- Rape, M. and S. Jentsch (2004). Productive RUpture: activation of transcription factors by proteasomal processing. *Biochim Biophys Acta* **1695**(1-3): 209-13.
- Reggiori, F. and H. R. Pelham (2002). A transmembrane ubiquitin ligase required to sort membrane proteins into multivesicular bodies. *Nat Cell Biol* **4**(2): 117-23.
- Richly, H., M. Rape, S. Braun, S. Rumpf, C. Hoegge and S. Jentsch (2005). A series of ubiquitin binding factors connects CDC48/p97 to substrate multiubiquitylation and proteasomal targeting. *Cell* **120**(1): 73-84.
- Robzyk, K., J. Recht and M. A. Osley (2000). Rad6-dependent ubiquitination of histone H2B in yeast. *Science* **287**(5452): 501-4.
- Rogers, S., R. Wells and M. Rechsteiner (1986). Amino acid sequences common to rapidly degraded proteins: the PEST hypothesis. *Science* **234**(4774): 364-8.
- Rothman, J. E. (1994). Mechanisms of intracellular protein transport. *Nature* **372**(6501): 55-63.
- Rouiller, I., B. DeLaBarre, A. P. May, W. I. Weis, A. T. Brunger, R. A. Milligan and E. M. Wilson-Kubalek (2002). Conformational changes of the multifunction p97 AAA ATPase during its ATPase cycle. *Nat Struct Biol* **9**(12): 950-7.
- Saeki, Y., Y. Tayama, A. Toh-e and H. Yokosawa (2004). Definitive evidence for Ufd2-catalyzed elongation of the ubiquitin chain through Lys48 linkage. *Biochem Biophys Res Commun* **320**(3): 840-5.
- Salghetti, S. E., A. A. Caudy, J. G. Chenoweth and W. P. Tansey (2001). Regulation of transcriptional activation domain function by ubiquitin. *Science* **293**(5535): 1651-3.

- Salghetti, S. E., M. Muratani, H. Wijnen, B. Futcher and W. P. Tansey (2000). Functional overlap of sequences that activate transcription and signal ubiquitin-mediated proteolysis. *Proc Natl Acad Sci U S A* **97**(7): 3118-23.
- Sambrook, J., E. F. Fritsch and T. Maniatis (1989). *Molecular Cloning*. CSH Laboratory Press.
- Schagger, H. and G. von Jagow (1987). Tricine-sodium dodecyl sulfate-polyacrylamide gel electrophoresis for the separation of proteins in the range from 1 to 100 kDa. *Anal Biochem* **166**(2): 368-79.
- Schauber, C., L. Chen, P. Tongaonkar, I. Vega, D. Lambertson, W. Potts and K. Madura (1998). Rad23 links DNA repair to the ubiquitin/proteasome pathway. *Nature* **391**(6668): 715-8.
- Scheffner, M., U. Nuber and J. M. Huibregtse (1995). Protein ubiquitination involving an E1-E2-E3 enzyme ubiquitin thioester cascade. *Nature* **373**(6509): 81-3.
- Schuberth, C., H. Richly, S. Rumpf and A. Buchberger (2004). Shp1 and Ubx2 are adaptors of Cdc48 involved in ubiquitin-dependent protein degradation. *EMBO Rep* **5**(8): 818-24.
- Schwarz, S. E., K. Matuschewski, D. Liakopoulos, M. Scheffner and S. Jentsch (1998). The ubiquitin-like proteins SMT3 and SUMO-1 are conjugated by the UBC9 E2 enzyme. *Proc Natl Acad Sci U S A* **95**(2): 560-4.
- Shanklin, J., E. Whittle and B. G. Fox (1994). Eight histidine residues are catalytically essential in a membrane-associated iron enzyme, stearyl-CoA desaturase, and are conserved in alkane hydroxylase and xylene monooxygenase. *Biochemistry* **33**(43): 12787-94.
- Shcherbik, N., Y. Kee, N. Lyon, J. M. Huibregtse and D. S. Haines (2004). A single PXY motif located within the carboxyl terminus of Spt23p and Mga2p mediates a physical and functional interaction with ubiquitin ligase Rsp5p. *J Biol Chem* **279**(51): 53892-8.
- Shih, S. C., D. J. Katzmann, J. D. Schnell, M. Sutanto, S. D. Emr and L. Hicke (2002). Epsins and Vps27p/Hrs contain ubiquitin-binding domains that function in receptor endocytosis. *Nat Cell Biol* **4**(5): 389-93.
- Skowyra, D., K. L. Craig, M. Tyers, S. J. Elledge and J. W. Harper (1997). F-box proteins are receptors that recruit phosphorylated substrates to the SCF ubiquitin-ligase complex. *Cell* **91**(2): 209-19.
- Sogaard, M., K. Tani, R. R. Ye, S. Geromanos, P. Tempst, T. Kirchhausen, J. E. Rothman and T. Sollner (1994). A rab protein is required for the assembly of SNARE complexes in the docking of transport vesicles. *Cell* **78**(6): 937-48.
- Sollner, T., S. W. Whiteheart, M. Brunner, H. Erdjument-Bromage, S. Geromanos, P. Tempst and J. E. Rothman (1993). SNAP receptors implicated in vesicle targeting and fusion. *Nature* **362**(6418): 318-24.
- Sommer, T. and S. Jentsch (1993). A protein translocation defect linked to ubiquitin conjugation at the endoplasmic reticulum. *Nature* **365**(6442): 176-9.
- Stewart, L. C. and M. P. Yaffe (1991). A role for unsaturated fatty acids in mitochondrial movement and inheritance. *J Cell Biol* **115**(5): 1249-57.

- Stukey, J. E., V. M. McDonough and C. E. Martin (1990). The OLE1 gene of *Saccharomyces cerevisiae* encodes the delta 9 fatty acid desaturase and can be functionally replaced by the rat stearyl-CoA desaturase gene. *J Biol Chem* **265**(33): 20144-9.
- Sun, Z. W. and C. D. Allis (2002). Ubiquitination of histone H2B regulates H3 methylation and gene silencing in yeast. *Nature* **418**(6893): 104-8.
- Swanson, R., M. Locher and M. Hochstrasser (2001). A conserved ubiquitin ligase of the nuclear envelope/endoplasmic reticulum that functions in both ER-associated and Matalpha2 repressor degradation. *Genes Dev* **15**(20): 2660-74.
- Taxis, C., R. Hitt, S. H. Park, P. M. Deak, Z. Kostova and D. H. Wolf (2003). Use of modular substrates demonstrates mechanistic diversity and reveals differences in chaperone requirement of ERAD. *J Biol Chem* **278**(38): 35903-13.
- Thrower, J. S., L. Hoffman, M. Rechsteiner and C. M. Pickart (2000). Recognition of the polyubiquitin proteolytic signal. *Embo J* **19**(1): 94-102.
- van Nocker, S., S. Sadis, D. M. Rubin, M. Glickman, H. Fu, O. Coux, I. Wefes, D. Finley and R. D. Vierstra (1996). The multiubiquitin-chain-binding protein Mub1 is a component of the 26S proteasome in *Saccharomyces cerevisiae* and plays a nonessential, substrate-specific role in protein turnover. *Mol Cell Biol* **16**(11): 6020-8.
- Vashist, S., W. Kim, W. J. Belden, E. D. Spear, C. Barlowe and D. T. Ng (2001). Distinct retrieval and retention mechanisms are required for the quality control of endoplasmic reticulum protein folding. *J Cell Biol* **155**(3): 355-68.
- Vashist, S. and D. T. Ng (2004). Misfolded proteins are sorted by a sequential checkpoint mechanism of ER quality control. *J Cell Biol* **165**(1): 41-52.
- Verma, R., R. Oania, J. Graumann and R. J. Deshaies (2004). Multiubiquitin chain receptors define a layer of substrate selectivity in the ubiquitin-proteasome system. *Cell* **118**(1): 99-110.
- Walker, J. E., M. Saraste, M. J. Runswick and N. J. Gay (1982). Distantly related sequences in the alpha- and beta-subunits of ATP synthase, myosin, kinases and other ATP-requiring enzymes and a common nucleotide binding fold. *Embo J* **1**(8): 945-51.
- Wang, C., L. Deng, M. Hong, G. R. Akkaraju, J. Inoue and Z. J. Chen (2001). TAK1 is a ubiquitin-dependent kinase of MKK and IKK. *Nature* **412**(6844): 346-51.
- Wang, Y., A. Satoh, G. Warren and H. H. Meyer (2004). VCIP135 acts as a deubiquitinating enzyme during p97-p47-mediated reassembly of mitotic Golgi fragments. *J Cell Biol* **164**(7): 973-8.
- Wiertz, E. J., D. Tortorella, M. Bogoy, J. Yu, W. Mothes, T. R. Jones, T. A. Rapoport and H. L. Ploegh (1996). Sec61-mediated transfer of a membrane protein from the endoplasmic reticulum to the proteasome for destruction. *Nature* **384**(6608): 432-8.
- Wilkinson, B. M., M. Regnacq and C. J. Stirling (1997). Protein translocation across the membrane of the endoplasmic reticulum. *J Membr Biol* **155**(3): 189-97.
- Wilkinson, C. R., M. Seeger, R. Hartmann-Petersen, M. Stone, M. Wallace, C. Semple and C. Gordon (2001). Proteins containing the UBA domain are able to bind to multi-ubiquitin chains. *Nat Cell Biol* **3**(10): 939-43.

- Yamaguchi, T., I. Dulubova, S. W. Min, X. Chen, J. Rizo and T. C. Sudhof (2002). Sly1 binds to Golgi and ER syntaxins via a conserved N-terminal peptide motif. *Dev Cell* **2**(3): 295-305.
- Ye, Y., H. H. Meyer and T. A. Rapoport (2001). The AAA ATPase Cdc48/p97 and its partners transport proteins from the ER into the cytosol. *Nature* **414**(6864): 652-6.
- Ye, Y., Y. Shibata, C. Yun, D. Ron and T. A. Rapoport (2004). A membrane protein complex mediates retro-translocation from the ER lumen into the cytosol. *Nature* **429**(6994): 841-7.
- Zhang, X., A. Shaw, P. A. Bates, R. H. Newman, B. Gowen, E. Orlova, M. A. Gorman, H. Kondo, P. Dokurno, J. Lally, *et al.* (2000). Structure of the AAA ATPase p97. *Mol Cell* **6**(6): 1473-84.
- Zhou, M. and R. Schekman (1999). The engagement of Sec61p in the ER dislocation process. *Mol Cell* **4**(6): 925-34.

ABBREVIATIONS

ADP	adenosine 5'-diphosphate
Amp	ampicillin
ATP	adenosine 5'-triphosphate
βGal	β-galactosidase
bp	base pairs
BSA	bovine serum albumin
cDNA	complimentary DNA
CCD camera	charged-coupled device camera
Ci	Curie
C-terminal	carboxyterminal
C-terminus	carboxy terminus
dATP	deoxyadenosine triphosphate
DMSO	dimethylsulfoxide
DNA	deoxyribonucleic acid
dNTP	deoxy nucleoside triphosphate
DTT	dithiothreitol
E1	ubiquitin activation enzyme
E2	ubiquitin conjugation enzyme
E3	ubiquitin ligase
E4	multiubiquitylation factor
EDTA	ethylenediaminetetraacidic acid
ER	endoplasmic reticulum
g	gram
<i>g</i>	gravitational constant ($6.6742 \times 10^{-11} \text{ N m}^2 \text{ kg}^{-2}$)
h	hours
Ig	immunoglobulin
IP	immunoprecipitation
IPTG	isopropyl-β-D-thiogalactopyranoside
k	kilo ($\times 10^3$)
kan	kanamycine
kb	kilo base pairs
kDa	kilo dalton
LB	Luria-Bertani
M	molar
m	milli ($\times 10^{-3}$)
μ	micro ($\times 10^{-6}$)
<i>MAT</i>	mating type
min	minutes
MOPS	3-N-Morpholinopropane sulfonic acid
mRNA	messenger RNA
MW	molecular weight
n	nano ($\times 10^{-9}$)
NEM	N-ethylmaleimide

NSF	NEM sensitive factor
N-terminal	aminoterminal
N-terminus	amino terminus
NP-40	Nonidet P-40
O/E	overexpression
OD _x	optical density at x nm
OLE-pathway	regulon for the transcription of the <i>OLE1</i> gene
PAGE	polyacrylamide gel electrophoresis
PBS	phosphate-buffered saline
PCR	polymerase chain reaction
PEG	polyethylene glycol
RING	<i>really interesting new gene</i> (E3 enzyme)
rpm	rounds per minute
RT	room temperature
S	sedimentation coefficient(Svedberg)
s	seconds
SDS	sodium dodecylsulfate
SNAP	soluble NSF attachment protein
SNARE	soluble NSF attachment protein receptor
TCA	trichloro acidic acid
t _{1/2}	half time
TBST	Tris-buffered saline with Tween-20
TEMED	N,N,N',N'-tetramethylethylenediamin
Tet	tetracycline
Tris	Tris(hydroxymethyl)aminomethane
U	Unit
Ub	ubiquitin
UBC	ubiquitin conjugating enzyme
Ubi-ProβGal	ubiquitin-proline-lacI-β-galactosidase
UFD	ubiquitin fusion degradation
UV	ultraviolet light
V	Volt
v/v	volume per volume
w/v	weight per volume
WT	wild type
YNB	yeast nitrogen base
YPD	yeast bactopectone dextrose

CURRICULUM VITAE

Name Sigurd Jürgen Braun
Adresse Bürgerschaft 5
79271 St.Peter im Schwarzwald
Geburtsdatum 18. Juni 1972
Geburtsort Freiburg i. Br.
Nationalität Deutsch

Schulbildung

1979 – 1992 Grund- und weiterführende Schule: Freie Waldorfschule Freiburg
Abschluss mit Abitur im Juni 1992

Studium

1992 – 1999 Albert-Ludwigs-Universität Freiburg
Diplomstudiengang Biologie
Diplomarbeit über „Untersuchung der Blaulicht-/UV-abhängigen
Chalconsynthase-Signaltransduktion in Petersiliezellkultur“
Fakultät für Biologie II in der Arbeitsgruppe von Prof. Eberhard Schäfer
(Betreuer: PD Dr. Hanns Frohnmeyer)
Abschluss mit Diplom Biologie im Januar 1999

Zivildienst

1999 – 2000 Max-Planck-Institut für Psychiatrie, München

Doktorarbeit

2000 – 2005 Max-Planck-Institut für Biochemie, Martinsried
Abteilung für Molekulare Zellbiologie (Prof. Stefan Jentsch)